Open access • Journal Article • DOI:10.1007/S11831-019-09327-X

Recent Trends in the Modeling and Quantification of Non-probabilistic Uncertainty

Matthias Faes, David Moens

Institutions: Katholieke Universiteit Leuven

Published on: 01 Jul 2020 - Archives of Computational Methods in Engineering (Springer Netherlands)

Topics: Uncertainty quantification and Probabilistic logic

Archives of Computational Methods in Engineering manuscript No.
(will be inserted by the editor)

Recent trends in the modeling and quantification of non-probabilistic uncertainty

Matthias Faes · David Moens

Received: date / Accepted: date

Abstract This paper gives an overview of recent advances in the field of non-probabilistic uncertainty quantification. Both techniques for the forward propagation and inverse quantification of interval and fuzzy uncertainty are discussed. Also the modeling of spatial uncertainty in an interval and fuzzy context is discussed. An in depth discussion of a recently introduced method for the inverse quantification of spatial interval uncertainty is provided and its performance is illustrated using a case studies taken from literature. It is shown that the method enables an accurate quantification of spatial uncertainty under very low data availability and with a very limited amount of assumptions on the underlying uncertainty. Finally, also a conceptual comparison with the class of Bayesian methods for uncertainty quantification is provided.

Keywords Non-probabilistic analysis · Fuzzy analysis · Inverse methods · Uncertainty quantification

1 Introduction

Nowadays, the design of functional components for use in demanding applications is largely founded on numerical approximations of the sets of differential equations that describe the physical processes in our everyday life. In this way, the dynamic and static responses of a complicated structural component to an estimated load can be predicted long before it has been produced. In the context of designing structural components, especially the Finite Element method [231] has become an indispensable part of the toolbox of a modern design engineer, as it proves to yield high-resolution predictions of the mechanical response of a structure to a

Matthias Faes
KU Leuven - Department of mechanical engineering
Post-doctoral Researcher of the Flemish Research Foundation (FWO)
E-mail: matthias.faes@kuleuven.be

David Moens
KU Leuven - Department of mechanical engineering
E-mail: david.moens@kuleuven.be

realistic load situation. In recent years, also extended FE methods have been proposed, including the computation of crack initiation and -propagation [42], various methods for Computational Flow Dynamics [205] and Isogeometric Analysis [99]. The use of these powerful numerical methods has led to an significant reduction in time-to-market and product development costs, as nearly all necessary design optimizations can be performed virtually instead of by means of prototype testing. These optimizations can include for example the minimization of the weight of the structure while maintaining its structural performance, or to maximize its reliability. As such, usually less costly prototype testing stages are needed in the design. Therefore, these numerical design methods are nowadays omnipresent in an industrial engineering context. Also in an academic context, the interest for numerical design methods is large, as illustrated by the number of published and cited papers on these subjects.

However, criticism exists with respect to purely virtual deterministic design optimizations. This criticism finds its root in the various sources of non-determinism that are commonly encountered when designing structural components. First, since most computations that involve the solution of (sets of) differential equations are based on numerical approximations, the obtained results diverge inherently from the true response of the system. This is, for example, caused by the discretization, truncation, linearization and/or inadequate approximations that are used to discretize the problem [109]. This issue was also addressed by Albert Einstein (see opening quote) during one of this lectures on geometry at the Prussian Academy of Sciences, where he stated that "As far as the laws of mathematics refer to reality, they are not certain, and as far as they are certain, they do not refer to reality".

Moreover, since nature itself is not deterministic, the material properties, modeled geometry of the structure, design loading and boundary conditions that are used to parametrize and construct the numerical model are also inherently non-deterministic (see e.g. [67, 157, 206, 111, 184] for a thorough discussion). An example of such natural non-determinism is the unknown process parameter variability during the part manufacturing which entails that the final part properties such as the mechanical strength or final dimensions cannot be determined deterministically in beforehand. A second example is the lack of knowledge on the exact loading conditions of the structure, as for example wind or snow loads on a building. Consequently, deterministic studies of the problem are inadequate when a reliable and economic and ecological design is pursued. Since the inherent non-determinism is neglected in this way, a large degree of conservatism in the design is needed to prevent premature failure. Unexpected premature failure of the structure due to an inadequate design usually entrails significant costs in terms of maintenance, insurance, legal actions and/or customer compensations, as well as a large damage to the reputation of the company. The economic impact is especially relevant for safety-critical applications such as aerospace, automotive, heavy machinery design, off-shore oil drilling or the nuclear sector, where moreover also irreparable human or ecological losses can occur upon failure. The necessary over-conservatism in the design not only impairs the economic cost of producing the component; it also leads to unnecessary weight gains, which is impermissible in such high-performance sectors. Therefore, during the last decades, numerous research initiatives have been taken to employ the large availability of computing power for the inclusion of non-determinism in FE models, rather than further refining the resolution of the used numerical methods. As such, the effect of various sources of non-determinism can

be incorporated already in early design stages, enhancing the credibility of the numerical models.

The class of techniques, methods and paradigms that are aimed at providing a quantitative characterization and/or reduction of non-determinism in numerical models are usually denoted as Uncertainty Quantification (UQ). Forward UQ methods start from a non-deterministic description of the model parameters and try to quantify the corresponding non-determinism in the model responses. This is for example highly relevant for the estimation of failure probabilities in the context of optimizing the reliability of the design. These methods are also commonly referred to as uncertainty propagation. Inverse UQ methods on the other hand are aimed at quantifying the non-determinism in the parameters of a numerical model, and start from e.g. a high-fidelity model or independent measurement data of measured system responses. In general, two large philosophies exist for UQ in FE analyses: the probabilistic and the possibilistic approach. Both approaches have their own advantages and limitations, which generally can be summarized as:

- Following a probabilistic approach, non-determinism is considered as the likelihood that a parameter assumes a certain value within a specified range, and is depicted as a joint probability density function (JPDF). This JPDF is propagated through the numerical model to infer the likelihood of obtaining a certain model response [188]. When non-deterministic quantities that are time or space-dependent are considered, the framework of random fields theory has already reached a high maturity [201]. Random fields are mostly specified by the spatial evolution of their first two statistical moments and a covariance function, which expresses the spatial dependence of the field variable under the rather strict assumption of statistical homogeneity of the random field. Application of these methods in practice often proves to be inconvenient due to the large amount of data necessary for the identification of a JPDF or the corresponding statistical moments, since this implies that the full joint likelihood for all parameter values should be quantified objectively. In this context, a review of literature shows that especially in industrial applications, many authors assume the data to follow a Gaussian distribution. This however can be a severe misjudgment of the non-deterministic data structure, resulting in an unrealistic assessment of the non-deterministic model behavior, and consequently, the design quality. Furthermore, these results often come at a very high computational cost, especially when very small failure probabilities are considered [49, 200]. In case no objective JPDF of the model parameters is available, this high computational cost is hard to justify.
- Possibilistic approaches such as interval methods consider only the crisp bounds on the non-deterministic values [132]. Fuzzy number approaches are an extension to interval methods as they assign a membership function to which all parameter values belong to a certain interval [90]. Following a possibilistic approach, the intervals or fuzzy numbers are propagated through the numerical model using specialized techniques to infer the worst-case responses of the structural component. However, interval methods are by definition not capable of defining dependence between different model responses, which might make them severely over-conservative with respect to the actual uncertainty in the model responses. As concerns non-deterministic quantities that are time or space-dependent, the concept of interval fields has been introduced only

very recently as non-probabilistic counterpart to random fields [130, 204, 202, 203, 180, 181]. These concepts alleviate the dependency problem to a large extent. In general, interval methods relax the need for the identification of a full probabilistic data description, which may be very cumbersome. Moreover, less expensive numerical procedures are necessary for the description of the non-determinism.

As such, it can be understood that both concepts complement each other perfectly, with their respective domains of applicability based on the availability of sufficient objective data and the nature of the processes that underlie the non-determinism.

However, to have an objective and realistic quantification of the non-determinism in the structural responses of the numerical design model, the description of the non-deterministic parameters of the numerical model should be made objectively and accurately. First, the most appropriate non-deterministic philosophy for describing the non-determinism should be selected. A lot of literature already deals with answering this question (see e.g. [49, 200, 11]). Secondly, the corresponding description of the non-determinism should be objectively quantified. Some parameters, such as plate thicknesses, are rather straightforward to quantify, as they can directly be measured. Material parameters such as non-isotropic Young's modulus or yield strength already pose a larger challenge, as they should be quantified in a destructive context, based on reference material samples. Finally, other parameters such as connection stiffness or damping coefficients are impossible to measure. In the two latter cases, indirect inverse UQ methods can provide a solution to alleviate the problems associated with a direct quantification approach. As concerns inverse UQ in a probabilistic sense, the class of Bayesian methods is considered the standard approach [7, 107], even when the non-deterministic model parameters are described by random fields [185, 127]. However, in the context of limited, insufficient, vague or ambiguous data, the construction of the necessary prior estimation of the joint probability density function of the non-deterministic parameter values is subjective. Moreover, this estimate, affects the quantified result to a large extent when insufficient independent measurement data are available. Moreover, generally expensive numerical procedures are needed since high-dimensional integrals need to be approximated numerically in this context. In a possibilistic context, methods for the inverse UQ of interval and fuzzy uncertainty have only been introduced very recently. Most of these methods are somehow based on a hypercubic approximation of the result of the interval numerical model, and therefore neglect possible dependence between the output parameters. As such, they are not capable of quantifying any dependence between the interval uncertain parameters of the numerical model, modeled as an interval field.

This paper aims at giving a recent overview of advances in the field of non-probabilistic techniques for the propagation and quantification of uncertainty. Also the topic of spatial and multivariate models for non-probabilistic uncertainty will be discussed. Probabilistic methods are not discussed in detail since the literature on the subject is already very extensive. For more information, the reader is referred to the review paper of Stefanou [188]. Furthermore, also an in-depth discussion on the applicability of probabilistic and non-probabilistic techniques is provided, expanding the currently available discussions with a treatment of multivariate and spatial uncertainty. Finally, a recent development in the field of interval

field quantification is discussed in detail and a case study is performed using this technique.

The paper is structured as follows:

- section 2 introduces recent developments in the area of interval and interval field analysis
- section 3 introduces recent developments in the area of fuzzy and fuzzy field analysis
- section 4 discusses the application of both probabilistic, interval and fuzzy approaches for the modeling and simulation of uncertainty in numerical models
- section 5 gives an overview of recently introduced inverse approaches for the quantification of interval and fuzzy model parameters based on a set of measured responses
- section 6 discusses a recently introduced method for the quantification of interval field uncertainty based on limited data in detail
- section 7 applies this method to a case study to illustrate its application and performance
- section 8 compares this novel method with the well-known probabilistic framework of Bayesian analysis
- section 9 lists the most important conclusions of this manuscript

2 Interval and interval field finite element method

In order to perform a structural design computation, usually sets of partial differential equations (PDE) have to be solved. The approximative solution of these PDE's is usually provided by means of a numerical model $\mathcal{M}(\boldsymbol{x})$, parametrized by a parameter vector $\boldsymbol{x}(\mathbf{r}) \in \mathcal{X} \subset \mathbb{R}^k$ with $\mathcal{X}$ the set of physically admissible parameters and $k \in \mathbb{N}$. For example, $\boldsymbol{x}(\mathbf{r})$ may contain inertial moments, clamping stiffness values or constitutive material parameters as a function of a spatial coordinate $\mathbf{r} \in \Omega \subset \mathbb{R}^d$ over the model domain Ω with dimension $d \in \mathbb{N}$. In case $\mathcal{M}(\boldsymbol{x})$ is constructed following a finite element approach, Ω is discretized by means of a set of finite elements, yielding d degrees of freedom (DOF). As such the problem is reduced to the solution of a set of equations.

The model $\mathcal{M}(\boldsymbol{x})$ provides a vector of model responses $\boldsymbol{y}(\mathbf{r}) \in \mathcal{Y} \subset \mathbb{R}^d$, with $\mathcal{Y}$ the set of admissible model responses and $d \in \mathbb{N}$, through a set of function operators $m_i,\ i = 1, \ldots, d$, which are defined as:

$$\mathcal{M}(\boldsymbol{x}) : y_i(\mathbf{r}) = m_i(\boldsymbol{x}(\mathbf{r})) \quad i = 1, \ldots, d \tag{1}$$

with $m_i : \mathbb{R}^k \mapsto \mathbb{R}$. Note that the dependence of $\boldsymbol{y}$ does not hold for e.g., structural dynamics applications. In that case d is the number of computed eigenmodes.

2.1 Interval theory

In an interval context, interval uncertain parameters $\boldsymbol{x^I}$ are propagated through a numerical model $m()$, in order to infer knowledge on the extrema in the model responses $\tilde{\boldsymbol{y}} = m(\boldsymbol{x^I})$. Two large groups of techniques are commonly applied, which are either based on trying to solve the set of interval-valued equations directly using

interval arithmetical approaches, or are aimed at finding the extreme responses of the numerical model following a global optimization approach.

The first application of interval arithmetic dates back to Archimedes, who bounded the approximation of π to lie in the interval $[223/71; 22/7]$. Modern era interval computations are based on Moore's interval arithmetic [146], who was in the late $1950's$ one of the first to apply interval calculus to real problems. Independently, similar ideas were presented by Warmus [210] and Sunaga [191]. This section provides a concise review of the basic interval arithmetical operations.

An *interval* or *interval scalar* is a convex subset of the domain of real numbers $\mathbb{R}$. By definition, an interval-valued parameter x is indicated using apex I: x^I. The set of possible values within x^I is bounded by the upper bound $\overline{x}$ and lower bound $\underline{x}$ of the interval. An interval is *closed* when both the upper and lower bound are a member of the interval. The domain of closed real-valued intervals is denoted as $\mathbb{IR}$. $x^I \in \mathbb{IR}$ is explicitly defined as:

$$x^I = [\underline{x}, \overline{x}] = \{x \in \mathbb{R} \mid \underline{x} \leq x \leq \overline{x}\} \tag{2}$$

The centre or midpoint of the interval is defined as :

$$\mu_{x^I} = \frac{\underline{x} + \overline{x}}{2} \tag{3}$$

and the corresponding interval radius is defined as:

$$\Delta x^I = \frac{\overline{x} - \underline{x}}{2} \tag{4}$$

An interval vector is a vector in which each element is an interval:

$$\boldsymbol{x^I} = \begin{Bmatrix} x_1^I \\ x_2^I \\ \vdots \\ x_n^I \end{Bmatrix} = \{\boldsymbol{x} \in \mathbb{R}^n \mid x_i \in x_i^I\} \tag{5}$$

with $\boldsymbol{x^I} \in \mathbb{IR}^n$, the domain of closed real-valued interval vectors of size n. Analogously, interval matrices are defined on $\mathbb{IR}^{n \times m}$. By definition, all indices in interval matrices and vectors are considered to be independent. Hence, an n-dimensional interval vector describes a hypercube in n-dimensional space. The vertices of this hypercube are determined by the lower and upper bounds of the interval scalar entries in the interval vector [132].

When the interval finite element model is solved using an interval arithmetical approach, standard arithmetic is augmented with definitions fot the addition, subtraction, multiplication and division of intervals:

$$x^I + y^I = \left[\underline{x} + \underline{y}; \overline{x} + \overline{y}\right] \tag{6a}$$

$$x^I - y^I = \left[\underline{x} - \overline{y}; \overline{x} - \underline{y}\right] \tag{6b}$$

$$x^I \cdot y^I = \left[\min\left(\underline{x}\underline{y}, \underline{x}\overline{y}, \overline{x}\underline{y}, \overline{x}\overline{y}\right), \max\left(\underline{x}\underline{y}, \underline{x}\overline{y}, \overline{x}\underline{y}, \overline{x}\overline{y}\right)\right] \tag{6c}$$

$$x^I / y^I = \begin{cases} x^I \cdot \left[\frac{1}{\overline{y}}, \frac{1}{\underline{y}}\right] & \text{if } 0 \notin y^I \\ \text{undefined} & \text{if } 0 \in y^I \end{cases} \tag{6d}$$

From the context, it should be clear whether interval arithmetical operations or regular arithmetical operations are performed. Addition and subtraction operations directly translate towards interval vectors and interval matrices, provided that the dimensions of the operands are compatible. Multiplication of interval matrices is performed analogously to *regular* matrices, albeit that the component multiplication is made using eq. 6c and addition using eq. 6a.

If $m(x)$ is continuous function on $\mathbb{R}$, the interval evaluation of the function is then:

$$m(x^I) = \left[\inf_{x \in x^I}(m(x)); \sup_{x \in x^I}(m(x)) \right] \tag{7}$$

with inf the infimum and sup the supremum. When the function $m()$ is monotonically increasing, the often costly determination of $\inf_{x \in x^I}$ and $\sup_{x \in x^I}$ can be replaced by [45]:

$$m(x^I) = [m(\underline{x}); m(\overline{x})] \tag{8}$$

which becomes:

$$m(x^I) = [m(\overline{x}); m(\underline{x})] \tag{9}$$

for monotonically decreasing functions. This is the basis for the vertex method.

2.2 Interval finite element analysis

Numerically, the interval FE procedure is equivalent to searching the input space, defined by a single interval for a model containing one parameter x or an hypercube for a model containing multiple parameters $\boldsymbol{x}$, for those parameter realizations that yield extrema in the output of the model $\boldsymbol{y}$. The first to describe this problem was allegedly Bulgakov as early as 1940 [18,19], who described the problem of estimating a dynamic system response under uncertain-but-bounded parameters.

Consider $\boldsymbol{x^I} \in \mathbb{IR}^k$ as the interval vector containing the k uncertain input parameters, while $m(\boldsymbol{x})$ is the numerical deterministic procedure yielding the multi-dimensional result $\boldsymbol{y} \in \mathbb{R}^d$ (see also eq. (1)). The interval FE method can then be expressed as finding the solution set $\tilde{\boldsymbol{y}}$:

$$\tilde{\boldsymbol{y}} = \left\{ \boldsymbol{y} \mid \boldsymbol{y} = m(\boldsymbol{x}), \boldsymbol{x} \in \boldsymbol{x}^I \right\} \tag{10}$$

which reads as "$\tilde{\boldsymbol{y}}$ is the set containing all output vectors $\boldsymbol{y}$, obtained by performing a deterministic numerical procedure to all vectors $\boldsymbol{x}$, contained in $\boldsymbol{x^I}$". As a point of attention, note that the result $\tilde{\boldsymbol{y}}$ of an interval FE computation is generally not expressed as an interval vector. By definition, all entries in an interval vector are decoupled. However, the underlying differential equations of the model provide a coupling between all model responses $\boldsymbol{y}$. Hence, non-physical model response vectors $\boldsymbol{y}$ are explicitly included in the interval FE result, causing a possibly large degree of over conservatism. This concept is also visualised in figure 1, where the d-dimensional uncertain solution set $\tilde{\boldsymbol{y}}$ and its hyper-cubic approximation $\boldsymbol{y}^I$ are shown as a cross-section on two arbitrary output quantities y_i and y_j. The interval results can become extremely conservative, as all possible dependency between the d output quantities in $\tilde{\boldsymbol{y}}$ is neglected. realizations of the output vector which are

in the hatched area in figure 1 are non-physical, even if they are included within $\boldsymbol{y}^I$.

In general, $\tilde{\boldsymbol{y}}$ spans a non-convex manifold in $\mathbb{R}^d$. As such, a closed form solution of $\tilde{\boldsymbol{y}}$ can only be obtained when an explicit analytical solution for $\boldsymbol{y} = f(\boldsymbol{x})$ exists. Even in that case, also the *dependency phenomenon* has to be tackled (see later in this section). Also, a general numerical solution to this problem is *NP-hard*.

Therefore, the exact solution set $\tilde{\boldsymbol{y}}$ can also be approximated by the construction of an uncertain realization set $\tilde{\boldsymbol{y}}_s$. This set is obtained by propagating q deterministic realizations $\boldsymbol{x}_{F,j}(\mathbf{r})$ of the interval field $\boldsymbol{x}^{\boldsymbol{I}}(\mathbf{r})$:

$$\tilde{\boldsymbol{y}}_s = \left\{ \boldsymbol{y}_{sj} \mid \boldsymbol{y}_{sj} = m(\boldsymbol{x}_{F,j}(\mathbf{r})), \boldsymbol{x}_{F,j}(\mathbf{r}) \in \boldsymbol{x}^{\boldsymbol{I}}(\mathbf{r}) \right\} \tag{11}$$

with $\boldsymbol{y}_{sj} \in \mathbb{R}^{d_s},\ 1, \ldots, q$ a vector containing the d output responses of the j^{th} deterministic model solution:

$$\boldsymbol{y}_{sj} = [y_{s1},\ y_{s2},\ ...,\ y_{sd}]^T \tag{12}$$

In practice, the response quantities that constitute $\boldsymbol{y}_{sj}$ depend on the considered model m. The q realizations should represent the solution set $\tilde{\boldsymbol{y}}$ as closely as possible. Therefore recent work has been focused on numerical approximative procedures aiming at finding the smallest conservative convex approximation of $\tilde{\boldsymbol{y}}$. In this context, two main strategies are found in literature: *global optimization* and *interval arithmetic*. *Global optimization* techniques use optimization algorithms to find the smallest conservative hypercube, whereas *interval arithmetic* techniques are fundamentally based on the interval arithmetic of Moore [144,146,145]. Both strategies are further discussed in detail.

2.2.1 Interval Arithmetic

Interval arithmetic techniques use Moore's interval calculus [144,146,145], as presented in section 2.1 for the solution of the interval FE problem, as introduced in eq. (10). The interval arithmetical approach directly translates the deterministic numerical procedure to an interval arithmetic equivalent. Basically, this consists of three steps [132]:

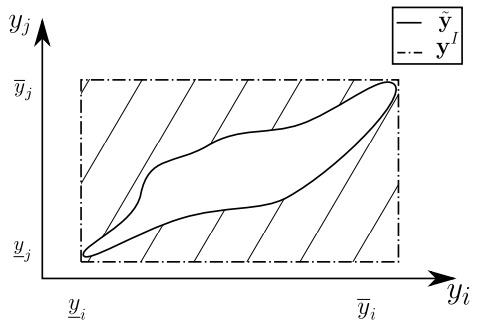

Fig. 1 Illustration of the concept of hyper-cubic approximation $\boldsymbol{y}^I$ of the uncertain solution set $\tilde{\boldsymbol{y}}$, shown as a cross-section on two arbitrary output quantities y_i and y_j of the result vector of the model [59].

1. the interval-valued parameters $\boldsymbol{x^I}$ are translated to interval element stiffness $\boldsymbol{K_e^I}$ and mass matrices $\boldsymbol{M_e^I}$ according to general finite element formulations (in for example an undamped dynamical model)
2. these interval element matrices are assembled into the interval system matrices, $\boldsymbol{K^I}$ and $\boldsymbol{M^I}$ for respectively the stiffness and mass matrices
3. these interval system matrices are used to approximate the solution of the analysis as:

$$\tilde{\boldsymbol{y}} = \left\{ \boldsymbol{y} \mid \boldsymbol{K} \in \boldsymbol{K^I}, \boldsymbol{M} \in \boldsymbol{M^I}, \boldsymbol{y} = m(\boldsymbol{K}, \boldsymbol{M}) \right\} \tag{13}$$

with m indicating the specific solution of the FE model (see eq. (1)).

The main advantage of the technique is its numerical efficiency because, as opposed to the global optimization approaches (see section 2.2.2), no iterative sampling of the deterministic numerical model is needed for the solution of the problem. However, an overestimation of the *true* interval width occurs in general since intervals cannot track parameter dependencies by definition. This overestimation originates from multiple occurrence of the same interval parameter in the arithmetic operations, and stems directly from the assumption that interval numbers are independent. This is also referred to as the *dependency phenomenon* [148], and can be expressed as:

$$x^I(y^I + z^I) \leq (x^I y^I) + (x^I z^I) \tag{14}$$

In practice, the degree of overestimation is proportional to the width of the intervals x^I and y^I and the number of uncertain parameters [182]. For a practical solution of a numerical model, this overestimation of the interval width occurs both during the interval arithmetical operations that are performed to construct and assemble the global system matrices, as in the as in the final approximation of the output of the procedure (i.e the solution phase). Furthermore, when secondary responses such as stresses are considered, this phenomenon is further amplified as these quantities dependent on both the interval stiffness matrix and the computed interval displacement vector [164, 182]. Inevitably, this leads to a serious over-estimation of the interval width of the output parameter, rendering the technique useless for practical design applications. The main body of research concerning interval arithmetic is therefore dedicated towards limiting the dependency phenomenon by keeping track of parameter dependencies throughout the interval arithmetical operations.

A first example of such an *improved interval arithmetical technique* is the element-by-element approach by Muhanna and Mullen [148]. In this technique, all elements in the FE mesh keep their own set of nodes and corresponding degree of freedom (DOF), meaning that a single DOF only corresponds to a single element, eliminating the interaction between the global stiffness matrix entries of different element stiffness matrices. The element connectivity is ensured by applying proper constraining on this full set of DOF. By doing this, an explicit formulation of the interval output is obtained. An extension to this technique was proposed by Muhanna and Mullen, replacing the constraining of the DOF by a *penalty matrix*, which is used to ensure the connectivity between the separate elements and acts like a large spring stiffness between the DOF of adjacent elements [149]. This method was shown to provide sharp bounds on problems containing axial and bending stiffness for HDOF FE-models, whilst not suffering from the curse of dimensionality [150].

Alternatively, Elishakoff and Miglis propose to use parametrized intervals, where the interval radius is parametrized using trigonometric functions[51]. The method seems to work well when an analytical inversion of the stiffness matrix is possible. However, approximative techniques for inverting the stiffness matrix should be applied for realistic FE models.

An alternative way of keeping track of the dependencies is introduced by Manson [118]. He proposes to use *affine arithmetic*, as earlier proposed by Comba and Stolfi [30], which is a more versatile extension of interval arithmetic. Affine arithmetic allows for keeping track of dependencies between operands and sub-formula, and as such enables the possibility of decreasing the dependency phenomenon. The principal idea of this method is to represent all k interval parameters using their affine form:

$$\langle x^I \rangle = x_0 + \sum_{i=1}^{k} x_i \hat{\epsilon}_i^I + x_e \hat{\epsilon}_e^I \tag{15}$$

with $\hat{\epsilon}_i^I \in [-1, +1]$ unknown symbolic real independent interval variables, which allow for keeping track of dependency through addition, subtraction and scalar multiplication. $x_e \hat{\epsilon}_e^I$ is an error term introduced to account for possible non-linear dependencies [35]. Muscolino and Sofi [153] further extended the ideas of Manson and elaborated on the symbolic interval variable, which they denote as *extra unitary interval* (EUI). It is defined such that following properties hold:

$$\hat{\epsilon}_i^I - \hat{\epsilon}_i^I = 0 \tag{16a}$$

$$\hat{\epsilon}_i^I \times \hat{\epsilon}_i^I \equiv (\hat{\epsilon}_i^I)^2 = [0, 1] \tag{16b}$$

$$\hat{\epsilon}_i^I \times \hat{\epsilon}_j^I = [-1, +1] \quad i \neq j \tag{16c}$$

$$x_i \hat{\epsilon}_i^I \pm y_i \hat{\epsilon}_i^I = (x_i \pm y_i) \hat{\epsilon}_i^I \tag{16d}$$

$$x_i \hat{\epsilon}_i^I \times y_i \hat{\epsilon}_i^I = x_i y_i (\hat{\epsilon}_i^I)^2 = x_i y_i [0, 1] \tag{16e}$$

with x_i and y_i finite numbers associated to the i^{th} EUI, $\hat{\epsilon}_i^I$. An interval is converted into its affine form as:

$$\langle x^I \rangle = \frac{1}{2}(\underline{x} + \overline{x}) + \frac{1}{2}(\overline{x} - \underline{x}) \hat{\epsilon}_x^I \tag{17}$$

where $\hat{\epsilon}_x^I$ symbolizes the EUI corresponding to the interval variable x^I. By associating an EUI to each interval variable, the dependency can be taken into account through the computations. Moreover, the over-conservatism in the matrix assembly phase is alleviated as the interval radius of the stiffness $\boldsymbol{\Delta K}$ can be written as as the superposition of the contribution of each separate interval parameter x_i^I (see [182] for the proof). The applicability of this so-called *improved interval analysis via extra unitary interval* has been demonstrated in the context of interval perturbation [153], interval arithmetic computations of truss structures [154], Timoshenko beams and Euler-Bernoulli beams subjected to spatial non-determinism [179, 181] or for the computation of natural frequencies of structures containing interval non-determinism [180].

A practical implementation of the affine arithmetic concept in Finite Element analysis was first proposed by Degrauwe et al. [35], who presented an algorithm to effectively solve an affine system of linear equations based on first and higher order Neumann expansions for the numerical computation of the inverse of a square

affine matrix. Sofi and Romeo [182] computed the inverse of the interval-valued stiffness matrix using the Interval Rational Series Expansion [151,152], showing that the series expansion convergence is independent of the number of DOF in the FE model $m()$. Moreover, they illustrated that also the bounds on secondary variables such as stresses are thus accurately predictable.

Although recently developed Interval Arithmetical techniques are proven to be able to compute sharp bounds on the interval uncertainty of responses of a numerical model within reasonable computational cost, their broad application is still limited. The main reason for this is that these techniques are inherently *intrusive*, meaning that they require specifically developed FE code for solving the numerical model subjected to parametric interval uncertainty. This is a large drawback, as it hinders the application of these techniques with proven and robust commercially available FE solvers.

2.2.2 Global optimization approach

The global optimization approach aims at finding the smallest conservative hyper-cubic approximation $\boldsymbol{y^I}$ of $\tilde{\boldsymbol{y}}$. This approximative hypercube $\boldsymbol{y^I}$ is calculated following an optimization approach, where $\underline{y}_i$ and $\overline{y}_i$ for each output quantity $\boldsymbol{y}_i$ of the solution interval vector $\boldsymbol{y^I}$ are determined by searching the hyper-cubic input domain, bounded by $\boldsymbol{x^I}$, the interval vector containing the non-determinism in the input parameters of the numerical model [132]. This optimization problem is explicitly defined as:

$$\begin{aligned} \underline{y}_i &= \min_{\boldsymbol{x} \in \boldsymbol{x^I}} m_i(\boldsymbol{x}) \qquad i = 1, ..., d \\ \overline{y}_i &= \max_{\boldsymbol{x} \in \boldsymbol{x^I}} m_i(\boldsymbol{x}) \qquad i = 1, ..., d \end{aligned} \tag{18}$$

where $y_i^I = [\underline{y}_i; \overline{y}_i]$ is i^{th} output quantity in the solution interval vector of the model and d is the number of output quantities in the model. If this optimization is successful (i.e., a global maximum and minimum are found), the smallest hyper-cubic approximation of $\tilde{\boldsymbol{y}}$ is obtained, as the dependency between the non-deterministic parameters is implicitly taken into account through the deterministic numerical computations. This particular property poses a significant advantage over the standard *interval arithmetic* approach as it makes *global optimization* insusceptible to the dependency phenomenon. Moreover, these methods are completely *non-intrusive*, as the steps concerning the uncertainty in the parameters are completely decoupled from the propagation of their deterministic realizations $y = m(x)$. This enables the possibility of using them in conjunction with high-performance, commercial FE codes, which facilitates the application to large-scale structures containing multiple DOF, as illustrated in e.g. [91,198,93,72,83].

Care should however be taken, as conservatism is not necessarily guaranteed unless the exact bounds of the (in general non-convex) goal function, defined in eq. 18 are found. Moreover, the computational cost of finding the solution is rather unpredictable as the convergence of the optimization procedures generally is highly problem dependent. However, according to Moens and Hanss [132], the goal function very often exhibits a smooth behavior with respect to the uncertain

parameters, facilitating the optimization procedure. As the technique provides exact bounds, global optimization techniques are more and more considered as the standard technique for solving interval problems. Usually, black box optimization routines are used in this context, employing only the input and output of the deterministic numerical model under consideration. Examples of optimization algorithms that are applied in this context are directional search [165,167,166], linear programming [114] or genetic algorithms [140,15,22]. Examples in literature show the broad applicability, with applications ranging from simple academic cases such as truss structures to geo-hydrodynamics [202] or the vibration of locally non-linear structures [20].

Generally, a high computational cost is associated with finding an accurate solution to the optimization problem posed in eq. (18). This is particularly true in an engineering design context, where often models that include millions of DOF or contain non-linearities are considered. Knowing that the number of function evaluations that are needed in the optimization increases exponentially with the number of uncertain parameters (this is also referred to as the *curse of dimensionality*), the computation time for a single model evaluation indeed drastically influences the total computation time for the solution of the interval model. Therefore, meta-models are commonly used for the representation of the deterministic numerical model. A response surface model models the output domain of a deterministic numerical model as a continuous function, based on some samples that are obtained by propagating a set of input parameters. The main challenge in this context is to build an accurate response surface model, while limiting the number of necessary function evaluations. In this context, higher-order polynomial functions [16] can be used to represent the deterministic model behavior, where the accuracy and complexity are determined by the polynomial degree. More data points are needed for higher-order polynomial response surface models. Also radial basis functions [125], sparse grids [112], Artificial Neural Networks [124,65, 160,38], Support Vector Machines [97,230] or Kriging interpolation schemes [120, 84] have been applied in this context. Recently, also interval predictor models [21, 31] have been introduced in this context and illustrated in range of applications [170,56]. Note that in fact, any surrogate model can be applied in this context. For a recent treatment on several techniques of surrogate models, the reader is referred to [190,78].

A highly accurate adaptive response surface method was introduced by De Munck et al. [33]. Following this method, a Kriging response model is initially constructed based on a small space filling design (using e.g., Latin Hypercube sampling). This Kriging model is then iteratively improved by sampling design points that show the highest *Maximum improvement*. This measure is based on the error estimation of the Kriging model with respect to the actual model behavior and assesses which points in the space that is spanned by the interval input parameters should be sampled to enhance the accuracy of the Kriging model optimally. As such, an accurate meta-model is obtained within limited computational cost. Other techniques have been introduced in this context by e.g. Crombecq et al. [32], who uses local linear approximations to assess the local non-linearity of the model response. In these non-linear zones, a higher sample density is used [177, 199].

In the case when the deterministic model response is monotonic with respect to the uncertain parameters, the Vertex method, as introduced by Dong and Shah

[45] is guaranteed to give an exact result for the optimization problem for interval problems, posed in eq. 18. The vertex method in fact provides a first-order response surface model approximation of the deterministic model response, as it constructs a linear interpolation between the model responses $\boldsymbol{y}_{sj}$, obtained by propagating the vertices of the hyper-cubic uncertain parameter set $\boldsymbol{x}^{\boldsymbol{I}}$, and is therefore a special case of the global optimization approach. This method knows wide application within the context of interval analysis (see e.g. [165, 23, 115, 1, 211, 220, 163, 155]). Moreover, it provides a convex estimation of the uncertain realization set when all vertex combinations are considered. However, the accuracy of the technique degrades rapidly when the model response is non-monotonic due to the limited number of sample points. Moreover, the computational cost of the vertex method increases exponentially with the number of uncertain input parameters, as 2^k function evaluations are needed for k interval uncertain parameters.

2.2.3 Perturbation methods

An alternative approach to the vertex methods is obtained by approximating the deterministic model evaluation around the centre points of the input parameters by means of a higher-order expansion scheme. This approximation then is used in the optimization scheme of eq. 18 to find a solution to the numerical model containing interval non-determinism.

As a regular perturbation approach is only applicable when the interval ranges on the parameters are sufficiently small or the model is linear, Qiu and Elishakoff proposed in this context an improved perturbation approach [162]. Specifically, they propose to divide the interval system matrices into equally spaced subinterval system matrices, which are then solved using a perturbation method [162]. However, many deterministic model evaluations are in that case needed to determine the local sensitivity indices for each subinterval. This also hinders application of this method for realistic design studies.

In the last 15 years, some work was presented in the context of interval perturbation by, among others, McWilliam [126], Chen et al. [24] and Deng et al. [37]. McWilliam presented a modified perturbation approach, based on first-order Taylor Series expansions, which in conjunction with a monotonicity assumption on the numerical model $m()$, proved to deliver a higher accuracy as compared to interval perturbation when the radii of the interval uncertain parameters increased [126]. Sim et al., who constructed in this context a first-order Taylor series approximation at the input parameter interval centre point to describe the effect of uncertain input parameter variations on mode shapes in a dynamical model [175]. A modified Taylor series expansion technique was proposed by Wang et al. [207], who propose to retain also higher order terms in expansion. Finally, Massa et al. [123, 122] introduced the Taylor Expansion with Extra Management (TEEM) technique to detect possible non-monotonicity in the objective function. They built a higher-order Taylor series expansion at the input parameter interval centre points to approximate the deterministic model behavior. Extrema in the input domain are searched by observing function evaluations in the vertex points, as well as the local derivatives at those locations. The Taylor expansion is used to speed up the evaluation of the deterministic model and its derivatives in the vertex points. Recently, many sub-types of perturbation methods for interval analysis

have been proposed (see e.g., [208, 222, 209]). However, their accuracy tends to degrade quickly when the width of the intervals increases, or when highly non-linear problems are considered. Latest trends in this context include the application of a Chebyshev series expansion [105] or dimension-wise approaches [219].

2.2.4 Hybrid approaches

Some advanced interval FE approaches combine both global optimization and interval arithmetic. In this context, Moens and Vandepitte [133] developed such a hybrid methodology to compute envelope frequency response functions based on the modal superposition principle. An optimization step is used in the modal analysis of the structure, whereas the actual modal superposition is done via interval arithmetic. The approach is also capable of handling damping [131].

2.3 Interval fields

Since intervals are inherently incapable of taking dependency into account, usually two extreme approaches are employed to model spatial uncertainty in an interval context. A first method exists in considering one independent interval per individual element in the FE model, neglecting all possible dependence throughout Ω. By neglecting dependence between two adjacent locations in Ω, discontinuous, and consequently possibly unphysical realizations of the uncertainty throughout the model are explicitly included in the mathematical representation of the spatial uncertainty. Moreover, the numerical cost of evaluating the model increases drastically as many interval uncertain parameters have to be considered in the analysis. This is particularly problematic for industrially sized FE models containing up to millions of nodes in their discretization. A second solution to this problem exists in considering all intervals in Ω completely coupled. Obviously, this poses in general a serious under-estimation of the spatial complexity of the uncertainty, possibly leading to strongly over-conservative estimates of the uncertainty in the model responses.

In an attempt for a more truthful representation of the spatial non-determinism, Moens et al. introduced the *explicit interval field* formulation [130] as an interval counterpart to the probabilistic random field framework for the modeling of spatial uncertainty under scarce data availability. The next sections describe two novel methods for performing interval field computations. Note that also other methods have been introduced, for instance based on local averaging techniques [39, 215]. Finally, a more generic method of defining inter-dependence between multiple intervals was introduced in [62].

2.3.1 Explicit interval fields

The description of an explicit interval field is based on the superposition of $n_b \in \mathbb{N}$ base functions $\boldsymbol{\psi}_i : \Omega \mapsto \mathbb{R}$, scaled by independent interval scalars $\boldsymbol{\alpha}_i^I$. The base functions $\boldsymbol{\psi}_i$ describe the spatial nature of the non-deterministic value that is modelled by the interval field over the model domain, and are unit-less. The interval scalars $\boldsymbol{\alpha}_i^I \in \mathbb{IR}$ on the other hand quantify the non-determinism of the

model parameters under consideration. An interval field $\boldsymbol{x}^I(\mathbf{r})$ is formally expressed as:

$$\boldsymbol{x}^I(\mathbf{r}) = \mu_{\boldsymbol{x}^I} + \sum_{i=1}^{n_b} \boldsymbol{\psi}_i(\mathbf{r})\alpha_i^I \tag{19}$$

When Ω is discretized into k finite elements $\Omega_e \subset \Omega$, the discretized base functions $\boldsymbol{\psi}_i(\mathbf{r}) \in \mathbb{R}^k$ interpolate the interval scalars α_i^I to dependent intervals for each element in Ω. As such, it is also clear that, when $n_b < k$, a reduction of the input space dimension is obtained. Furthermore, since all $\boldsymbol{\alpha}_i^I$ remain independent, commonly applied techniques for the propagation of the uncertainty can be applied directly.

The solution of the numerical model $\mathcal{M}$ containing interval field uncertain parameters $\boldsymbol{x^I}(\mathbf{r})x\mathbf{r}$ is aimed at finding those realizations of the interval field that yield extrema in the set of model responses $\tilde{\boldsymbol{y}}(\mathbf{r})$, obtained by propagating the interval field:

$$\tilde{\boldsymbol{y}}(\mathbf{r}) = \left\{ \boldsymbol{y}_i(\mathbf{r}) \mid \boldsymbol{y}_i(\mathbf{r}) = \mathcal{M}\left(\boldsymbol{x}_{\boldsymbol{F},\boldsymbol{j}}\left(\mathbf{r}\right)\right); \boldsymbol{x}_{\boldsymbol{F},\boldsymbol{j}}\left(\mathbf{r}\right) \in \boldsymbol{x}^I(\mathbf{r}); i = 1, \ldots, q \right\} \tag{20}$$

with $q \in \mathbb{N}$ the number of propagated realizations of the interval field. $\tilde{\boldsymbol{y}}(\mathbf{r})$ is obtained using one of the methods discussed in section 2.2.

For practical application, the base functions $\boldsymbol{\psi}_i(\mathbf{r})$ in (19) should translate expert knowledge of the analyst on the spatial nature of the uncertainty to a mathematical formulation in an intuitive way, while delivering a realistic representation of this uncertainty. The definition as such can be based either on knowledge of the production process or other engineering judgment, but can also be based on direct [102] or indirect [59,55] measurement data. Two methods for the construction of $\boldsymbol{\psi}_i(\mathbf{r})$ were introduced very recently by the authors:

Inverse Distance Weighting interpolation was recently applied by [61] in the context of interval field modeling. The core idea is to control the complexity of the field realizations by selecting appropriate control point locations $\mathbf{r}_i$ inside the model domain Ω. Based on these control point locations, the base functions $\boldsymbol{\psi}_i(\mathbf{r})$ are constructed according to:

$$\boldsymbol{\psi}_i(\mathbf{r}) = \frac{w_i(\mathbf{r})}{\sum_{j=1}^{n_b} w_j(\mathbf{r})} \tag{21}$$

with $w_i(\mathbf{r}) \in \Omega$ and $i = 1, \ldots, n_b$:

$$w_i(\mathbf{r}) = \frac{1}{[d(\mathbf{r}_i, \mathbf{r})]^p} \tag{22}$$

with $p \in \mathbb{R}^+$ and they should be designed as such that they preserve the independence of $\boldsymbol{\alpha}^I$.

Based on this approach, the number of control points and their location in Ω directly affect the spatial nature of the interval field realizations. As such, these parameters can be either tuned by an analyst to represent the actual spatial uncertainty as closely as possible, or quantified following an inverse approach using indirect measurement data [59,55]. This technique is mostly suited for modelling spatial interval uncertainty in case of non-homogeneous, localised spatial uncertainty, as the definition and construction of the interval field requires no assumptions on isotropy.

Local interval field decomposition was introduced by the authors in [101, 100] and starts also from the explicit formulation of the interval field, as introduced in eq. (19). The spatial complexity of the interval field realizations is limited by imposing an upper bound to their gradients.
Specifically, four global non-deterministic parameters are defined to bound all realizations $\boldsymbol{x_{F,j}}$ of the interval field $\boldsymbol{x^I}(\mathbf{r})$

$$\underline{\mu}_x \leq \mu_{x^I} \leq \overline{\mu}_x \tag{23a}$$

$$\forall \mathbf{r} \in \Omega : \boldsymbol{x_{F,j}} - \mu_{x^I} \leq \boldsymbol{s}_{x,max} \tag{23b}$$

$$\forall \mathbf{r} \in \Omega : \mu_{x^I} - \boldsymbol{x_{F,j}} \geq -\boldsymbol{s}_{x,max} \tag{23c}$$

$$-\frac{\partial x}{\partial \mathbf{r}}\Big|_{max} \leq \frac{\partial \boldsymbol{x_{F,j}}}{\partial \mathbf{r}} \leq \frac{\partial x}{\partial \mathbf{r}}\Big|_{max} \tag{23d}$$

with $\boldsymbol{s}_{x,max}$ the maximum absolute value of the deviation from the mean value. In practice, this achieved by defining the base functions $\boldsymbol{\psi_i(r)}$ as identically shaped, piecewise second order polynomial functions for each separate element, which are located at the element midpoints [101, 100].
The method provides the analyst with an intuitive tool to model the spatial dependency of the interval field using a limited set of intuitive parameters. However, a major disadvantage is computational cost as the dimension of the space spanned by the uncertain input parameters is equal to the number of elements in the model. This is particularly problematic in the case of industrially sized FE models containing up to millions of DOF. Recently, also a method to construct such base functions from a limited set of measurement data was introduced very recently [102].

2.3.2 Affine arithmetical interval fields

To extend the concepts of affine arithmetic for modeling dependencies in intervals to modeling spatial uncertainty, Sofi and coworkers [180, 178, 181, 179] introduced a dimensionless interval field $\boldsymbol{B^I}(\mathbf{r})$ with unit range (i.e. $\boldsymbol{\Delta B}(\boldsymbol{x}) < 1$) in the definition of the parameter interval field $\boldsymbol{x^I}(\mathbf{r})$ via:

$$\boldsymbol{x^I}(\mathbf{r}) = \mu_{x^I}\left(1 + \boldsymbol{B^I}(\mathbf{r})\right) \tag{24}$$

which is related to the deviation $\boldsymbol{s_x^I}(\mathbf{r})$ from the mean function via:

$$\boldsymbol{s_x^I}(\mathbf{r}) = \mu_{x^I} \cdot \boldsymbol{B^I}(\mathbf{r}) \tag{25}$$

Subsequently, they define a deterministic, symmetric, non-negative, bounded function $\Gamma_B(\mathbf{r}_i, \mathbf{r}_j),\ \mathbf{r}_i, \mathbf{r}_j \in \Omega$, based on this dimensionless interval field $\boldsymbol{x^I}(\mathbf{r})B\mathbf{r}$ as:

$$\Gamma_B(\mathbf{r}_i, \mathbf{r}_j) = mid\left(\boldsymbol{B^I}(\mathbf{r_i}) \cdot \boldsymbol{B^I}(\mathbf{r_j})\right) \tag{26}$$

with $mid(\cdot)$ an operator that returns the midpoint of the interval between the brackets. Note that this function only gives the correct result when extra unitary intervals, as defined in eq. 16, are used in order to prevent the *dependency phenomenon*. Sofi and Muscolino argue in [179] that $\Gamma_B(\mathbf{r}_i, \mathbf{r}_j)$ can be regarded as a possibilistic counterpart for the stochastic auto-correlation function that is used for describing the auto-covariance in a random field [180, 178, 181, 179]. Therefore,

a Karhunen-Loève-like decomposition is applied to $\Gamma_B(\mathbf{r}_i, \mathbf{r}_j)$, where the dimensionless interval function $\boldsymbol{B}^{\boldsymbol{I}}(\mathbf{r})$ is expanded as a N-truncated summation series of deterministic functions and extra unitary intervals:

$$\boldsymbol{B}^{\boldsymbol{I}}(\mathbf{r}) = \sum_{i=1}^{N} \sqrt{\lambda_i} \boldsymbol{\psi}_i(\mathbf{r}) \hat{e}_i^I \tag{27}$$

λ_i and $\psi_i(\mathbf{r})$ are respectively the eigenvalues and eigenvectors corresponding to the solution of following eigenvalue problem:

$$\int_{\Omega} \Gamma_B(\mathbf{r}_i, \mathbf{r}_j) \psi_i(\mathbf{r}_i) d\mathbf{r} = \lambda_i \boldsymbol{\psi}_i(\mathbf{r}) \tag{28}$$

which is analogous to the homogeneous Fredholm equation of the second kind that is often encountered in the context of random fields [14], be it that the autocorrelation function is replaced by $\Gamma_B(\mathbf{r}_i, \mathbf{r}_j)$. As such, the interval field is given as:

$$\boldsymbol{x}^{\boldsymbol{I}}(\mathbf{r}) = \mu_{x^I} \left(1 + \sum_{i=1}^{N} \sqrt{\lambda_i} \boldsymbol{\psi}_i(\mathbf{r}) \hat{e}_i^I \right) \tag{29}$$

However, note that by replacing the independent, identically distributed random variables in the truncated KL series expansion with interval variables, the optimal convergence properties of the expansion, as described in [186], are no longer guaranteed to hold.

3 Fuzzy and fuzzy field finite element method

3.1 Fuzzy numbers and membership functions

The fuzzy number description of uncertain model parameters is based on the *fuzzy set* concept, as introduced by Zadeh [224] as a tool to scientifically represent vague linguistic information, and is a natural extension of the interval concept. An interval is defined by crisp bounds on the *membership* of a parameter in the interval (i.e., the parameter is either a member of the interval or not). A fuzzy set extends this principle by introducing a *membership level*, which expresses the degree to which a parameter is thought to be encapsulated by the bounds of an interval. It thus provides a gradual transition from the linguistic statement "the parameter lies completely outside the interval" to "the parameter lies completely within the interval". The membership of each element x in the domain X with respect to the fuzzy set $\hat{x}$ is described by the *membership function* $\eta_{\hat{x}}(x) : X \mapsto [0; 1]$:

$$\hat{x} = \{(x, \eta_{\hat{x}}(x)) \mid x \in X; \eta_{\hat{x}}(x) \in [0; 1]\} \tag{30}$$

In case $\eta_{\hat{x}}(x) = 1$ (i.e., the membership level is 1), x is certainly a member of the fuzzy set $\hat{x}$. On the contrary, when $\eta_{\hat{x}}(x) = 0$, x is definitely not a member of $\hat{x}$. When $0 < \eta_{\hat{x}}(x) < 1$, the membership is uncertain. Different types of membership functions are applicable for fuzzy analysis, with triangular and Gaussian membership functions being the most popular. When multiple fuzzy parameters are considered, a *joint membership function* $\eta_{\hat{\boldsymbol{x}}}(x_1, x_2, \cdots, x_k)$ is defined as:

$$\eta_{\hat{\boldsymbol{x}}}(x_1, x_2, \cdots, x_k) = \min\left(\eta_{\hat{x}_1}(x_1), \eta_{\hat{x}_2}(x_2), ..., \eta_{\hat{x}_k}(x_k)\right) \tag{31}$$

Zadeh's extension principle [226,228,227,225] provides the necessary tools to find the membership function $\eta_{\hat{y}}(y)$ of a fuzzy output quantity $\hat{y}$, given k fuzzy input parameters $\hat{x}_1$,$\hat{x}_2$,...,$\hat{x}_k$ of the numerical model that is used to approximate the solution of the design problem under consideration.

$$\eta_{\hat{y}}(y) = \begin{cases} \sup_y \left(\eta_{\hat{\boldsymbol{x}}}(x_1, x_2, \cdots, x_k)\right) & \text{if} \quad \exists y = m(x_1, x_2, ..., x_k) \\ 0 & \text{otherwise} \end{cases} \tag{32}$$

Following the extension principle, the solution to a fuzzy arithmetical numerical model requires a multidimensional optimization scheme, possibly imposing a considerable computational cost. Therefore, other, less costly methods for the solution of the fuzzy propagation problem have been proposed in recent years. An excellent and complete overview of the application of fuzzy arithmetic to non-deterministic numerical simulations is given in the book of Hanss [90].

3.2 Propagation of Fuzzy non-determinism

3.2.1 α-cut method

As concerns the numerical propagation of Fuzzy non-determinism, the α-cut method provides an extension of interval methods towards solving a numerical model having fuzzy uncertain parameters. The membership function $\eta_{\hat{x}_i}(x_i)$ of the i^{th} input parameter is subdivided into N_α equally spaced intervals of width $\Delta\mu = \frac{1}{N_\alpha}$. This yields an interval for each membership level η_{α_j}:

$$x_{i,\alpha}^I = \{x_i \in X_i \mid \eta_{\hat{x}_i}(x_i) \geq \alpha\} \tag{33}$$

with the discrete values of the $N_\alpha + 1$ intervals equal to:

$$\eta_{\alpha_j} = \frac{j}{N_\alpha}, \qquad j = 0, \cdots, N_\alpha \tag{34}$$

An α-cut as such contains all elements x_i that *at least* belong to $\hat{x}$ *at least* to the degree α. Subsequently, an interval analysis is performed on these intervals. According to Moens and Hanss [132], it can be shown that the obtained output intervals are intersections of the output membership functions at membership level α, and are therefore an α-cut of the output membership function. The α-cut procedure therefore provides a discretization of the membership function $\eta_{\hat{y}_i}(y_i)$, of which the resolution depends on the α-cut discretization of the input membership functions $\eta_{\hat{x}_i}(x_i)$. The interval propagation methods that are presented in section 2.2 are then straightforwardly applied to the propagation of each α-cut. A visualisation of the technique is given in figure 2, where fuzzy parameters $\hat{x}_1$ and $\hat{x}_2$ are propagated to two fuzzy responses $\hat{y}_1$ and $\hat{y}_2$ following the α-cut procedure. Applications of the α-cut method for the propagation of fuzzy parametric uncertainty are given e.g., by [141].

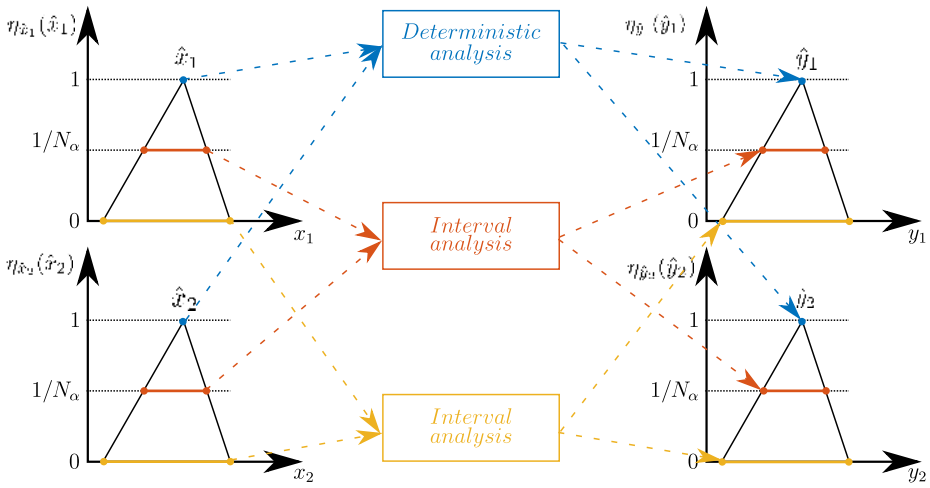

Fig. 2 Graphical representation of the α-cut procedure, applied to two fuzzy input parameters $\hat{x}_1$ and $\hat{x}_2$ of a monotonic model $m()$, for the computation of two fuzzy responses $\hat{y}_1$ and $\hat{y}_2$.

3.2.2 Transformation method

The transformation method was introduced by Hanss [87,89,90] as an extension to the vertex method in the context of propagating fuzzy uncertainty through a possibly non-monotonic numerical model. A *reduced transformation method*, *general transformation method* [87] and an *extended transformation method* [89] have been introduced. In general, the transformation method provides an efficient numerical procedure for solving the optimization problem that is associated with the extension principle (eq. (32)).

As a first step, the membership functions $\eta_{\hat{x}_1}(x_1), \eta_{\hat{x}_2}(x_2), \cdots, \eta_{\hat{x}_k}(x_k)$ of k fuzzy input parameters $\hat{x}_1, \hat{x}_2, \cdots, \hat{x}_k$ are decomposed into N_α intervals $x_{i,j}^I$ with $i = 1, \cdots, k$ and $j = 0, \cdots, N_\alpha$ at each α-level of the fuzzy variable using eq. (33). Subsequently, these input intervals $x_{i,j}^I$ are transformed into arrays $\hat{X}_{i,j}$. A distinction is made, based on the monotonicity of the numerical model $m()$. In general, the *general* form of the transformation method should be used. However, in case of strict monotonicity, the less computationally intensive *reduced* form of the transformation method can be used. The *reduced* form can also be used when only one fuzzy parameter is considered. This choice determines the structure of the transformed arrays $\hat{X}_{i,j}$.

The reduced transformation method constructs a hyper-cubic approximation in $\mathbb{R}^k$ for each α-cut, and the vertices of this hypercube are propagated through the deterministic model. This in fact corresponds to applying the vertex method for each α-cut of the fuzzy parameters. The obtained responses are then recombined into a fuzzy number by assigning the correct α-level to them, while ensuring convexity of the fuzzy number. The general transformation method on the other hand is also capable of dealing with non-monotonic models $m()$ by dividing each α-cut into $N_\alpha - j + 1$ intervals, where the bounds coincide with the midpoints of the intervals of the higher α-level. The vertices of these intervals are then combinatorially propagated while keeping track of their mutual relation. The resulting

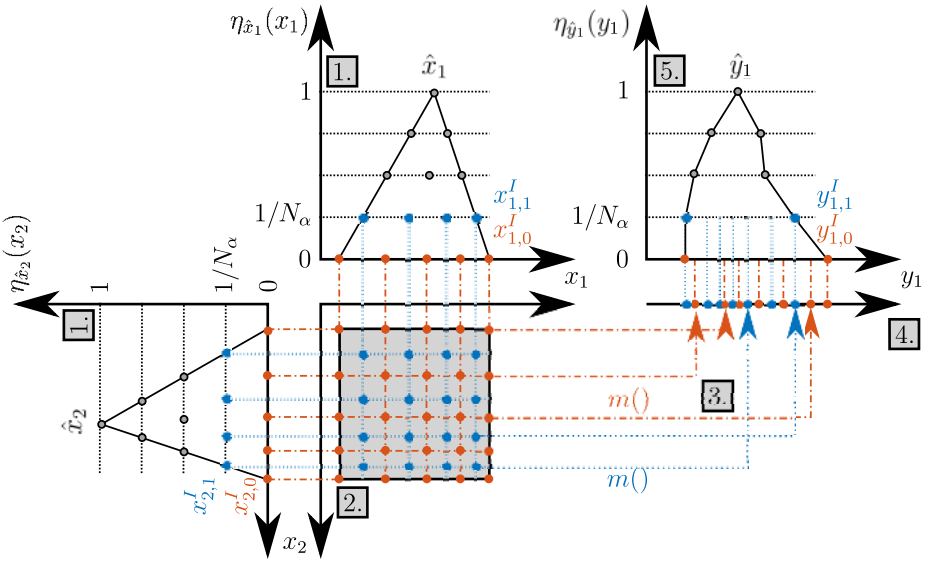

Fig. 3 Graphical representation of the general transformation method, applied to two fuzzy input parameters $\hat{x}_1$ and $\hat{x}_2$ of a non-monotonic model $m()$, for the computation of a fuzzy response $\hat{y}_1$.

fuzzy numbers are then analogously obtained as using the reduced transformation method.

The general transformation method is illustrated in figure 3. This figure shows two triangular fuzzy numbers $\hat{x}_1$ and $\hat{x}_2$, which are parameters of a non-monotonic function $m()$. The subsequent steps for the transformation method are indicated as the corresponding numbers in the grey boxes. The fuzzy numbers are first discretized into $N_\alpha + 1$ intervals $x^I_{1,j}$ and $x^I_{2,j}$ for $j = 0, \cdots, N_\alpha$. The vertices of these intervals are then combined in a combinatorial way, which can be visualized as a rectangular grid in $\mathbb{R}^2$ for each separate α-cut. The general transformation method is used since $m()$ is non-monotonic. The third step consists of propagating each vertex in the rectangular grid of each α level through $m()$ to the response variable y_1. In figure 3, this is illustrated as the blue and orange arrows. The non-monotonicity of $m()$ is evident from the fact that an increase in e.g. x_2 first increases y_1 after which the value decreases again. In the fourth step, the output intervals are recomposed for each membership level. Finally, the fuzzy output variable $\hat{y}_1$ is recomposed from the output intervals. In this example, only the steps for the 0^{th} and 1^{st} membership level (i.e. $\mu = 0$ and $\mu = 1/N_\alpha$) are illustrated.

Additionally to obtaining the fuzzy response variables $\hat{\boldsymbol{y}}$ of a numerical model $m()$, parametrized by fuzzy input variables $\hat{\boldsymbol{x}}$, both the reduced and general transformation method also provide a degree of influence of each $\hat{x}_i,\ i = 1, \cdots, k$ on each $\hat{y}_i,\ i = 1, \cdots, d$, [87,92]. Since for each fuzzy parameter $\hat{x}_i,\ i = 1, \cdots, k$ the same combinations of values are tested for each α-level, the effect of each fuzzy parameter is tested independently of all other parameters, enabling the possibility of determining the extent to which it contributes to the overall uncertainty. The degree of influence is also referred to as *gain factor* [88]. Additionally, Hanss and Klimke show that also the total differential can be used, when the model functions

$m()$ are available in analytical form, which in most cases leads to similar results [92].

Note however that $\sum_{j=1}^{N_\alpha} j^k$ deterministic function evaluations are needed for a fuzzy model evaluation, making the general transformation method very demanding when a fine α-level discretization is used in conjunction with a deterministic model having a high number of fuzzy parameters. When the model $m()$ is strictly monotonic, this is reduced to $1 + N_\alpha \cdot 2^k$ model evaluations. This however still proves to be intractable when a high number of fuzzy-valued parameters are considered in the model due to the exponential scaling of the number of necessary deterministic model evaluations.

In order to relieve this computational burden, the short transformation method was introduced by Donders et al. [43,44] as method for reconstructing fuzzy frequency response functions (FRF) within limited computational burden. The method is founded on the assumption that sampling deterministic points on a single diagonal of the input hypercube (the so-called *critical diagonal*) is sufficient for assessing the FRF uncertainty. As such, $1 + 2^k + 2 \cdot (N_\alpha - 1)$ deterministic model evaluations are needed. However, determining the *critical diagonal* in the work of Donders et al. [43,44] follows a procedure where $2^k + 1$ model evaluations at the lowest membership level are performed, which still becomes intractable when the number of parameters becomes too large.

3.3 Fuzzy fields

The concept of interval fields can easily be extended towards fuzzy fields. Considering the explicit interval field definition, as presented in eq. (19). When the n_b interval scalars $\boldsymbol{\alpha^I}$ are replaced by n_b fuzzy numbers, a fuzzy field is obtained:

$$\hat{\boldsymbol{x}}(\mathbf{r}) = \sum_{i=1}^{n_b} \hat{\boldsymbol{\alpha}} \boldsymbol{\psi}(\mathbf{r}) \tag{35}$$

where $\boldsymbol{\psi}(\mathbf{r})$ can analogously be defined as explained for interval fields and $\hat{\boldsymbol{\alpha}}$ is a vector of fuzzy numbers with joint-membership function $\eta_{\hat{\boldsymbol{\alpha}}}(\alpha_1, \alpha_2, \ldots, \alpha_{n_b})$. The only applications of fuzzy fields to the knowledge of the authors is in a geo-hydrodynamic case [203], and more recently in a study towards types of dependence in fuzzy analysis [75].

4 Application of different concepts for the modeling of non-determinism

In this section, the applicability of the probabilistic and possibilistic concept for the forward and inverse quantification of parametric non-determinism is compared and discussed. First, both philosophies are compared in the context of forward propagating the non-deterministic parameters through the numerical model (i.e. quantification of the non-determinism in the model responses as a result of non-deterministic model parameters). This comparison is made, based on the nature of the non-determinism, the ability to account for dependence and correlation, and the design phase in which the methods are applied. Secondly, the application of

both philosophies for the identification and quantification of uncertainty in the parameters of the model based on measured system responses, is compared in terms of necessary data, computational cost and obtained information. Hereto, first the relevant terminology is repeated.

4.1 Terminology

As mentioned in the introduction, computing a numerical approximation of a set of differential equations is prone to many sources of non-determinism. Therefore, an extensive amount of literature has been dedicated to this subject. In literature, a large number of terms such as *error*, *uncertainty* and *variability* are used interchangeably, and the link to the underlying nature of the non-determinism is often rather nebulous. Therefore, before elaborating on the details of the probabilistic and possibilistic frameworks for the representation and quantification of non-determinism, this section aims at giving a concise but clear overview of the corresponding terminology that is commonly found in literature. In this section, the terminology that was proposed by Oberkampf et al. [157] is presented with the refinements that were made by Moens and Vandepitte [134], as well as the terminology that was proposed by Elishakoff [48]. Finally, the distinction between *aleatory* and *epistemic* uncertainty is explained, as this has some implications for inverse UQ methods.

4.1.1 Variability, uncertainty and error

According to Oberkampf et al. [157], *variability*, *uncertainty* and *error* are respectively defined according to definitions 1 to 3.

Definition 1 *Variability is the variation which is inherent to the modeled physical system or the environment under consideration.*

In general, a variable quantity is a quantity that differs between nominally identical parts or from place to place or time to time within the same realization of a part. The former is also commonly referred to as *inter-variability*, whereas the latter is referred to as *intra-variability* [171]. Some examples of variability are manufacturing tolerances, measurable scatter in the mechanical properties of a material or identifiable randomness in the working conditions of the considered structure. Elishakoff also refers to this type of non-determinism as *randomness* [48].

Definition 2 Uncertainty is defined as a potential deficiency in any phase or activity of the modeling process that is due to a lack of knowledge.

Uncertainty means that there exists a deterministic value for the model parameter under consideration, but it is not or insufficiently accurately known. The word *potentially* indicates that this deficiency does not necessarily occurs during the modelling process. In the context of numerical modelling, usually parameter uncertainty and uncertainty stemming from the modelling approximations that were used in the idealization of reality are considered in literature (see e.g. [67, 157, 206, 111, 184]). The former is a direct result of uncertainty on the parameters of the

numerical model. These can be insufficiently characterized material parameters, naturally varying loading situations or parameters that are hard to quantify such as damping values in a dynamic model. The latter refers to approximations that were deliberately made by the analyst to e.g., reduce the model complexity (such as the discretization of a Finite Element model) or assumptions on the linearity of the simulated system, or unintended simplifications due to a lack of understanding [117]. Elishakoff refers to uncertainty as either *imprecision* or *vagueness*, when the non-determinism is respectively caused by a lack of knowledge or an ambiguous description of the parameter [48]. Examples of the latter are linguistic statements such as a *stiff* joint or *thin* plate.

Definition 3 An error is defined as a recognizable deficiency in any phase of modeling or simulation that is not due to a lack of knowledge.

The most obvious source of errors are human errors in the modeling process of the physical system under consideration. Besides, also modeling errors caused by the mathematical description of the physical system or errors such as rounding, truncation, incomplete convergence due to the numerical procedure are considered in this category. Sometimes, errors in the coding of the mathematical model are also considered as a part of the numerical model uncertainty [109]. This is however very hard to quantify, and is moreover more a problem of verifying the computer code [158]. This verification is thoroughly discussed in the Los Alamos report on model validation and verification [194]. Therefore, modeling errors should not be taken into consideration in the modelling of the non-determinism.

Moens and Vandepitte [134] made a refinement on the definition of variability and uncertainty, as they are not necessarily mutually exclusive. A variability can be expressed as a range of possible values and the likelihood of each value within this range. In this context, Moens makes a distinction between *certain variability* and *uncertain variability*. An uncertain variability occurs when no or limited statistical information is available on the range or likelihood of each value within this range of the variable parameter. This is especially relevant when modeling the non-determinism as stochastic processes or random fields, as usually a large amount of statistical information is needed in order to construct an objective and credible probabilistic description of the variability.

An analogous thought experiment can be made for uncertainties. An *invariable uncertainty* has by nature a deterministic value, which cannot be accurately modeled due to a lack of knowledge. Conversely, a *variable uncertainty* is an uncertain parameter which exhibits variability.

4.2 Description and propagation of non-determinism

4.2.1 Type of non-determinism

Based on the nature of the non-determinism, the distinction between uncertain variabilities, certain variabilities and invariable uncertainty that was made in section 4.1, is employed. According to Moens and Vandepitte, these should be treated as follows [134]:

Certain variability For a *certain variability*, the probabilistic concept in its *frequentist* interpretation is highly suited, as available information on the range of possible values and likelihood of each value within this range can perfectly be described using a PDF. However, all necessary information for the construction of a JPDF, such as the likelihood of, and correlation between all non-deterministic quantities should be available in order to prevent an inaccurate or unreliable assessment of the non-deterministic model behaviour [134]. Therefore, application of this theory in practice often proves to be inconvenient, due to the large amount of data necessary for the identification of a PDF or the corresponding statistical moments [50].

The interval concept on the other hand only requires a range of possible values. A conversion from a probabilistic description of a certain variability to an interval description is therefore straightforward when a bounded PDF is used. In this case, the likelihood of each value within this range is lost. In the case when an unbounded PDF (e.g., a Gaussian PDF) is used, realistic bounds should be chosen by the analyst. Under the assumption that the likelihood in the tails is too low to be of realistic interest, this is usually obtained by selecting k standard deviations from the mean, with k usually larger than 3. Note that this introduces subjectivity in the analysis, as this truncation of the range of possible values that are attributed to the variable parameter is largely based on the expert knowledge of the analyst.

In the context of Fuzzy analysis of certain variabilities, some methods have been proposed to derive a fuzzy number membership function (interpreted as *plausibility density function*) from a probability density function [29,47,161]. The conversion is based on the consistency principle, which states that the plausibility of an event is greater than or equal to its probability.

Hence, even when the complete PDF $f_X(x)$ is known, an infinite number of possibilistic representations exist. Therefore, the conversion from a probability density function to a fuzzy membership function always introduces subjectivity, based on the judgment of the analyst, and should only be interpreted in a subjective sense.

Uncertain variability Uncertain variabilities or variable uncertainties can be modeled as well using the *frequentist* probabilistic framework. However, in order to obtain a reliable representation of the uncertain variability, the analysis should be performed using different PDF functions. In theory, all possible PDF functions should be regarded. In practice however, the analyst selects a few probabilistic models based on engineering judgment and expert knowledge on the non-deterministic quantities [134]. In this context, a review of literature shows that especially in industrial applications, many authors assume the data to follow a Gaussian distribution [200]. This can be a severe misjudgment of the non-deterministic data structure, resulting in an unrealistic assessment of the non-deterministic model behavior, and consequently, the design quality. Alternatively, also the maximum entropy principle can be used for constructing the PDF function, as this provides the least informative prior [103,104].

The interval concept on the other hand is perfectly suited for the description of uncertain variabilities, as no information on the likelihood of each value within the range of possible values is needed. As such, considerably less objective information is necessary to construct the interval description of the uncertain variability. However, when no or insufficient objective information on the actual range of parameter values is present, subjectivity can also be incorporated by the analyst. This might

happen in e.g. early design stages, when many decisions on the final geometry still have to be made, or when dealing with complicated joint connections that are simplified in the modelling process. In the former case, the interval description as such corresponds with the range of values that are deemed possible by the analyst in that specific stage of the design. As the design process continues and more information on the final geometry becomes available, the interval boundaries are as such adapted. In the latter case, the interval description is used to account for the effect of approximations that were used to model the complicated joints. As such, the boundaries do not change when the design process advances. However, the subjectivity that is present in the latter estimation can be alleviated by using indirect measurements and appropriate uncertainty quantification techniques.

Finally, for the analysis of uncertain variability, also hybrid techniques have been introduced such as imprecise probabilities [68–70,197,9,216,77], fuzzy randomness [141,142,136,139,138,137,12] and methods based on Dempster-Shafer theory [36,174,159,196,172,2]. Basically, these techniques employ Bayesian statistical descriptors, intervals or fuzzy sets to describe a class of CDF functions, lying between two extreme CDF functions that are constructed by superimposing these non-deterministic descriptions on the first few statistical moments of the probabilistic description of the uncertain variability. Especially imprecise probabilities currently gain a lot of attention [10]. Also extensions towards imprecise field descriptions have been proposed recently [40].

Invariable uncertainty The representation of invariable uncertainty using the probabilistic approach in a frequentist interpretation is not recommended. Moens and Vandepitte state that *"... for an invariable uncertainty the information contained in the random quantity does not represent the variation of the quantity in the final product, since by definition the invariable uncertainties are considered to be constant..."* [134]. This means that representing the lack of knowledge on the value of an invariable quantity as a variation herein, results in an unrealistic non-deterministic model behavior, and consequently unreliable and inaccurate model results. In this context, Teichert [193] also indicates that for the representation of invariable uncertainty, care should be taken in employing the probabilistic concept. When the lack of knowledge on the modeled quantity is represented as a PDF, the variability attributed to that parameter does not represent a physical variability. Therefore it should also not be interpreted as such. This perfectly coincides with the *Bayesian* interpretation of probabilistic non-determinism. Therefore, following a Bayesian interpretation, it is possible to describe an invariable uncertain parameter. However, this description might be highly subjective.

When applying interval or fuzzy methods for the representation of invariable uncertainty is completely subjective and can only be based on the expert opinion of the analyst. As such, it should only be interpreted as a subjective estimation of the model responses. Specifically for fuzzy methods, the α-cut procedure can be regarded as a large scale sensitivity analysis.

As a final remark, care should be taken when a model is used containing both variable and uncertain quantities. In that case it is imperative to distinguish between both interpretations and treat them accordingly in the numerical procedure as described by Hoffman and Hammonds [95].

4.2.2 Multivariate and spatial non-determinism

The probabilistic framework for uncertainty representation, be it in a frequentist or Bayesian interpretation, is highly suited for the description of multivariate non-deterministic quantities. This is a direct result from the explicit definitions that are directly available in this framework to describe mutual dependence and covariance. Probabilistic methods are also directly applicable in the context of non-deterministic quantities that do not have constant statistical descriptors in the time and/or spatial domain through the definition of auto-covariance and auto-correlation. Since these probabilistic methods for the description of multivariate and spatial non-determinism already have reached a high degree of maturity, they are already widely applied in various domains ranging from geotechnical applications [119, 96, 41, 229], the study of (the effect of) random material properties [223, 128, 27] or the evaluation of flow dynamics [213, 169]. As such, probabilistic random fields are often considered as the standard approach to model spatial or multivariate non-deterministic quantities.

However, some critical remarks have to be made when using the random field concept for the representation of spatial non-determinism in a practical engineering context. When the complete covariance function is known (e.g. by fitting it to an elaborate set of objective measurement data), discretization of the random field is rather straightforward and can be applied without resorting to series expansions for the representation of the random field covariance. However, in order to obtain the complete covariance structure of the random field, data with a high statistical and spatial resolution are needed. The argumentation for the former prerequisite is based on the need for an objective estimation of the statistical structure of the non-determinism, whereas the latter is of specific importance to ensure that the spatial effect is accurately quantified.

In realistic engineering practice such data are generally not available as the necessary experimental campaign is both time consuming and very costly. Therefore, the analyst usually has to resort to subjective assumptions on the probabilistic nature of the spatial non-determinism. First, hypotheses on the non-deterministic nature of the spatially uncertain parameter considering the most applicable probability distribution function and spatial isotropy and homogeneity need to be made. Moreover, the covariance of the random field is usually modeled using a predefined auto-covariance function. The spatial behavior of this function is largely determined by the *correlation length*. The value of this correlation length is in practice usually chosen subjectively, based on the engineering judgment of the analyst.

The interval framework on the other hand is less suited for the description of multivariate non-deterministic quantities, as intervals are by definition independent. As such, the description of dependence and correlation are not readily available within the interval framework. Therefore, the *pure* interval framework will be over-conservative in this context. Moreover, due to the lack of an interval measure for dependence, the description of spatial interval uncertainty proves to be a non-trivial task. Application of interval methods has been mainly illustrated in low dimension problems (see e.g. [218, 129]), but also some more realistic applications have been introduced so far [64, 4, 214].

In the context of spatially coupled interval uncertain parameters, the concept of interval fields provides a solution to some extent. However, the interval field concepts suffer largely from the same problems as their probabilistic coun-

terparts considering the objective modeling of the spatial nature of the uncertain phenomenon. As an example, when applying the inverse distance weighting interpolation technique, subjectivity is present in the selection of the control points and the exponent of the distance weighting. Moreover, the application of interval fields to practical problems is still very scarce in literature (see e.g., [130, 202, 204, 100]). This is however also partially explained by the relatively recent introduction of these techniques as compared to the well-established framework of random fields.

4.2.3 Design phase

In an engineering context, the different non-deterministic concepts all have their own area of application. Specifically, Moens and Vandepitte [134] propose following distinction:

- In an early design phase, when still selecting the most appropriate concept, many design questions are still open. Some model properties are only known vaguely, whereas others are still completely undefined. As such, the non- determinism in the model is mostly caused by uncertainty instead of variability. Therefore, interval and fuzzy methods are more applicable in this stage. Specifically the fuzzy concept is useful as it gives a measure for the sensitivity of the design boundaries. Moreover, it is highly suited to handle linguistic variables.
- Then, as the design evolves further, more decisions on the final design are being made. Therefore, most parameters such as e.g., plate thickness values are known up to a certain range. Uncertainty is in this context still the predominant factor, as the lack of knowledge on the final geometry in general still exceeds the variability that is caused by the production process. Therefore, interval methods are more applicable.
- Finally, as the design is in its final stage, most numerical studies are performed in the context of validation and reliability estimation. Therefore, variability is the most important source of non-determinism. Hence, the probabilistic approach is in this context best suited.

The different formalisms for the description of non-determinism are highly complementary, with the transition between the different concepts being gradual. As such, the final choice of the most appropriate modeling approach should be made by the analyst, based on the considerations that are given above.

5 Inverse approaches for quantifying interval fields

This section deals with the state-of-the-art in the quantification of interval and fuzzy uncertainty that is present in a set of model parameters, denoted respectively $\boldsymbol{x}^{\boldsymbol{I}}$ and $\hat{\boldsymbol{x}}$, based on measurements of the model responses $\tilde{\boldsymbol{y}}_m$. Analogously to the propagation of fuzzy uncertainty, the identification and quantification of fuzzy uncertainty is usually performed using interval techniques for each α-level of the input fuzzy numbers.

5.1 $\mathcal{L}_2$ norm based techniques

Mostly, inverse identification and quantification of both interval and fuzzy uncertainty are based on a squared $\mathcal{L}_2$ norm formulation of the difference between a set of measured responses, obtained by performing repeated experimental tests on the structure under consideration in close correspondence to the numerical model, and the prediction of the numerical model that has interval or fuzzy uncertain parameters. In the remainder, the methods are explained in an interval context, keeping in mind that they just have to be applied for each membership level in a fuzzy context. Usually, the identification is performed as a two-step process, where first the midpoints of the interval (or fuzzy) uncertain parameters are determined following a deterministic model updating procedure:

$$\min \left(\mu_{\boldsymbol{y}_s^I}(x^I) - \mu_{\boldsymbol{y}_m^I}\right)^T W \left(\mu_{\boldsymbol{y}_s^I}(x^I) - \mu_{\boldsymbol{y}_m^I}\right) \tag{36}$$

where $\mu_{y_m^I}$ denotes the midpoint (or statistical average) of the measurement vector set and W is a weighting matrix that can be used to normalise the different terms in the response vectors. $\boldsymbol{y_s^I} = m(\boldsymbol{x^I})$ is the interval result of propagating the parametric interval uncertainty $\boldsymbol{x^I}$ through the numerical model $m()$.

Examples of methods that first use a deterministic updating step in the identification and quantification of interval (or fuzzy) uncertainty can be found in e.g. [81, 80, 82, 66, 38]. Sometimes, regularization steps are included to prevent ill-posedness of the updating problem [3, 195].

This deterministic model updating step is then followed by the actual inverse identification of the interval (of fuzzy) description of the uncertain model parameters. The objective that is minimised in this context is expressed as the squared $\mathcal{L}_2$ norm over the difference in interval radii between the intervals on the output parameters of the numerical model and intervals that are fitted around each measured response [38]:

$$\min \left(\Delta \boldsymbol{y}_s(x^I) - \Delta \boldsymbol{y}_m\right)^T W \left(\Delta \boldsymbol{y}_s(x^I) - \Delta \boldsymbol{y}_m\right) \tag{37}$$

Alternatively two separate squared $\mathcal{L}_2$ norm formulations are constructed and summed, expressing respectively the difference between the upper and lower bounds of these intervals [173, 66, 63, 17]:

$$\begin{aligned} \min &\left(\underline{\boldsymbol{y}}_s(x^I) - \underline{\boldsymbol{y}}_m\right)^T W \left(\underline{\boldsymbol{y}}_s(x^I) - \underline{\boldsymbol{y}}_m\right) + \\ &\left(\overline{\boldsymbol{y}}_s(x^I) - \overline{\boldsymbol{y}}_m\right)^T W \left(\overline{\boldsymbol{y}}_s(x^I) - \overline{\boldsymbol{y}}_m\right) \end{aligned} \tag{38}$$

Different optimization algorithms have been proposed in this context. Gabriele and Valente [74] solved eq. (36) - (38) using an interval Branch & Bound algorithm named *Interval Intersection Method*, which was first presented by Hansen et al. [85]. The bounding part of the algorithm is performed by first checking the inclusion monotonicity of the result of the interval FE computation, as well as that the interval uncertain measurements are included in the result of the interval FE model. They also compared the method to (deterministic) sensitivity based model updating, showing that it is computationally less efficient in a deterministic model updating setting [73]. Moreover, practical implementations are only

shown for interval scalar uncertainty, which was moreover limited to only two parameters. Alternatively, Fedele et al. [66,217] use adjoint optimization methods in conjunction with coarse-to-fine regularization [54]. Erdogan and Bakir used in this context a hybrid combination of a Genetic Algorithm and Particle Swarm based on a perturbation-based propagation, which was implemented on a distributed memory parallel cluster [173]. Boulkaibet et al. [17] on the other hand used meta-heuristic optimizers such as Ant Colony Optimization [46] and Particle Swarm Optimization [108], leading to a heavy computational burden. Fang et al. [63] performed the $\mathcal{L}_2$ norm minimization by introducing an interval response surface model. Finally, Deng et al. [38] used radial basis function neural networks as a surrogate for the identification to limit the computational expense of the inverse identification.

By first introducing a deterministic model updating step in the identification, the number of parameters that can be identified is ideally maximally equal to the number of measured responses to ensure uniqueness of the solution. Moreover, when the responses are highly correlated, even less uncertain parameters can be identified. This is caused by rank deficiency in the Jacobian (and consequently the Hessian) matrices of commonly used iterative non-linear optimization algorithms such as the Gauss-Newton approach [156] when there are more uncertain parameters than unique data points. This leads to an infinite number of solutions to the optimization problem [147]. Minimum norm solutions have been proposed in the context of a deterministic model updating context [156], alleviating this problem. However, it is not guaranteed that this minimum norm solution also corresponds to the physical solution of the problem, as this is merely a mathematical tool to alleviate the ill-posedness of the problem.

Moreover, the solution of the problem as such becomes very sensitive to small modeling errors due to an inaccurate inversion of the Hessian [86], when it becomes near-singular. Finally, as this deterministic model updating procedure precedes the interval methods, special care should be taken to avoid such problems as to prevent offsetting the interval variables with respect to their actual value.

5.2 Inverse fuzzy quantification

In the context of fuzzy model updating, Haag et al. [81,80,82] introduced a methodology that is conceptually different as compared to the minimization of the $\mathcal{L}_2$-norm. Since fuzzy numbers are an extension of interval analysis, the method can also be used in an interval context. After first deterministically identifying the midpoints of the fuzzy input parameters $\hat{x}$, a linear map between the fuzzy input parameters and fuzzy responses $\hat{y}$ is constructed. Then, the distance between the boundaries of the α-cut intervals of $\hat{x}$ with the identified midpoint is minimized, while ensuring that the fuzzy FE models still encompasses the spread in the measured responses $\tilde{\boldsymbol{y}}_m$ completely. Moreover, they defined a model validity criterion as a measure for the total uncertainty that is captured by the fuzzy numbers $\hat{\boldsymbol{x}}$ and $\hat{\boldsymbol{y}}$ both at the input and output side of the FE model. The computation of this criterion is based on the concept of relative imprecision [90]. When multiple solutions to the identification procedure exist, the one with the lowest model validity criterion value should be selected [81,80,82].

5.3 Kriging based approach

In the context of interval uncertainty quantification, Khodaparast et al. propose a Kriging predictor meta-model [110]. First, they perform a deterministic model updating procedure (as illustrated in eq. (36)) to identify the interval midpoints. From this, an initial k-dimensional hypercube is constructed. Then, a deterministic set of input parameters is identified by means of deterministic model updating for each separate measurement point and the initial hypercube is adjusted to firmly circumscribe the set of identified model parameters. The method was also illustrated using the AIRMOD test structure [76], and was later extended towards Fuzzy uncertainty quantification [84]. However, in this extension, no measure was taken to ensure convexity of the resulting fuzzy numbers.

5.4 Concluding remarks

In the context of the inverse quantification of scalar interval uncertainty, recently important steps have been made. Techniques based on an $\mathcal{L}_2$ norm minimization provide a first step, but some inherent problems are still there as elaborated, especially in the context of non-uniqueness and ill-posedness of the solution. Some authors alleviate this problem by including regularization in the optimization problem.

Furthermore, none of the introduced methods is able to keep track of dependence between the model responses, as they all either explicitly or implicitly assume a hyper-cubic output domain. Another fundamental issue with this approach is that by representing the scatter in the responses that are grouped in a set of measurement data $\tilde{\boldsymbol{y}}_m$ as an (hyper-cubic) interval vector, the dependency between these responses is neglected completely as intervals are independent by definition. As such, physically infeasible combinations of responses are also considered as belonging to the measurement data set. Moreover, important information that is captured in the dependency between these responses is lost, whereas it serves as a possible solution to the non-uniqueness and ill-posedness of the interval quantification. Finally, by performing this hyper-cubic approximation, it is not possible to quantify coupled interval uncertainty following these methods, e.g., in the context of interval field modeling.

6 An interval approach for inverse interval field quantification

This section presents a recently introduced method for the quantification of spatial interval uncertainty based on a limited set of measured responses of the system. Instead of adapting a hyper-cubic representation of the measurement data and interval finite element model responses, a convex set approach is used that is capable of maintaining linear dependence between the responses. The general overview of this procedure is illustrated in figure 4. The following sections will provide a detailed explanation of each step that is shown in this figure. The ideas discussed here are an overview of methods first presented in [58], [59], [61] and [57].

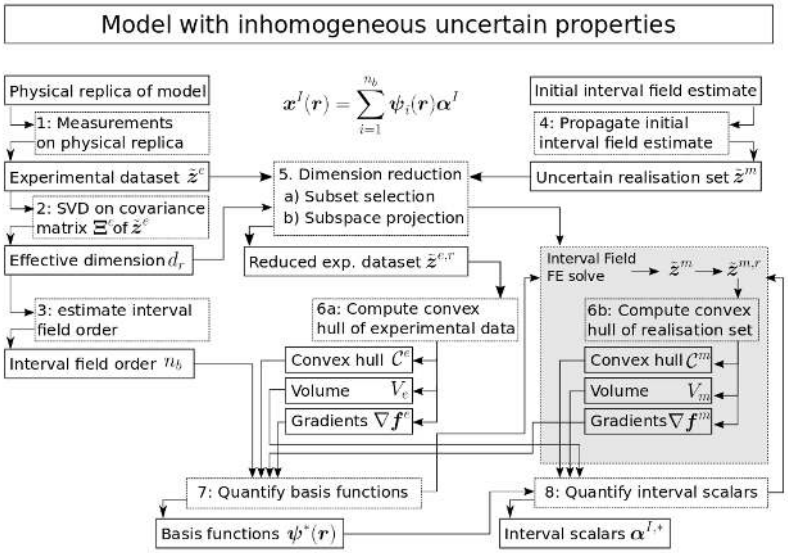

Fig. 4 General overview of the methodology

6.1 Steps 1 & 6(ab): Measurement data and convex hulls

The measurement data that are used for the identification are usually obtained through an experimental procedure where a real-life model is physically tested repeatedly in close relation to the FE model under consideration. The model responses, measured on the j^{th} test replica are grouped in the vector $\boldsymbol{y}_{mj} \in \mathbb{R}^{d_m}$:

$$\boldsymbol{y}_{mj} = [y_{m1},\ y_{m2},\ ...,\ y_{md_m}]^T \tag{39}$$

These responses are subsequently used to construct a measurement set $\tilde{\boldsymbol{y}}_m$, which is defined as:

$$\tilde{\boldsymbol{y}}_m = \left\{ \boldsymbol{y}_{mj} \mid j \in 1, ..., t \right\} \tag{40}$$

with the cardinality of $\tilde{\boldsymbol{y}}_m$ equal to t, the number of conducted physical experiments. For the sake of simplicity but without any further limitation to the validity of the proposed approach, it is assumed here that the experimental procedure gives information on the same response quantities which are modeled in the simulation model. In general, this may not be true and it would imply that a suitable data reduction or interpolation technique should be selected for an objective and correct comparison between measurement and simulation data.

Central to the development of the inverse interval field quantification method is the representation of the uncertainty in the measurement data set $\tilde{\boldsymbol{y}}_m$ and the uncertainty that is represented by the uncertain realization set $\tilde{\boldsymbol{y}}_s$, as introduced in eq. (20) as a convex hull. Indexes m and s indicate that $\boldsymbol{y}$ is considered as belonging to respectively the measurement data or the result of the interval field finite element model ($s$imulation). In general, the convex hull of a finite set of vectors in Euclidean space is defined as the smallest possible convex set, containing

the vectors in $\tilde{\boldsymbol{y}}_s$ and it is the intersection of all possible convex sets containing these vectors. For the realization set, this is explicitly defined as:

$$\tilde{\boldsymbol{y}}_s^C = \left\{ \sum_{j=1}^{q} \beta_j \boldsymbol{y}_{sj} \mid (\forall j : \beta_j \geq 0) \wedge \sum_{j=1}^{q} \beta_j = 1 \; ; \; \boldsymbol{y}_{sj} \in \tilde{\boldsymbol{y}}_s \right\} \tag{41}$$

where $\boldsymbol{\beta}$ is a vector of weighting factors, such that all β_j are non-negative and sum to one [13]. In the specific case when $\tilde{\boldsymbol{y}}_s$ is computed following a global optimization approach (see also eq. 18), $\boldsymbol{y}^{\boldsymbol{I}}$, the hyper-cubic approximation of $\tilde{\boldsymbol{y}}$, and $\tilde{\boldsymbol{y}}_s^C$ span the same uncertain solution set. The convex hull $\tilde{\boldsymbol{y}}_m^C$ of $\tilde{\boldsymbol{y}}_m$ is similarly calculated as:

$$\tilde{\boldsymbol{y}}_m^C = \left\{ \sum_{j=1}^{t} \beta_j \boldsymbol{y}_{mj} \mid (\forall j : \beta_j \geq 0) \wedge \sum_{j=1}^{t} \beta_j = 1 \right\} \tag{42}$$

This concept is illustrated in figure 5, where an interval field $\boldsymbol{x}^{\boldsymbol{I}}(\mathbf{r})$ with $n_b = 3$ input interval scalars is propagated using the transformation method yielding $q = 2^3 = 8$ deterministic realizations. The figure shows the cross-section of the convex hull $\tilde{\boldsymbol{y}}_s^C$ with the $\{y_i, y_j\}$ plane of two different arbitrary model responses.

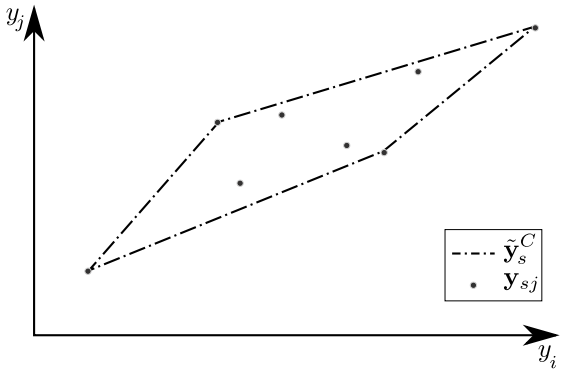

Fig. 5 Illustration of the convex hull principle on an uncertain simulation set $\tilde{\boldsymbol{y}}_s$, obtained by propagating an interval field $\boldsymbol{x}_F^I(\mathbf{r})$ with $n_b = 3$ input dimensions using the transformation method, leading to 8 realizations of $\boldsymbol{y}_{sj}$. The convex hull $\tilde{\boldsymbol{y}}_s^C$ has d_s dimensions, but only the cross-section with the $\{y_i, y_j\}$ plane of two arbitrary model responses is shown (reproduced from [59]).

Also the d_s-dimensional volume $\mathcal{V}_s$ of $\tilde{\boldsymbol{y}}_s^C$ is computed , as it can intuitively be interpreted as a measure for the uncertainty that is present in the data, and hence a generalization of the one-dimensional interval width to higher dimensions. This estimate of the uncertainty is more accurate than the hyper-cubic volume since it takes dependence between responses explicitly into account. In general, the d_s-dimensional volume $\mathcal{V}_s$ of $\tilde{\boldsymbol{y}}_s^C$ can be expressed as a d_s-dimensional integral over the region bounded by $\tilde{\boldsymbol{y}}_s^C$:

$$\mathcal{V}_s = \int_{\tilde{\boldsymbol{y}}_s^C} \cdots \int \quad dy_{s1} \; dy_{s2} \; ... \; dy_{sd_s} \tag{43}$$

A similar expression exists for the d_m-dimensional volume $\mathcal{V}_m$ of $\tilde{\boldsymbol{y}}_m^C$:

$$\mathcal{V}_m = \int_{\tilde{\boldsymbol{y}}_m^C} \cdots \int \quad dy_{m1}\ dy_{m2}\ ...\ dy_{md_m} \tag{44}$$

Finally, Minkowski-Weyl's theorem [212] states that for any polyhedron, there always exists a duality in its representation (i.e. as a set of vertices (a convex hull) or as a set of half-spaces (a set of linear inequalities)). As such, $\tilde{\boldsymbol{y}}_m^C$ and $\tilde{\boldsymbol{y}}_s^C$ can be rewritten as a set of linear inequalities:

$$\tilde{\boldsymbol{y}}_s^C \equiv \boldsymbol{A}_s \boldsymbol{y}_s^T - \boldsymbol{b}_s \geq 0 \tag{45a}$$

$$\tilde{\boldsymbol{y}}_m^C \equiv \boldsymbol{A}_m \boldsymbol{y}_m^T - \boldsymbol{b}_m \geq 0 \tag{45b}$$

with $\boldsymbol{A}_s \in \mathbb{R}^{h_s \times d_s}$, $\boldsymbol{A}_m \in \mathbb{R}^{h_m \times d_m}$, $\boldsymbol{b}_s \in \mathbb{R}^{h_s}$, $\boldsymbol{b}_m \in \mathbb{R}^{h_m}$,$\boldsymbol{y} \in \mathbb{R}^{d_s}$ and $\boldsymbol{y}_m \in \mathbb{R}^{d_m}$. Apex T denotes the transpose. The variable $\boldsymbol{y}$ is a general vector of responses. The number of half-spaces h_m and h_s that are needed to determine $\tilde{\boldsymbol{y}}_m^C$ and $\tilde{\boldsymbol{y}}_s^C$ respectively are given by the Quickhull algorithm, and are dependent on the vectors of measurement data and model responses that are present in these sets. Specifically, the vertices constituting $\tilde{\boldsymbol{y}}_m^C$ and $\tilde{\boldsymbol{y}}_s^C$ are used to construct these sets of hyperplanes.

6.2 Steps 2-3: Interval field dimension

In the identification and quantification of interval field uncertainty, the first step is the identification of the interval field dimension (i.e., the order of the interval field series expansion as introduced in eq. (19)). This discussion is based on the work presented in [61]. This is also illustrated in figure 4.

The core idea for this identification is that the *effective* dimension of the convex hull of the uncertain realization set $\tilde{\boldsymbol{y}}_s^C$ should be equal to the *effective* dimension d_r of the convex hull of the measurement data set $\tilde{\boldsymbol{y}}_m^C$. The term *effective* infers that in general the combination of d system responses does not necessarily represent a d-dimensional manifold in $\mathbb{R}^d$, e.g. due to a high degree of dependence between certain responses. The *effective* dimension d_r of the convex hulls is in that case lower as compared to the space $\mathbb{R}^d$ in which they are defined [61].

In order to compute the *effective* dimension of the measurement data set $\tilde{\boldsymbol{y}}_m$, the covariance matrix $\boldsymbol{\Gamma}_m$ of $\tilde{\boldsymbol{y}}_m$ is computed over the t replica that are measured for each response in $\tilde{\boldsymbol{y}}_m$. These replica are concatenated for each response j in a vector $\boldsymbol{y}_{mj}^t \in \mathbb{R}^t$. $\boldsymbol{\Gamma}_m$ is as such defined as:

$$\boldsymbol{\Gamma}_m = \begin{bmatrix} var(\boldsymbol{y}_{m1}^t) & cov(\boldsymbol{y}_{m1}^t, \boldsymbol{y}_{m2}^t) & \dots & cov(\boldsymbol{y}_{m1}^t, \boldsymbol{y}_{md_m}^t) \\ cov(\boldsymbol{y}_{m2}^t, \boldsymbol{y}_{m1}^t) & var(\boldsymbol{y}_{m2}^t) & \dots & cov(\boldsymbol{y}_{m2}^t, \boldsymbol{y}_{md_m}^t) \\ \vdots & & \ddots & \vdots \\ cov(\boldsymbol{y}_{md_m}^t, \boldsymbol{y}_{m1}^t) & cov(\boldsymbol{y}_{m1}^t, \boldsymbol{y}_{m2}^t) & ... & var(\boldsymbol{y}_{md_m}^t) \end{bmatrix} \tag{46}$$

The measurement data set is used as a reference, as the *effective* dimension of the uncertain realization set $\tilde{\boldsymbol{y}}_s$ is therefore not objective as it depends on an initial estimate of the constituting uncertainty. Note that this covariance matrix is a tool to assess the dependence between model responses, and hence should not be

interpreted as the effective variability in the full output dimension. Subsequently, a singular value decomposition of $\boldsymbol{\Gamma}_m$ is performed such that:

$$\boldsymbol{\Gamma}_m = \boldsymbol{\Phi}_m \boldsymbol{\Lambda}_m \boldsymbol{\Phi}_m^T \tag{47}$$

with $\boldsymbol{\Lambda} \in \mathbb{R}^{d_m \times d_m}$ the diagonal matrix of the ordered eigenvalues $\lambda_1 \leq \lambda_2 \leq \cdots \leq \lambda_{d_s}$ of $\boldsymbol{\Gamma}_m$, and $\boldsymbol{\Phi}_m \in \mathbb{R}^{d_m \times d_m}$ a matrix containing the orthogonal eigenvectors $\boldsymbol{\phi}_{m,j} \in \mathbb{R}^{d_m},\ j = 1, ..., d_m$. Finally, the *effective* dimension d_r of the convex hull of the measurement data set $\tilde{\boldsymbol{y}}_m^C$ is then defined such that:

$$\sum_{i=1}^{d_r} \frac{\lambda_{m,i}}{tr(\boldsymbol{\Gamma}_m)} \geq 1 - \epsilon \tag{48}$$

with $tr(\boldsymbol{\Gamma}_m)$ the trace of the covariance matrix, and ϵ the approximation error, which should be a very small number.

The correct number of base functions n_b should then be selected such that an uncertain realization set $\tilde{\boldsymbol{y}}_s$ is obtained which has at least the same *effective* dimension as the measurement data set. The idea behind this, is that when n_b is increased, the dimension of the hyper-cubic uncertainty on the input parameters of the deterministic model $m()$ is increased as more independent interval scalars are considered. Furthermore, since more base functions $\boldsymbol{\psi}(\mathbf{r})$ are considered, the interval field can have a higher spatial complexity.

In case of a strictly monotonic model $m()$, n_b can be chosen to be equal to d_r. However, when non-monotonicity is present in the numerical model, it is not assured that the effective dimension that is identified in the model responses is obtained by following the above explained heuristic. This is caused by the general inability of finding the extreme vertices of the convex hull of the uncertain realization set $\tilde{\boldsymbol{y}}_s^C$ in polynomial time and approximative techniques should be applied (see section 2.2). Indeed, when the extreme vertices are not contained in $\tilde{\boldsymbol{y}}_s^C$, the computation of d_r might be biased. Furthermore, since non-monotonicity infers that response vectors that are initially at the boundary of $\tilde{\boldsymbol{y}}_s^C$ might shift to its interior when additional basis functions and corresponding interval scalars are included in the interval field definition, also the quantification of n_b might prove to be cumbersome. This is however highly dependent on the specific properties of the non-monotonic function, and is therefore not treated in general detail.

6.3 Step 5: Dimension reduction

The numerical computation of the convex hull and the corresponding multi-dimensional volume is made using the QHULL library, which uses the "Quickhull" algorithm, as developed by Barber et al.. This is a generalization of the Quicksort algorithm to higher dimensions [5]. Care should be taken when computing high dimensional convex hulls, as the time complexity of the *Quickhull* computation of a convex hull is in a worst case scenario equal to:

$$\mathcal{O}\left(\left\lfloor v_c^{\frac{d_s}{2}} \right\rfloor / \left\lfloor \frac{d_s}{2} \right\rfloor !\right) \tag{49}$$

with v_c the number of vertices of $\tilde{\boldsymbol{y}}_s^C$ [5]. This means that the computational cost of the algorithm scales exponentially with the dimension d_s of the space $\mathbb{R}^{d_s}$ in

which the uncertain realization $\tilde{\boldsymbol{y}}$ set is defined, and linearly with the number of vertices. As such, when more responses of the interval FE model are considered for the identification, the computation time of the convex hull increases drastically. This is also sometimes referred to as the *curse of dimensionality*.

However, as already explained in section 6.2, the effective dimension d_r of this convex hulls is in general lower than the dimension of the vector space in which it is defined. Based on this notion, two reduction methods were recently presented. The first method retains the physical responses of the measurement data set $\tilde{\boldsymbol{y}}_m$ and the uncertain realization set $\tilde{\boldsymbol{y}}_s$, and as such delivers a *physical space* of responses. This method is denoted the *subset selection method* and was presented in [59]. The second method projects the measurement data set and the uncertain realization set to a lower-dimensional vector space $\mathbb{R}^{d_r}$. Hence, the responses in these sets do not necessarily represent physical quantities. This method is denoted the *projection method* and was first presented in [61].

6.3.1 Subset selection method

The subset selection method reduces the dimension of the vector space in which the convex hull is defined by selecting those responses that contribute the most to the uncertainty that is modeled.

Specifically, a reduced result vector consisting of selected output quantities $\boldsymbol{y}_{sj}^r \subset \boldsymbol{y}_{sj}$ with $\boldsymbol{y}_{sj}^r \in \mathbb{R}^{d_r}$, $\boldsymbol{y}_{sj} \in \mathbb{R}^{d_s}$ and $d_r \ll d_s$ is constructed as such that a maximum amount of information on the constituting uncertainty at the input side of the model is maintained. The reduced uncertain realization set $\tilde{\boldsymbol{y}}_s^r$, based on these reduced result vectors is then defined as:

$$\tilde{\boldsymbol{y}}_s^r = \left\{ \boldsymbol{y}_{sj}^r \mid \boldsymbol{y}_{sj}^r \subset \boldsymbol{y}_{sj} = f(\boldsymbol{x}^{\boldsymbol{I}}(\mathbf{r})), \boldsymbol{x}_{\boldsymbol{F},\boldsymbol{j}}(\mathbf{r}) \in \boldsymbol{x}^{\boldsymbol{I}}(\mathbf{r}) \right\} \tag{50}$$

with $\boldsymbol{y}_{sj}^r$ a vector containing the d_r selected output responses out of the full-dimensional output $\boldsymbol{y}_{sj}$ of the deterministic solution of the propagation of the j^{th} input uncertainty realization, with $j \in [1, q]$:

$$\boldsymbol{y}_{sj}^r = [y_{s1},\ y_{s2},\ ..,\ y_{sd_r}] \tag{51}$$

A first step in the subset selection procedure is the determination of the dimension d_r of the vector space $\mathbb{R}^{d_r}$ in which $\tilde{\boldsymbol{y}}_s^r$ has to be defined. In fact, the number of responses that should be retained is equal to the effective dimension of either the convex hull of the measurement data set or the convex hull of the result of the interval field FE analysis. This is caused by the notion that the effective dimension of both sets should be equal, as the dimension n_b of the interval field $\boldsymbol{x}^{\boldsymbol{I}}(\mathbf{r})$ should be set to ensure this equality (see eq. (46) to (48)). By definition, the effective dimension of the convex hull is the number of non-zero orientations in that convex hull (see also 6.2).

The subset that is selected should furthermore be sensitive to changes to the input intervals of the model. In order to take into account the coupling between the considered responses, a modified version of the interval sensitivity, as proposed by Moens & Vandepitte in [135], is employed. In its original form, the interval sensitivity is defined as :

$$s_{il} = \frac{\partial r_{y_l}}{\partial r_{x_i}} \tag{52}$$

with r_{y_l} and r_{x_i} the interval radius of respectively the l^{th} model response and the i^{th} interval scalar at the input of the model. This concept is further expanded to consider the sensitivity of multiple output responses and their dependence w.r.t. changes in the interval uncertainty at the input side of the model $m()$. Specifically, the sensitivity s_{il} of the volume $\mathcal{V}_{s,l}^r$ of the d_r-dimensional convex hull $\tilde{\boldsymbol{y}}_{s,l}^{r,C}$ of the l^{th} candidate reduced uncertain realization set $\tilde{\boldsymbol{y}}_{s,l}^r$ with respect to changes in the interval radius $\Delta\alpha_i$ of a locally defined interval scalar α_i of $\boldsymbol{x}^{\boldsymbol{I}}(\mathbf{r})$ is calculated as:

$$s_{il} = \frac{\partial \mathcal{V}_{s,l}^r}{\partial \Delta\alpha_i} \tag{53}$$

In order to facilitate the comparison between different candidate reduced uncertain realization sets based on the sensitivity, normalized relative interval sensitivities $s_{il}^{n,r}$ are more relevant, as they give the relative width of the intervals and are dimensionless. The normalized relative interval sensitivity is defined as:

$$s_{il}^{n,r} = \frac{\partial \mathcal{V}_{s,l}^r}{\partial \Delta\alpha_i} \cdot \frac{\Delta\alpha_i}{\mathcal{V}_s} \cdot \frac{1}{s_i^r} \tag{54}$$

with:

$$s_i^r = \sum_j s_{il}^r = \sum_j \frac{\partial \mathcal{V}_{s,l}^r}{\partial \Delta\alpha_i} \cdot \frac{r_{\alpha_i}}{\mathcal{V}_s} \tag{55}$$

and s_{il}^r the non-normalized relative interval sensitivity.

Finally, also the dependence between the q realizations of a response within a candidate $\boldsymbol{y}_{sj,l}^r$ is computed in order to prevent the selection highly dependent responses. This dependence is in this context computed as the aspect ratio ν of the convex hull $\tilde{\boldsymbol{y}}_{s,l}^{r,C}$ of that candidate reduced uncertain realization set $\tilde{\boldsymbol{y}}_{s,l}^r$. When all responses are completely dependent, these responses describe a line in $\mathbb{R}^{d_r}$, and the aspect ratio of $\tilde{\boldsymbol{y}}_s^C$ tends to zero. On the other hand, the aspect ratio will approach unity when the responses are completely independent. Hence, it can be regarded as a measure for the dependence. In general, the multidimensional aspect ratio is calculated as the ratio between the smallest and largest eigenvalue of the covariance matrix $\boldsymbol{\Xi}_c^r$ of $\tilde{\boldsymbol{y}}_{s,l}^r$:

$$\nu_l = \frac{min(\boldsymbol{\Lambda}_c^r)}{max(\boldsymbol{\Lambda}_c^r)} \tag{56}$$

with $\boldsymbol{\Lambda}_c^r \in \mathbb{R}^{d_r \times d_r}$ the diagonal matrix containing the ordered d_r eigenvalues of $\boldsymbol{\Xi}_c^r \in \mathbb{R}^{d_r \times d_r}$, the covariance matrix of $\tilde{\boldsymbol{y}}_{s,l}^r$. $\boldsymbol{\Xi}_c^r$ is calculated similarly to $\boldsymbol{\Gamma}$ of $\tilde{\boldsymbol{y}}_s$, as shown in equation (46), where instead of the complete result vector $\boldsymbol{y}_{sj}$, the candidate reduced result vectors $\boldsymbol{y}_{sj,l}^r$ are used for the computation of the covariance matrix $\boldsymbol{\Xi}_c^r$.

In order to select the optimal subset, a metric μ_{il} combining the sensitivity of all possible subsets and dependence between the dimensions of these subsets is calculated for each separate locally defined interval $i = 1, ..., k$:

$$\mu_{il} = |s_{il}^{n,r}| \nu_l \tag{57}$$

with $s_{il}^{n,r} \in [-1;1]$ and $\nu \in [0;1]$. Since only the magnitude of the sensitivity is important, the absolute value is considered. The optimal subset exhibits a maximal value of μ_{il} among all candidate reduced uncertain realization sets, yielding following optimization problem:

$$l^* = argmax \left(\sum_{i=1}^{k} \mu_{il} \right) \tag{58}$$

Intuitively, this means that a subset of responses is searched that is maximally sensitive to changes in the input intervals, but where the uncertainty is evenly distributed among the considered responses. The solution of eq. (57) can be either be obtained following a *brute-force* approach when the number of considered responses is relative low, or in a global optimization approach for larger models. Following a brute-force approach, the candidate reduced uncertain realization sets and their convex hull $\tilde{\boldsymbol{y}}_{s,l}^{r,C}$ with corresponding volume $\mathcal{V}_{s,l}^{r}$ are computed for each possible d_r-dimensional responses $\boldsymbol{y}_{sj,l}^{r}$ that can be deduced from the result vector $\boldsymbol{y}_{sj}$. Based on these combinations, the optimal subset is selected using the subset selection metric (see eq. (57)). The number of convex hull computations is in that case:

$$\binom{d_m}{d_r} = \frac{d_m!}{d_r!(d_m - d_r)!} \tag{59}$$

and $n_b + 1$ interval field computations are needed for the estimation of the sensitivities. Alternatively, also adjoint approaches can be used.

6.3.2 Projection method

Also the projection method is based on the concept of *effective* dimension, as elaborated in section 6.2. Instead of selecting a subset of responses, the method projects $\tilde{\boldsymbol{y}}_m$ and $\tilde{\boldsymbol{y}}_s$ to a lower dimensional basis $\mathcal{B} \in \mathbb{R}^{d_r}$, which is constructed using the orthogonal eigenvectors of the covariance matrix of the measurement data set, since these data usually provide the most objective information on the uncertainty at hand. As such, a *reduced* realization set $\tilde{\boldsymbol{y}}_s^r$ and *reduced* measurement data set $\tilde{\boldsymbol{y}}_m^r$ are obtained. However, d_r can still be prohibitively large when realistic numerical models and/or measurement sets containing numerous responses are considered. In that case, $\tilde{\boldsymbol{y}}_s^r$ and $\tilde{\boldsymbol{y}}_m^r$ are further projected onto lower-dimensional subspaces $\mathcal{B}_i^+ \subset \mathcal{B}$.

As a first step of the reduction, equations (46) to (48) are employed to compute d_r . Then, an orthogonal basis $\mathcal{B}$ is constructed in $\mathbb{R}^{d_r}$ based on the eigenvectors $\phi_{m,j}$ of the covariance matrix corresponding to the d_r largest eigenvalues in $\boldsymbol{\Lambda}_m$. This basis is thus defined as:

$$\mathcal{B} = \text{span}\{\phi_{m,d-d_r}, \phi_{m,d-d_r+1}, \dots \phi_{m,d}\} \tag{60}$$

with $\phi_i \in \mathbb{R}^d$. $\mathcal{B}$ is oriented according the the d_r directions in $\tilde{\boldsymbol{y}}_m^C$ that show the largest variance.

For the actual reduction $\mathbb{R}^d \mapsto \mathbb{R}^{d_r}$, the realizations $\boldsymbol{y}_{sj}$, $j = 1, \dots, q$ in $\tilde{\boldsymbol{y}}_s$ are first concatenated in a matrix $\tilde{\boldsymbol{Y}}_s \in \mathbb{R}^{d \times q}$:

$$\tilde{\boldsymbol{Y}}_s = [\boldsymbol{y}_{s1}, \boldsymbol{y}_{s2}, \dots, \boldsymbol{y}_{sq}] \tag{61}$$

The measured replica $\boldsymbol{y}_{mj}$, $j = 1..., t$ are analogously concatenated in a matrix $\tilde{\boldsymbol{Y}}_m \in \mathbb{R}^{d\times t}$:

$$\tilde{\boldsymbol{Y}}_m = [\boldsymbol{y}_{m1}, \boldsymbol{y}_{m2}, \ldots, \boldsymbol{y}_{mt}] \tag{62}$$

$\tilde{\boldsymbol{Y}}_s$ and $\tilde{\boldsymbol{Y}}_m$ are then projected onto $\mathcal{B}$ such that:

$$\tilde{\boldsymbol{Y}}^r_s = \left(\tilde{\boldsymbol{Y}}^T_s \mathcal{B}\right)^T = [\boldsymbol{y}^r_{s1}, \boldsymbol{y}^r_{s2}, \ldots, \boldsymbol{y}^r_{sq}] \tag{63}$$

with $\tilde{\boldsymbol{Y}}^r_s \in \mathbb{R}^{d_r\times q}$ for the uncertain realization set, and:

$$\tilde{\boldsymbol{Y}}^r_m = \left(\tilde{\boldsymbol{Y}}^T_m \mathcal{B}\right)^T = [\boldsymbol{y}^r_{m1}, \boldsymbol{y}^r_{m2}, \ldots, \boldsymbol{y}^r_{mt}] \tag{64}$$

with $\tilde{\boldsymbol{Y}}^r_m \in \mathbb{R}^{d_r\times t}$ for the measurement data set.

However, when realistic numerical models and measurement data sets containing thousands of responses are considered, the computation of the convex hulls $\tilde{\boldsymbol{y}}^C_s$ and $\tilde{\boldsymbol{y}}^C_m$ of the reduced sets $\tilde{\boldsymbol{Y}}^r_s$ and $\tilde{\boldsymbol{Y}}^r_m$ still might take prohibitively long as d_r still might be too large for efficient computation due to intricate dependence structures between these responses. Therefore, it is proposed to further reduce the dimension of both data sets by further projecting $\tilde{\boldsymbol{Y}}^r_m$ and $\tilde{\boldsymbol{Y}}^r_s$ onto d^+_r-dimensional subspaces, where each subspace is defined by a lower-dimensional orthogonal basis $\mathcal{B}^+_i \subset \mathcal{B},\ i = 1, \ldots, \binom{d_r}{d^+_r}$, constructed as a subset of $\mathcal{B}$, with $d^+_r << d_r$ and $\binom{d_r}{d^+_r}$ the binomial coefficient. In this way, the time complexity of the computation of the convex hull becomes

$$\mathcal{O}\left(\left\lfloor v_c^{\frac{d^+_r}{2}} \right\rfloor / \left\lfloor \frac{d^+_r}{2} \right\rfloor ! \times \binom{d_r}{d^+_r}\right) \tag{65}$$

Therefore, as long as d^+_r is a very small number, the computational cost of calculating $\binom{d_r}{d^+_r}$ d^+_r dimensional convex hulls reduces drastically with respect to computing 1 d_r dimensional convex hull. This implies that only the $d^+_r - 1$ order interactions between model responses are retained in the analysis, since the higher order interactions are lost in the projection. Herein, $d^+_r = 1$ is the limit case where only the hyper-cubic approximation of $\tilde{\boldsymbol{y}}^r_s$ and $\tilde{\boldsymbol{y}}^r_m$ is retained. This however does not limit the accuracy of the method as long as $d^+_r \geq 2$, since by considering the convex hulls over the response sets, all higher-order interactions (i.e., quadratic interactions and higher) between model responses are already linearised. Therefore, no further approximations of the dependence structure of both sets is made as compared to considering only the convex hull.

Then, $\tilde{\boldsymbol{Y}}^r_m$ and $\tilde{\boldsymbol{Y}}^r_s$ are projected onto each d^+_r dimensional subspace defined by $\mathcal{B}^+_i \subset \mathcal{B}$. Furthermore, by considering $\binom{d_r}{d^+_r}$ bases, the projection and computation of the convex hull has become embarrassingly parallel, as it is has been split in the computation of $\binom{d_r}{d^+_r}$ independent low dimensional convex hulls. The i^{th} orthogonal basis $\mathcal{B}^+_i$ is defined as:

$$\mathcal{B}^+_i = \text{span}\{\phi_{m\mathcal{I}_{i,1}}, \phi_{m\mathcal{I}_{i,2}}, \ldots \phi_{m\mathcal{I}_{i,d^+_r}}\} \tag{66}$$

with $\mathcal{I}_i$ an index set containing the d^+_r indices for the i^{th}, $i = 1, ..., \binom{d_r}{d^+_r}$ subspaces of the vector space by $\mathcal{B}$. The reduced sets $\tilde{\boldsymbol{Y}}^{r+}_{s,\mathcal{B}^+_i} \in \mathbb{R}^{d^+_r\times q}, i = 1, \ldots, \binom{d_r}{d^+_r}$ and

$\tilde{\boldsymbol{Y}}^{r+}_{m,\mathcal{B}_i^+} \in \mathbb{R}^{d_r^+ \times t}, i = 1, \ldots, \binom{d_r}{d_r^+}$ are then obtained by projecting $\tilde{\boldsymbol{Y}}^{r}_{m}$ and $\tilde{\boldsymbol{Y}}^{r}_{s}$ onto each of these subspaces:

$$\begin{aligned} \tilde{\boldsymbol{Y}}^{r+}_{s,\mathcal{B}_i^+} &= \left(\tilde{\boldsymbol{Y}}^{T}_{s}\mathcal{B}_i^+\right)^T \\ &= \left[\boldsymbol{y}^r_{s1,\mathcal{B}_i^+}, \boldsymbol{y}^r_{s2,\mathcal{B}_i^+}, \ldots, \boldsymbol{y}^r_{sq,\mathcal{B}_i^+}\right], \quad i = 1, \ldots, \binom{d_r}{d_r^+} \end{aligned} \tag{67a}$$

$$\begin{aligned} \tilde{\boldsymbol{Y}}^{r+}_{m,\mathcal{B}_i^+} &= \left(\tilde{\boldsymbol{Y}}^{T}_{m}\mathcal{B}_i^+\right)^T \\ &= \left[\boldsymbol{y}^r_{m1,\mathcal{B}_i^+}, \boldsymbol{y}^r_{m2,\mathcal{B}_i^+}, \ldots, \boldsymbol{y}^r_{mq,\mathcal{B}_i^+}\right], \quad i = 1, \ldots, \binom{d_r}{d_r^+} \end{aligned} \tag{67b}$$

Finally, the uncertain realization set $\tilde{\mathbf{y}}^r_{s,i}$ and measurement data set $\tilde{\mathbf{y}}^r_{m,i}$ that are projected onto $\mathcal{B}_i^+$, the i^{th} subspace of $\mathcal{B}$, are explicitly defined as:

$$\tilde{\boldsymbol{y}}^r_{s,i} = \left\{\boldsymbol{y}^r_{sj,\mathcal{B}_i^+} \mid j = 1, \ldots, q\right\} \quad i = 1, \ldots, \binom{d_r}{d_r^+} \tag{68}$$

$$\tilde{\boldsymbol{y}}^r_{m,i} = \left\{\boldsymbol{y}^r_{mj,\mathcal{B}_i^+} \mid j = 1, \ldots, t\right\} \quad i = 1, \ldots, \binom{d_r}{d_r^+} \tag{69}$$

Note that the notation is simplified as compared to eq. (67) for the sake of clarity. Finally, also $\tilde{\boldsymbol{y}}^C_{s,i}$ and $\tilde{\boldsymbol{y}}^C_{m,i}$ are computed based on $\tilde{\boldsymbol{y}}_{s,i}$ and $\tilde{\boldsymbol{y}}_{m,i}$, for each $i = 1, \ldots, \binom{d_r}{d_r^+}$:

$$\tilde{\boldsymbol{y}}^C_{s,i} = \left\{ \sum_{j=1}^{t} \beta_j \boldsymbol{y}^r_{sj,\mathcal{B}_i^+} \;\mid\; (\forall j : \beta_j \geq 0) \wedge \sum_{j=1}^{t} \beta_j = 1 \;;\; \boldsymbol{y}^r_{sj,\mathcal{B}_i^+} \in \tilde{\mathbf{y}}^r_{m,i} \right\} \tag{70}$$

$$\tilde{\boldsymbol{y}}^C_{m,i} = \left\{ \sum_{j=1}^{t} \beta_j \boldsymbol{y}^r_{mj,\mathcal{B}_i^+} \;\mid\; (\forall j : \beta_j \geq 0) \wedge \sum_{j=1}^{t} \beta_j = 1 \;;\; \boldsymbol{y}^r_{mj,\mathcal{B}_i^+} \in \tilde{\mathbf{y}}^r_{m,i} \right\} \tag{71}$$

Also the corresponding multidimensional volumes $V_{s,i}$ and $V_{m,i}$ are thus computed. The main advantage of this method over the subset selection method, is that all measured responses are explicitly taken into account in the identification procedure, as compared to only a (small) subset of the responses. As such, all available information is used in the identification and quantification. Evidently, this also makes the identification more prone to outliers in the data. Therefore, adequate data pre-processing should be applied prior to performing this reduction method.

6.4 Step 7: Basis function quantification

In order to accurately quantify the interval field model $\boldsymbol{x}^{\boldsymbol{I}}(\mathbf{r})$ of the spatial uncertainty in the parameters of the numerical model $\mathcal{M}$, the constituting base functions $\boldsymbol{\psi}_i(\mathbf{r})$ have to be quantified objectively. An initial estimation of these basis functions can be based on expert knowledge of the analyst (e.g. from experimental

data or knowledge on the manufacturing process). However, since available expert knowledge is in most realistic industrial design cases scarce, ambiguous or subjective, this initial estimate has to be improved and/or validated based on experimentally obtained measurement data. This section presents a method to perform such quantification, and is based on the work presented in [61].

After the identification of the interval field basis dimension, as explained in section 6.2, the base functions of the interval field expansion (eq. (19)) should be identified. This as such constitutes the sixth step in the general overview given in figure 4. For the identification of the base functions $\boldsymbol{\psi}_i$, the convex hull of the uncertain realization set $\tilde{\boldsymbol{y}}_s^C$ and the convex hull of the measurement data set $\tilde{\boldsymbol{y}}_m^C$ are represented as a set of d_s-dimensional half-spaces, following Minkowski-Weyl's theorem [212] (see eq. (45)). These sets of half-spaces in fact represent the linear inequalities that describe boundaries of the corresponding convex hull and they consist of a set of vector-valued functions $\boldsymbol{f}_s(\boldsymbol{\alpha}^I, \boldsymbol{\psi}(\boldsymbol{r}))$, which depend on the interval field that is defined on the parameters at the input of $\mathcal{M}$. Considering only the crisp boundary of $\tilde{\boldsymbol{y}}_s^C$ yields a set of linear equalities:

$$\boldsymbol{f}_s(\boldsymbol{\alpha}^I, \boldsymbol{\psi}(\boldsymbol{r})) = [f_1, f_2, ..., f_{h_s}]^T = \boldsymbol{A}_s \boldsymbol{y}_s^T - \boldsymbol{b}_s = \boldsymbol{0} \tag{72}$$

with $\forall f_i, i = 1, ..., h_s : \mathbb{R}^d \mapsto 0$. These functions are analogously defined for the measurement data set:

$$\boldsymbol{f}_m = [f_1, f_2, ..., f_{h_m}]^T = \boldsymbol{A}_m \boldsymbol{y}_m^T - \boldsymbol{b}_m = \boldsymbol{0} \tag{73}$$

In order to quantify the basis functions $\boldsymbol{\psi}^*(\boldsymbol{r})$ that govern the spatial nature of the uncertainty captured by $\tilde{\boldsymbol{y}}_m^C$, a squared $\mathcal{L}_2$-norm of the difference between the gradients of the half-spaces that bound $\tilde{\boldsymbol{y}}_m^C$ and $\tilde{\boldsymbol{y}}_s^C$ is minimized:

$$\boldsymbol{\psi}^*(\boldsymbol{r}) = \text{argmin} \left(\left\| \nabla \boldsymbol{f}_s \left(\boldsymbol{\alpha}^I, \boldsymbol{\psi}(\boldsymbol{r}) \right) \big|_{\boldsymbol{\alpha}^I = \boldsymbol{\alpha}_0^I} - \nabla \boldsymbol{f}_m \right\|_2^2 \right) \tag{74}$$

where the interval field $\boldsymbol{x}^{\boldsymbol{I}}(\mathbf{r})$ can either be evaluated using an initial guess on the interval scalars, or by using identified interval scalars using the method presented in section 6.5. In the specific case when the base functions $\boldsymbol{\psi}(\mathbf{r})$ are constructed using inverse distance weighting (see eq. (21)), the optimization problem reduces to finding the correct control point locations $\boldsymbol{r}_i$.

As explained in section 2.3, the definition of the basis functions $\boldsymbol{\psi}(\boldsymbol{r})$ controls the coupling between these local intervals at the element level. In the following, it is illustrated how these local intervals at element level impact the gradient of $\boldsymbol{f}_s$, and hence, how these gradients can aid the quantification of the correct basis functions. This explanation is based on a two-dimensional system response $\{y_o, y_p\}$, when considering the propagation of two realizations of $\boldsymbol{x}^{\boldsymbol{I}}(\mathbf{r})$, l_1 and l_2. First, the interval field $\boldsymbol{x}^{\boldsymbol{I}}(\mathbf{r})$ is decomposed into its midpoint function $\mu(\boldsymbol{x}^{\boldsymbol{I}}(\mathbf{r}))$ and the deviation from this midpoint function $\Delta\boldsymbol{x}^{\boldsymbol{I}}(\mathbf{r})$:

$$\boldsymbol{x}^{\boldsymbol{I}}(\mathbf{r}) = \mu(\boldsymbol{x}^{\boldsymbol{I}}(\mathbf{r})) + \Delta\boldsymbol{x}^{\boldsymbol{I}}(\mathbf{r}) = \sum_{i=1}^{n_b} \boldsymbol{\psi}_i \mu_{\alpha_i} + \sum_{i=1}^{n_b} \boldsymbol{\psi}_i \Delta\alpha_i \tag{75}$$

with $\mu()$ the midpoint function of the field and $\Delta()$ the radius of the interval. In order to approximate ∇f_h, the responses $y_{o,l1}, y_{o,l2}, y_{p,l1}$ and $y_{p,l2}$ are expressed

as a truncated Taylor series expansion around $\mu(\alpha_i)$:

$$y_{o,l1} = y_o(\mu(\boldsymbol{x}^{\boldsymbol{I}}(\mathbf{r}))) + \sum_{j=1}^{k} \frac{\partial \boldsymbol{y}_o}{\partial x_j} \Delta \boldsymbol{x}_F^{l1}(\boldsymbol{r}) \tag{76}$$

with $x_j,\ j = 1, \cdots, k$ the value of the j^{th} element in the FE model $m()$ and $\Delta \boldsymbol{x}_F^{l1}(\boldsymbol{r})$ the l_1^{th} realization of the deviation function of the interval field $\boldsymbol{x}^{\boldsymbol{I}}(\mathbf{r})$, as expressed in eq. (75). Note that a Taylor series expansion is in general not accurate enough for the actual uncertainty propagation. In this case however, this method provides an intuitive illustration of the effect of the basis functions on the gradient of the half-space under consideration and is hence used for explanatory reasons. For notational efficiency, denote the local sensitivity matrix $\mathcal{S} \in \mathbb{R}^{d_s \times k}$:

$$\mathcal{S} = \begin{bmatrix} \frac{\partial y_1}{\partial x_1} & \frac{\partial y_1}{\partial x_2} & \cdots & \frac{\partial y_1}{\partial x_k} \\ \frac{\partial y_2}{\partial x_1} & \frac{\partial y_2}{\partial x_2} & \cdots & \frac{\partial y_2}{\partial x_k} \\ \vdots & \vdots & \ddots & \vdots \\ \frac{\partial y_{d_s}}{\partial x_1} & \frac{\partial y_{d_s}}{\partial x_2} & \cdots & \frac{\partial y_{d_s}}{\partial x_k} \end{bmatrix} \tag{77}$$

This matrix describes the sensitivity of each model response $y_i,\ i = 1, ..., d_s$ to changes in the local element value $x_i,\ i =, ..., k$ for each element in Ω. $\mathcal{S}_i$ denotes the i^{th} column of the local sensitivity matrix , while with $\mathcal{S}_{:i}$, the i^{th} row is considered.

Now consider one half-space equality f_h that corresponds to the h^{th} bounding half-space of $\tilde{\boldsymbol{y}}_s^C$. For the considered case, this can be expressed as:

$$\nabla f_h = \frac{y_{o,l2} - y_{o,l1}}{y_{p,l2} - y_{p,l1}} \tag{78}$$

with:

$$y_{o,l1} = y_o\left(\mu\left(\boldsymbol{x}^{\boldsymbol{I}}(\mathbf{r})\right)\right) + \sum_{j=1}^{k} \mathcal{S}_{jo} \sum_{i=1}^{n_b} \boldsymbol{\psi}_i \Delta \alpha_i^{l1} \tag{79}$$

$$y_{o,l2} = y_o\left(\mu\left(\boldsymbol{x}^{\boldsymbol{I}}(\mathbf{r})\right)\right) + \sum_{j=1}^{k} \mathcal{S}_{jo} \sum_{i=1}^{n_b} \boldsymbol{\psi}_i \Delta \alpha_i^{l2} \tag{80}$$

$$y_{p,l1} = y_n\left(\mu\left(\boldsymbol{x}^{\boldsymbol{I}}(\mathbf{r})\right)\right) + \sum_{j=1}^{k} \mathcal{S}_{jp} \sum_{i=1}^{n_b} \boldsymbol{\psi}_i \Delta \alpha_i^{l1} \tag{81}$$

$$y_{p,l2} = y_p\left(\mu\left(\boldsymbol{x}^{\boldsymbol{I}}(\mathbf{r})\right)\right) + \sum_{j=1}^{k} \mathcal{S}_{jn} \sum_{i=1}^{n_b} \boldsymbol{\psi}_i \Delta \alpha_i^{l2} \tag{82}$$

with $\mathcal{S} \in \mathbb{R}^{d_s \times k}$, $\boldsymbol{\psi}_i \in \mathbb{R}^{k \times 1}$ and $\Delta \alpha_i^{l_{1,2}} \in \mathbb{R}^1$. From these equations, it is seen how the n_b interval scalars and base functions translate to local values for all k elements in Ω, and are further translated towards a system response. Filling in these expressions in the expression for the gradient (eq. (78)) and rearranging some terms yields:

$$\nabla f = \frac{\sum_{j=1}^{k} \mathcal{S}_{jo} \sum_{i=1}^{n_b} \boldsymbol{\psi}_i \Delta(\alpha_i^{l2} - \alpha_i^{l1})}{\sum_{j=1}^{k} \mathcal{S}_{jp} \sum_{i=1}^{n_b} \boldsymbol{\psi}_i \Delta(\alpha_i^{l2} - \alpha_i^{l1})} \tag{83}$$

From this equation, it is clear that three terms affect the gradient. First, the respective elements in the local sensitivity matrix have an important influence, as they are a measure for how the model translates the local interval uncertainty $\boldsymbol{x}^I$ at element level towards the model responses $\boldsymbol{y}$. This is a linearization of the general case, where this propagation is performed by the functions $m_i()$ of the numerical model $\mathcal{M}$. These factors are constant as long as the same model $m()$ is considered for each propagation of the uncertainty, which is usually the case. Furthermore, also the relative difference between the scalar values of the realizations of the interval scalars (i.e., α_i^{l2} and α_i^{l1}) of the interval field affect ∇f. This term is however constant since the gradients in eq. (74) are evaluated for a given $\boldsymbol{\alpha}^I$, also this term is constant. As such, ∇f is only affected by the $\boldsymbol{\psi}_i$ of the interval field. Hence, minimizing the discrepancy between the gradients of the half-spaces of $\tilde{\boldsymbol{y}}_s^C$ and $\tilde{\boldsymbol{y}}_m^C$ should allow for their quantification.

It should be noted that the above argumentation for the method only holds when the model is monotonic. This is caused by the fact that in general, propagating the interval field realizations that are obtained by taking the vertices of the hyper-cubic set of interval scalars through a non-monotonic model does not necessarily yield the vertices of the convex hull of the uncertain realization set, thus complicating the computation of the gradient of the half-spaces considerably. This however can be solved by using appropriate propagation techniques, keeping in mind that the obtained gradients can be severely biased when extreme vertices are missing in $\tilde{\boldsymbol{y}}_s^C$. Moreover, it should be noted that in case non-monotonic models are considered, continuity of the objective function that is introduced in eq. (74) is no longer guaranteed, as the response vectors $\boldsymbol{y}_{sj}$ that are initially at the boundaries of $\tilde{\boldsymbol{y}}_s^C$ can shift to its interior. This leads to a discontinuous change in the gradients of the convex hull, and consequently eq. (74).

In a generic engineering context, the size t of the measurement data set is usually limited. This may bias the comparison of the gradients of $\tilde{\boldsymbol{y}}_m^C$ to the gradients of the convex hull over the uncertain realization set $\tilde{\boldsymbol{y}}_s^C$, especially when the extreme responses of the structure are not contained in $\tilde{\boldsymbol{y}}_m$. In order to overcome this, a minimum-volume convex polytope is constructed around $\tilde{\boldsymbol{y}}_m^C$ having the same number of vertices as $\tilde{\boldsymbol{y}}_s^C$, in analogy to the ideas of Elishakoff and Sarlin presented in [52,53]. The shape of this convex polytope is completely up to the data, as long as the number of vertices between the two is equal. The principal idea behind this method is to *expand* the information that is contained in the measured responses by taking the topology of the uncertain realization set (in terms of number of vertices) into consideration, as computed by the numerical model. This is valid as long as the problem at hand is strictly monotonic with respect to the physical parameters under consideration. It is worth noting that the number of vertices present in the uncertain realization set $\tilde{\boldsymbol{y}}_s$ follows directly from the computation of the effective dimension d_r of the measurement data set $\tilde{\boldsymbol{y}}_m$, as proposed in section 6.2, and is therefore also directly computed using the measurement data set $\tilde{\boldsymbol{y}}_m$, which is an objective estimate. As such, the experimental burden for the determination of the gradients of the half-spaces bounding $\tilde{\boldsymbol{y}}_m^C$ shifts from finding the extreme vertices towards finding a suitable set of extreme responses that constitute the boundaries of $\tilde{\boldsymbol{y}}_m^C$.

However, the corresponding experimental campaign should be performed carefully, as a lack of extreme responses might severely bias the gradients, and con-

sequently, the identification. To quote the famous statistical Ronal Fisher [71] (1938): "To call in the statistician after the experiment is done may be no more than asking him to perform a post-mortem examination: he may be able to say what the experiment died of.". Although the term *statistician* is not entirely applicable in the context of interval non-determinism, the core idea behind this quote is still valid as it stresses the importance of a close collaboration between experimentalists and analysts. Indeed, an accurate identification of the spatial interval uncertainty calls for an intelligently designed experimental campaign (e.g., according to a Design Of Experiments approach) in order to obtain sufficient experimental responses. As such, an accurate estimate of the spatial topology of the interval field can be obtained. The exact design of such experimental campaign is evidently highly case-dependent, and should be performed with utmost care, based on some expert knowledge. Furthermore, it should be stresses that as compared to quantifying random field uncertainty, obtaining some extreme responses in an intelligently designed test campaign should prove to be less cumbersome as compared to experimentally obtaining an entire auto-covariance function.

6.5 Step 8: Interval scalar quantification

As a final step, also the interval scalars $\boldsymbol{\alpha}^I$ in eq. (19) are quantified. The presented method can equally be applied for the identification and quantification of scalar interval uncertainty, contained in an interval vector $\boldsymbol{x}^I \in \mathbb{IR}^k$, with k the number of parameters in the model. The methods presented in this section are first introduced in [59] and [60].

Identification of $\boldsymbol{\alpha}^I \in \mathbb{IR}^{n_b}$, the interval vector that is used for the construction of an interval field $\boldsymbol{x}^I(\mathbf{r})$, as shown in eq. (19), is obtained through the minimization of a cost function $\delta(\boldsymbol{\alpha}^I)$, which expresses the discrepancy between the uncertain realization set $\tilde{\boldsymbol{y}}_s$ of the IFE simulation and the measurement set $\tilde{\boldsymbol{y}}_m$. The construction of $\delta(\boldsymbol{\alpha}^I)$ is based on the geometrical properties of shape and size of both hulls $\tilde{\boldsymbol{y}}_m^C$ and $\tilde{\boldsymbol{y}}_s^C$ and it contains three terms.

First, the difference between the multidimensional volumes $\mathcal{V}_m$ and $\mathcal{V}_s$ of the respective hulls is computed, as this is a measure for the amount of uncertainty captured by the convex hull. Also the multidimensional volume $\mathcal{V}_o$ of the intersection $\tilde{\boldsymbol{y}}_o$ of $\tilde{\boldsymbol{y}}_m^C$ and $\tilde{\boldsymbol{y}}_s^C$ is taken into account. The intersection between $\tilde{\boldsymbol{y}}_m^C$ and $\tilde{\boldsymbol{y}}_s^C$ is formally defined as:

$$\tilde{\boldsymbol{y}}_o = \tilde{\boldsymbol{y}}_s^C \cap \tilde{\boldsymbol{y}}_m^C \tag{84}$$

and can be computed as the set of all $\boldsymbol{y}_j$ complying with both sets of linear inequalities:

$$\tilde{\boldsymbol{y}}_o = \left\{ \boldsymbol{y}_j \;\middle|\; \boldsymbol{A}_o \boldsymbol{y}_j^T - \boldsymbol{b}_o^T \leq 0 \wedge \boldsymbol{y}_j \in \mathbb{R}^d \right\} \tag{85}$$

with $\boldsymbol{A}_o \in \mathbb{R}^{(h_m+h_s)\times d}$:

$$\boldsymbol{A}_o = [\boldsymbol{A}_m; \boldsymbol{A}_s]^T \tag{86}$$

and $\boldsymbol{b}_o \in \mathbb{R}^{(h_m+h_s)}$:

$$\boldsymbol{b}_o = [\boldsymbol{b}_m; \boldsymbol{b}_s]^T \tag{87}$$

Finally, the objective function $\delta(\boldsymbol{\alpha}^I)$ should contain a desirable descent direction for the specific case when the intersection between $\tilde{\boldsymbol{y}}_s^C$ and $\tilde{\boldsymbol{y}}_m^C$ is empty (i.e.,

$\tilde{\boldsymbol{y}}_o = \emptyset$), as the applied optimization algorithm would otherwise get trapped in a local minimum of the optimization function δ. This condition may occur when the analyst's initial knowledge on the input parameters of the FE model has a large bias with respect to the actual uncertainty in the model. In this specific case, there is no descent direction for the optimization algorithm that ensures overlap between $\tilde{\boldsymbol{y}}_s^C$ and $\tilde{\boldsymbol{y}}_m^C$. Therefore, also the squared $\mathcal{L}_2$ norm of the difference between $\boldsymbol{c}_m$ and $\boldsymbol{c}_s$ is incorporated in the discrepancy metric. $\boldsymbol{c}_m$ and $\boldsymbol{c}_s$ are defined as the geometrical center of gravity of $\tilde{\boldsymbol{y}}_s$ and $\tilde{\boldsymbol{y}}_m$:

$$\begin{aligned} \boldsymbol{c}_m &= \frac{1}{t}\sum_{j=1}^{t} \boldsymbol{y}_{mj} \\ \boldsymbol{c}_s &= \frac{1}{q}\sum_{j=1}^{q} \boldsymbol{y}_{sj} \end{aligned} \tag{88}$$

Combining these three elements, $\delta(\boldsymbol{\alpha}^I)$ is constructed according to:

$$\delta(\boldsymbol{\alpha}^I) = \left(\Delta\mathcal{V}_m^2 + w_o \Delta\mathcal{V}_o^2 + \Delta c^2\right) \tag{89}$$

with:

$$\Delta\mathcal{V}_m = 1 - \frac{\mathcal{V}_s(\boldsymbol{\alpha}^I)}{\mathcal{V}_m} \tag{90a}$$

$$\Delta\mathcal{V}_o = 1 - \frac{\mathcal{V}_o(\boldsymbol{\alpha}^I)}{\mathcal{V}_m} \tag{90b}$$

$$\Delta c = \left\| \boldsymbol{c}_m - \boldsymbol{c}_s(\boldsymbol{\alpha}^I) \right\|_2 \tag{90c}$$

and w_o a weighting factor. This weighting factor is of specific importance when the measurement data set is very small, or when insufficient samples are located on the boundaries of $\tilde{\boldsymbol{y}}_m^C$. In that case, more weight in the optimization is given to maximizing the overlap between the uncertain realization set and the measurement data set, to ensure that all measurement points are included in the identified interval field. As such, this part of $\delta(\boldsymbol{\alpha}^I)$ acts as a barrier function, penalizing a lack of overlap. Finally, $\boldsymbol{\alpha}^{I,*}$, the interval vector containing the identified interval scalars is finally computed as:

$$\boldsymbol{\alpha}^{I,*} = argmin\ \delta(\boldsymbol{\alpha}^I) \tag{91}$$

Due to the general non-linearity of $\delta(\boldsymbol{\alpha}^I)$, the minimization is performed following an iterative optimization procedure. Specifically, the sequential quadratic programming (SQP) algorithm is employed for this reason [156]. It is an iterative optimization algorithm that optimizes the non-linear objective function by minimizing a series of quadratic approximations of $\delta(\boldsymbol{\alpha}^I)$. During each iteration of the SQP algorithm, $\tilde{\boldsymbol{y}}_s^C$, $\mathcal{V}_s$, $\mathcal{V}_o$ and $\boldsymbol{c}_s$ are computed using eq. (11) - eq. (88) in order to obtain $\delta(\boldsymbol{\alpha}^{\boldsymbol{I}})$.

In case the projection method is used to reduce the computational cost of the quantification procedure, the identification of the multivariate interval uncertainty

at the input parameters of the model is obtained by incorporating this reduction into eq. (89), which yields:

$$\delta(\boldsymbol{\alpha_i^I}) = \sum_{i=1}^{\binom{d_r}{d_r^+}} \left(\Delta\mathcal{V}_{m,i}^2 + w_o \cdot \Delta\mathcal{V}_{o,i}^2 + \Delta c_i^2 \right) \tag{92}$$

with:

$$\Delta\mathcal{V}_{m,i} = 1 - \frac{\mathcal{V}_{s,i}(\boldsymbol{\alpha_i^I})}{\mathcal{V}_{m,i}} \tag{93a}$$

$$\Delta\mathcal{V}_{o,i} = 1 - \frac{\mathcal{V}_{o,i}(\boldsymbol{\alpha_i^I})}{\mathcal{V}_{m,i}} \tag{93b}$$

$$\Delta c_i = \left\| \boldsymbol{c}_{m,i} - \boldsymbol{c}_{s,i}(\boldsymbol{\alpha_i^I}) \right\|_2 \tag{93c}$$

where $\boldsymbol{c}_{s,i}$ and $\boldsymbol{c}_{m,i}$ are the centers of gravity of respectively $\tilde{\boldsymbol{y}}_{s,i}^C$ and $\tilde{\boldsymbol{y}}_{m,i}^C$. Note that for notational simplicity, the subscript $\mathcal{B}_i^+$ is simplified to i.

7 Illustration: pressure vessel

This case study applies the method that is presented in section 6 to a quasi-static model where the FE model responses are the nodal displacements. In this case study, it is assumed that all responses in the model domain are measurable without noise at the exact locations of the nodes of the FE model. Evidently, this is not true in realistic experimental cases. Nonetheless, the case study serves as a good illustration of the full interval field quantification procedure. This case study was first presented in [61].

7.0.1 Deterministic model

The methods are applied to an axisymmetric finite element model of a cast pressure vessel with spatially uncertain Young's modulus. It is assumed that the distribution of Young's modulus is continuous over the model domain, and that this uncertainty stems from heterogeneity in the post-casting cooling time. The model is discretized using 208 axisymmetric triangular elements with 6 nodes (CTRIAX6), yielding 954 degrees of freedom. Axissymmetric constraints are applied to the nodes at the top and bottom of the geometry. A uniform pressure load P of 50 MPa is applied to the model, and the model is solved for the nodal displacements u_x and u_y. The geometry of the pressure vessel, together with the finite element discretization and boundary conditions, is illustrated in figure 6, with the x-axis being the symmetry axis.

For illustrative purposes, but without loss of generality, it is considered that all responses are measurable at the exact nodal locations of the FE model. Should this not be the case, then the same non-measured responses should be omitted from the uncertain realization set.

For benchmarking purposes, measurement data are numerically generated by means of Monte Carlo sampling from a predefined interval field. The base functions of the interval field are constructed using inverse distance weighting interpolation (see also eq. (21)), with the control points located at the $\boldsymbol{r}_1 = 67^{th}$

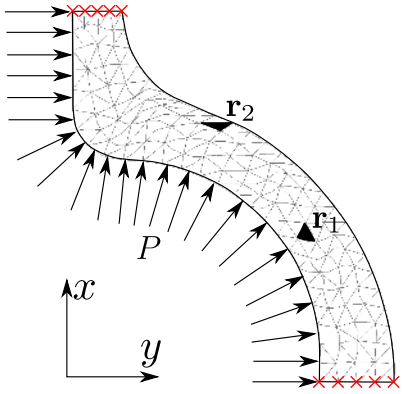

Fig. 6 Model discretization and boundary conditions. (reproduced from [61])

and $\boldsymbol{r}_2 = 134^{th}$ element of the model, corresponding to different cross-sectional areas of the cast part. These locations are also indicated in figure 6. The corresponding interval scalars are chosen to be respectively $\boldsymbol{\alpha_1} = [200; 220]\ GPa$ and $\boldsymbol{\alpha}_2 = [200; 210]\ GPa$. Four measurement data sets are constructed, containing respectively $4^*, 50, 100$ and 250, and the performance of the presented interval field identification is tested with respect to these measurement sets. Specifically, the set containing 4 specimens is constructed by propagating the vertices of the known interval field, yielding the exact gradients of the bounding half-spaces.

7.0.2 Steps 2-3: Interval field dimension

The first step in the quantification procedure is the quantification of the number of base functions (i.e. interval field dimension) of the underlying interval field $\boldsymbol{x^I}(\mathbf{r})$. This quantity should be selected such that the propagation of the interval field yields an uncertain realization set $\tilde{\boldsymbol{y}}_s$ with the same effective dimension of the uncertainty that is captured in the measurement data set.

Figure 7 shows the approximation error ϵ, as defined in eq. (48), when a measurement set $\tilde{y}_m \in \mathbb{R}^{954}$ consisting of either 50, 100 or 250 replicas is represented in a d_r dimensional vector space (i.e., when the *effective* dimension is approximated as d_r). Since the considered model is strictly monotonic, it can be deduced from this figure that $n_b = 2$ for all measurement data sets, as the approximation error $\epsilon < 1 \cdot 10^{-06}$. This analysis also indicates that the identification of the dimension of the interval field that underlies the measurement data set is robust against the measurement data set size.

7.0.3 Step 5: Uncertain realization set model reduction

The FE model consists of 954 degrees of freedom, rendering a computation of $\tilde{\boldsymbol{y}}_m^C$ and $\tilde{\boldsymbol{y}}_s^C$ computationally intractable, taking into account the computational complexity presented in eq. (49). In this case study, the projection method, as presented in section 6.3.2 is applied to project $\tilde{\boldsymbol{y}}_m$ and $\tilde{\boldsymbol{y}}_s$ onto a lower-dimensional

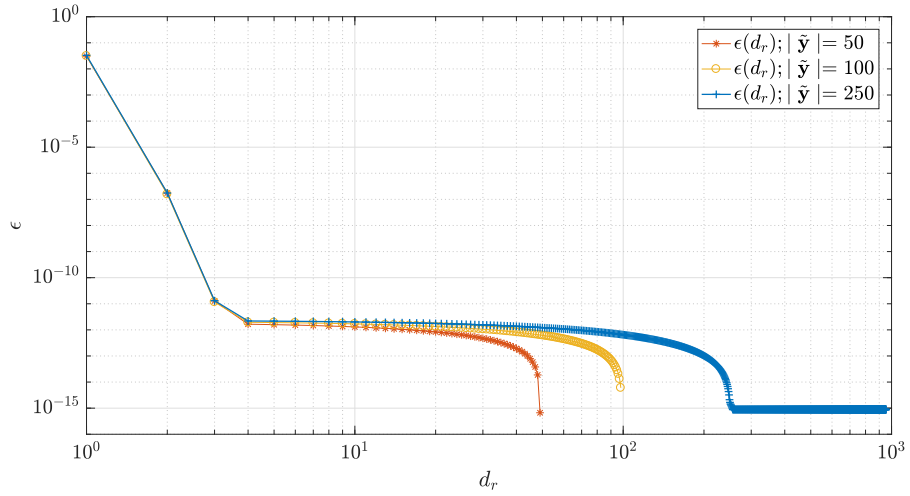

Fig. 7 Approximation error ϵ, as defined in eq. (48), when a measurement set $\tilde{y}_m \in \mathbb{R}^{954}$ consisting of either 50, 100 or 250 replicas is represented in a d_r dimensional vector space (reproduced after [61]).

orthogonal basis with $d_r = 2$ using eq. (60) - (64). This follows from the computation of the effective dimension of $\tilde{\boldsymbol{y}}_m$, as illustrated in figure 7. Figure 8 shows these reduced measurement data sets, together with their respective convex hull $\tilde{\boldsymbol{y}}_m^C$ and minimum volume quadrilateral for all datasets $\tilde{\boldsymbol{y}}_m$. The latter is included to account for measurement data scarcity, as explained in section 6.4.

7.0.4 Step 7: Base function identification

The quantification of the correct basis functions for the interval field series expansion (eq. (19)) is obtained by solving the minimization problem introduced in eq. (74) using an integer implementation of the genetic algorithm (GA) with a population size of 10 specimens and a cross-over fraction of 0.75. The GA is deemed to be converged after 20 stalling generations. This optimization problem is solved for all considered data sets.

The results of the converged optimization are shown in table 1 for the four considered data sets. As may be noted, a perfect identification is only achieved when the extreme realizations are included in $\tilde{\boldsymbol{y}}_m$, as is the case for the data set with 4 replica. Since the 4 replica correspond to the extreme vertices of the interval field, the estimation of the gradients is exact. Also in the other cases, a good approximation of the underlying base functions $\boldsymbol{\psi}_i(\mathbf{r})$ is obtained, as clearly control points in the close vicinity of the correct ones were selected. This is furthermore illustrated in figure 9.

7.0.5 Step 8: Interval scalar quantification

A final step of this illustrative example consists of identifying the interval scalars of the interval field. Also here, the identification is performed using the three data

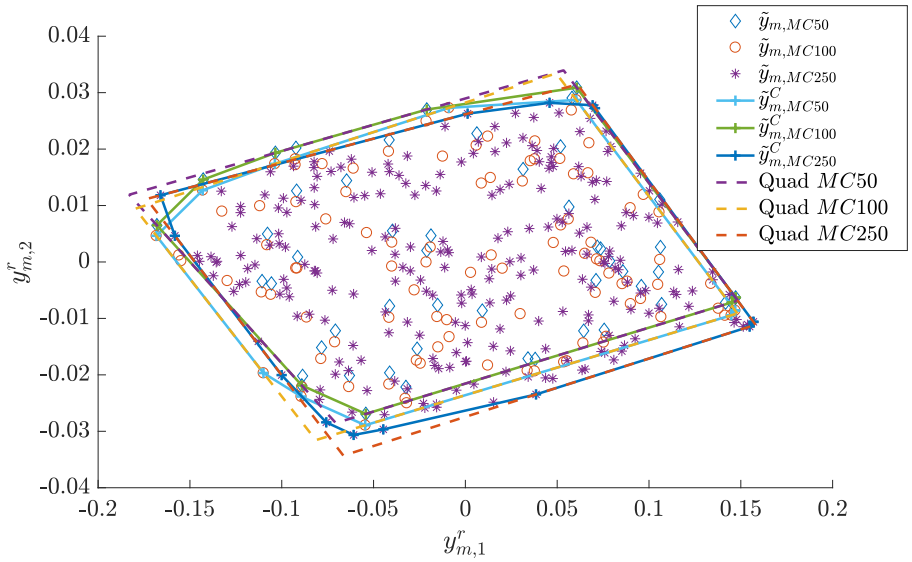

Fig. 8 Reduced measurement data sets, together with their respective convex hull $\tilde{\boldsymbol{y}}^C_m$ and minimum volume polytope for all datasets $\tilde{\boldsymbol{y}}_m$, projected onto the $d_r = 2$-dimensional orthogonal basis $\mathcal{B}$.

Table 1 Result of the identification in terms of identified set of base functions (denoted by the location of their corresponding locally defined interval) and global minimum of the objective function (eq. (74)) as a function of $|\tilde{\boldsymbol{y}}_m|$. The control points of the *goal* base functions are illustrated in yellow.

$\lvert\tilde{\boldsymbol{y}}_m\rvert$	Identified set	error
50	$\boldsymbol{r}_1, \boldsymbol{r}_2 = \{74, 142\}$	0.0013
100	$\boldsymbol{r}_1, \boldsymbol{r}_2 = \{66, 124\}$	$4.26 \cdot 10^{-05}$
250	$\boldsymbol{r}_1, \boldsymbol{r}_2 = \{67, 133\}$	$8.22 \cdot 10^{-05}$
4*	$\boldsymbol{r}_1, \boldsymbol{r}_2 = \{67, 134\}$	0

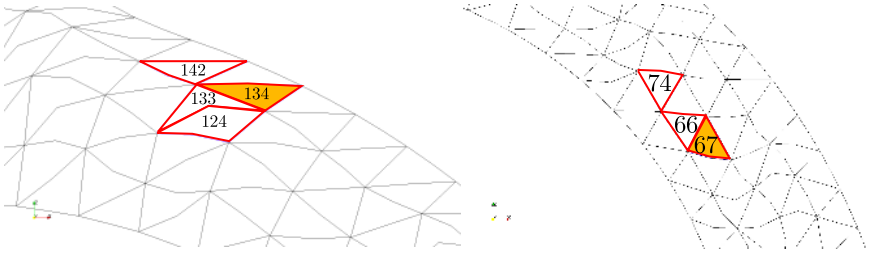

Fig. 9 Element locations of the elements where control points were placed for the construction of the base functions $\boldsymbol{\psi}_i$ of the interval field $\boldsymbol{x}^{\boldsymbol{I}}(\mathbf{r})$ that was used to construct $\tilde{\boldsymbol{y}}_m$ ($\{67, 164\}$), as well as the identified control points (reproduced from [61]).

sets consisting of 50, 100 and 250 samples, based on the quantified basis functions. Also, an interval scalar quantification is performed on a dataset containing 250 samples, but with basis functions that are based on an expert guess. For this case, it is assumed that an expert estates that the control points of the interval field are

located as $\mathbf{r}_1, \mathbf{r}_2 = \{10, 60\}$ (i.e.,the middle element in the second row of elements (counting from the bottom) and the middle element one row under the correct base functions). This corresponds to one reasonable estimate and one estimate that is comparably far off.

This quantification is obtained by solving the optimization problem introduced in (89) using a sequential quadratic programming algorithm [156]. The initial estimate for this optimization problem is arbitrarily set as $\boldsymbol{\alpha}_1 = [120; 150]\ GPa$ and $\boldsymbol{\alpha}_2 = [120; 150]\ GPa$, which is completely disjunct with respect to the interval scalars that were used to construct the measurement data set. For a more rigorous study to the influence of the initial estimate on the optimization problem, the reader is referred to [59].

The results of the converged optimization are shown in table 2. As concerns those cases where the identified basis functions are used, an accurate quantification is obtained. The quality of the quantification is also rather insensitive to the size of the data set. However, the case where an expert estimate is used for the basis functions, the quantified intervals are very wide even though the same convergence criterion was used for the optimization solver. This is explained by the notion that these basis functions map the globally defined interval scalars to local intervals at the element level. Consequently, when this mapping is not correct, the dependence between these local intervals is biased with respect to reality, and the model responses will not conform to the measurement data. Note that the minimum of eq. (89) is obtained by encompassing all measurement data when w_o is set sufficiently large. Since the projection method takes all response data into account by projecting it onto a lower-dimensional basis, the minimum can only be obtained with very wide intervals when the global to local map of the interval uncertainty is incorrect. Conversely, when the subset selection method is used for the reduction of the dimension of the data sets, the intervals will be quantified such that $\tilde{\boldsymbol{y}}_s$ encompasses only the corresponding subset of measured responses. Hence, this estimate will in general not be conservative for the entire interval field when the global to local mapping provided by the basis functions is incorrect.

Table 2 Results of the identification for the three measurement data sets, where the interval scalars are located at the control points of the identified base functions, as well as as the result of the identification of the interval scalars located at the control points of base functions that are constructed on expert knowledge of the analyst (indicated as 250_{eb}).

$\lvert\ \tilde{\boldsymbol{y}}_m\ \rvert$	Initial Estimate	Identified scalars	iterations
50	$\boldsymbol{\alpha}_1 = [120; 150]\ GPa$	$\boldsymbol{\alpha}_1 = [200.05; 220.78]\ GPa$	22
	$\boldsymbol{\alpha}_2 = [120; 150]\ GPa$	$\boldsymbol{\alpha}_2 = [200.11; 209.59]\ GPa$	
100	$\boldsymbol{\alpha}_1 = [120; 150]\ GPa$	$\boldsymbol{\alpha}_1 = [199.34; 220.55]\ GPa$	30
	$\boldsymbol{\alpha}_2 = [120; 150]\ GPa$	$\boldsymbol{\alpha}_2 = [199.81; 209.87]\ GPa$	
250	$\boldsymbol{\alpha}_1 = [120; 150]\ GPa$	$\boldsymbol{\alpha}_1 = [200.06; 219.86]\ GPa$	31
	$\boldsymbol{\alpha}_2 = [120; 150]\ GPa$	$\boldsymbol{\alpha}_2 = [200.08; 209.85]\ GPa$	
250_{eb}	$\boldsymbol{\alpha}_1 = [120; 150]\ GPa$	$\boldsymbol{\alpha}_1 = [158.51; 241.46]\ GPa$	23
	$\boldsymbol{\alpha}_2 = [120; 150]\ GPa$	$\boldsymbol{\alpha}_2 = [179.04; 249.29]\ GPa$	

7.0.6 Concluding remarks

This case study illustrates that theoretically, the presented method is equally applicable to quasi-static FE models, and that also in this context highly accurate results can be obtained. However, three major issues are neglected in this context. First, it was assumed that all nodal displacements were measurable, whereas in practice, considerably more responses throughout Ω are obtained when for instance full field strain measurement techniques such as Digital Image Correlation [116] are applied. Secondly, it was also assumed that all measured responses were obtained at a location in Ω that corresponds perfectly with the location of a node of the FE model. Finally, all noise effects were omitted. Evidently, this does not correspond to a realistic case study, and further refinements of the method need to be made.

However, still some interesting novel insights were provided by this case study. First, it is shown that an exact identification is obtained within reasonable computational cost when the extreme vertices are present in the measurement data set. However, this is in reality intractable. Therefore, these are extrapolated from the other responses on the boundaries of the measurement data set and the effective dimension of the set. Using this extrapolation, it is shown that an accurate identification of the base functions is obtained, even when these vertices are not obtained in the measurement data set. However, the accuracy of the identification strongly depends on the number of responses on the boundary, and degenerates when insufficient responses on the boundary of $\tilde{\boldsymbol{y}}_m^C$ are obtained. Moreover, the effect of using one incorrect basis function on the identified interval field is also illustrated. It is shown that when the interval scalar identification is performed using the projection method for reducing the dimension of the result vectors, the interval bounds become over-conservative in order to completely capture the measurement data. It should be noted that this over-conservatism only occurs in conjunction with the projection method, as all model responses are projected onto a lower-dimensional basis. Indeed, when a subset of responses is selected in this context, the interval scalars are quantified such that they provide an accurate uncertain realization set for those responses only. This set is not necessarily conservative at all for the entire interval field.

8 Inverse approaches in engineering design

Direct comparison of probabilistic (Bayesian) methods and interval/fuzzy concepts for the identification and quantification of multivariate uncertainty is a non-trivial task due to the inherently different philosophy that both techniques are based on. Interval methods are based on the idea that the true value of the uncertain parameter is located between two crisp boundaries, without making inference on the likelihood of each value within that interval. As such, interval UQ methods approach the problem from the *outside*, as they usually provide the analyst with the extreme bounds between which the uncertain parameter is deemed to lie. Bayesian methods on the other hand start from assigning a degree of plausibility to each value of these uncertain parameters within a range and updating this likelihood based on independent data as to infer the most plausible parameter values. As such, Bayesian methods approach the uncertainty from the *inside* by

searching the most probable point, and specifying how the probability decreases away from this point.

Bayesian methods are widely applied in various domains ranging from economics and finance [94,106], marketing [168], over biology [98], to artificial intelligence [113] and structural mechanics [6,8,121,26,25,221], and applications range from small-scale problems to large-scale problems [143,160]. Also their application to the quantification of random fields has been illustrated numerous times [34,28, 187]. Interval methods for inverse UQ on the other hand are introduced only very recently, and their application is mainly limited to purely numerical or small-scale problems.

8.1 Obtained information

When applying Bayesian techniques, a full description of the joint degree of plausibility of each parameter over a range is obtained. However, in order to obtain an objective result, a sufficiently accurate prior estimate of the uncertainty is needed in conjunction with sufficient experimental data. When only scarce experimental data are available, as is usually the case in realistic experimental cases, the prior distribution influences the obtained quantification to a large extent. The obtained results are in this case highly subjective, which limits their credibility. This effect is further amplified when the prior is highly biased with respect to the actual parameter values [189].

In order to obtain a more objective prior, techniques such as the maximum entropy principle [79,103,104,183] have been introduced, alleviating this subjectivity. However, objective in a certain sense and based on a solid mathematical foundation, it is not guaranteed that the maximum entropy principle also yields the physically most probable point. For example, when only information on the range of the non-deterministic parameter is available, the maximum entropy principle yields the uniform distribution as being most appropriate as this distribution has the highest information entropy given the available data. However, with only information on the range, there is no guarantee that each point between the predefined bounds is equally probable. Therefore, while being objective (i.e., independent on estimates of the analyst), the obtained distribution does not correspond to reality. This small-scale example illustrates indeed that this approach is only guaranteed to give a truthful estimation when sufficient data are available to effectively assess the accuracy of the estimated probability distribution.

Interval quantification methods on the other hand deliver crisp bounds between which the uncertain parameter is believed to lie. The main advantage hereof is that each dataset can be uniquely described by an interval. Therefore, this method is inherently objective as no subjective estimates and approximations on the underlying probabilistic nature of the non-determinism are made to steer the quantification process. As long as the measurement data are obtained in an optimised way (i.e., such that they completely capture the needed scatter in the responses that results from the uncertainty that is studied), interval methods moreover provide sufficient information for worst-case analyses. However, it is not possible to assess the reliability of the designed structure using purely interval-based methods.

8.2 Multivariate uncertain parameters and responses

As Bayesian methods are founded on the elaborate probabilistic theory, they are inherently capable of identifying jointly non-deterministic parameters. This is usually attained by defining a joint plausibility function, which is inferred analogously as to a univariate identification problem. It should be noted that the definition of the prior distribution could prove in this context more challenging. Bayesian methods are also easily extendible towards the identification and quantification of key random field parameters such as the statistical moments and/or correlation length, albeit in the Bayesian interpretation of uncertainty. As such, a degree of plausibility is obtained for these parameters.

Intervals are by definition not capable of describing dependency between different variables. As such, the identified non-determinism is inherently decoupled as well, and thus no information on the dependence is obtainable. The recent developments discussed in this paper remediate this shortcoming of the paradigm. Interval fields allow for modeling spatial uncertainty in an interval context, and the discussed quantification method allows for their inverse quantification.

8.3 Computational cost

When no asymptotic approximations of the posterior are attainable in the Bayesian framework, computationally expensive Markov Chain Monte Carlo procedures are needed for its construction. As convergence of these chains in general needs numerous forward propagations to full convergence, MCMC in conjunction with realistic FE models proves to be very computationally demanding. Therefore, often surrogate models are employed, which introduce additional uncertainty if applied improperly. The computational burden is further aggravated by the fact that most MCMC algorithms are very hard or impossible to code in parallel. Finally, the implementation of such Bayesian identification schemes using MCMC proves to be a non-trivial task.

Interval models on the other hand prove to be less computationally intensive as their probabilistic counterparts. This is particularly true when interval arithmetical approaches are employed for the propagation of the interval FE problem. Also in the context of applying global optimization approaches, a reasonable computational cost is obtained when Newton-type optimisers are applied. When combinatorial methods such as the vertex or transformation method are applied, an exponential scaling of the computational cost is obtained with respect to the number of uncertain parameters. Moreover, in the state-of-the-art of inverse identification and quantification of interval uncertain model parameters, also some metaheuristic optimization techniques such as Particle Swarm, Genetic algorithms and Ant Colony optimization are applied. These techniques increase the computational burden heavily as they usually need thousands of interval model evaluations for convergence.

8.4 Measurement data uncertainty

Both techniques may suffer from uncertainty in the measurement data, as often (aleatory) variability is present due to random measurement errors. Therefore measurement system noise is present, as well as biased results due to systematic deviations of the measurement devices due to insufficient calibration. Usually, the order of magnitude of this non-determinism is considerably lower as compared to the one attributed to the numerical model, as long as necessary measurement standards are taken into account and the measurement instruments are properly calibrated. This can be asserted by determining the repeatability and reproducibility of the measurement system [192, 67]. This noise is only problematic when the stability of the minimization of the $\mathcal{L}_2$ norm error that is commonly used in classical probabilistic or interval uncertainty quantification is not ensured due to near rank-deficiency of the corresponding sensitivity matrices (see also section 5). Bayesian techniques are expected to be more robust to these phenomena, as the prior information that is incorporated into the analysis serves as some sort of regularization [176].

8.5 Type of the non-determinism

When considering the identification and quantification of non-deterministic values, an analyst is mostly confronted with either uncertain variability or invariable uncertainty. Both techniques are, apart from the above considerations, equally applicable for the identification and quantification of such non-determinism. Their applicability for invariable uncertainty is straightforward, as the Bayesian method provides a *plausibility* for a range of possible values for this uncertainty, whereas the interval methods provide the analyst with crisp bounds in between which the uncertainty is deemed to be located. As concerns uncertain variability, Bayesian methods should be applied to obtain a plausibility corresponding to the hyperparameters of some hypothesized distributions. Interval methods on the other hand provide also in this context the analyst with crisp bounds for the uncertain variable parameter.

9 Conclusions

This paper discusses non-probabilistic concepts for the forward and inverse quantification of parametric model uncertainty. A survey of interval, fuzzy and convex set approaches is presented both for the modeling and propagation of spatial uncertainty is also provided. Recent advances in interval fields are also discussed. These methods provide a tool to allow for the modeling of spatial uncertainty despite the fact that intervals are independent by definition. Several techniques are discussed and their advantages and drawbacks highlighted. The interval method on the one hand requires very few data points to already provide an analyst with a crisp and objective estimate of the constituting uncertainty. The fuzzy method on the other hand requires the definition of a membership function, which is inherently subjective. Therefore, this class of methods is more regarded either as a subjective tool to transparently incorporate expert knowledge into the design, or as an excellent means to assess the sensitivity of the model to the crisp interval

boundaries. Also a comparison with probabilistic methods is briefly recalled and extended towards the modeling of multi-variate and spatial uncertainty.

Furthermore, a recent survey of inverse methods for non-probabilistic uncertainty quantification is given. The core idea of these methods is to use a set of measured responses to infer the bounds on the uncertainty that is present in the model parameters. The first step in all these methods is the hyper-cubic approximation of the measurement data set, followed by an iterative optimization approach that maps the hyper-cubic result of the interval finite element computation to the hyper-cube of measured data. However, this hyper-cubic representation omits all information on the dependence between these model responses. In this paper, it is discussed how this prevents the quantification of spatial interval uncertainty at the input side of the model, but also gives rise to possible problems with non-uniqueness and ill-posedness of the corresponding optimization problem.

Finally, a very recent development in the context of interval field quantification is presented in full detail. The method starts is based on the computation of the convex hull of the uncertain output set, which originates from propagating the input interval field through the interval FE solver on the one hand, and the calculation of the convex hull of the measurement data on the other hand. The quantification of the interval field at the input side of the model is then obtained by minimizing some well-defined objective functions that describe the discrepancy between both convex hulls. Also two methods to reduce the computational cost that is associated with the computation of the convex hulls are discussed in detail. Two case studies are also highlighted: A case study concerning a quasi-static axisymmetric model of a cast pressure vessel is included to illustrate the method. In this case study, numerically generated measurement data are used to illustrate the performance of the interval field identification and quantification method in the context of quasi-static FE models. To limit the computational cost, the projection method is used to project the set of measurement data and the prediction of the numerical model onto a lower-dimensional basis. It is illustrated that an accurate identification of the base functions is attainable, as long as sufficient extreme responses are enclosed in the measurement data set. The accuracy however degrades when insufficient responses are available. Also, when already one base function for the construction of the interval field is selected inaccurately, the obtained results become quickly very conservative. Both issues stress the need for both an intelligently designed experimental campaign as for identifying the base functions from the measurement data instead of constructing them using expert knowledge.

Finally, also a conceptual comparison with Bayesian methods is given in this paper. This comparison highlights the complementary nature of both approaches. More research is however needed to address specific questions such as to objectify the selection of the most appropriate method given a dataset.

Acknowledgements The authors would like to acknowledge the financial support of the Flemish Research Foundation in the context of the research grant HIDIF (High dimensional interval fields), as for the post-doctoral research grant of Matthias Faes.

Conflict of interest statement

On behalf of all authors, the corresponding author states that there is no conflict of interest.

References

1. Abdel-Tawab, K., Noor, A.K.: Uncertainty analysis of welding residual stress fields. Computer Methods in Applied Mechanics and Engineering **179**(3-4), 327–344 (1999). DOI 10.1016/S0045-7825(99)00045-6
2. Agarwal, H., Renaud, J.E., Preston, E.L., Padmanabhan, D.: Uncertainty quantification using evidence theory in multidisciplinary design optimization. Reliability Engineering & System Safety **85**(1), 281–294 (2004)
3. Ahmadian, H., Mottershead, J., Friswell, M.: Regularisation methods for finite element model updating. Mechanical Systems and Signal Processing **12**(1), 47–64 (1998)
4. Balu, A., Rao, B.: High dimensional model representation based formulations for fuzzy finite element analysis of structures. Finite Elements in Analysis and Design **50**, 217–230 (2012)
5. Barber, C.B., Dobkin, D.P., Huhdanpaa, H.: The quickhull algorithm for convex hulls. ACM Transactions on Mathematical Software **22**(4), 469–483 (1996). DOI 10.1145/235815.235821
6. Beck, J.L., Au, S.K.: Bayesian updating of structural models and reliability using markov chain monte carlo simulation. Journal of Engineering Mechanics **128**(4), 380–391 (2002)
7. Beck, J.L., Katafygiotis, L.S.: Updating models and their uncertainties. i: Bayesian statistical framework. Journal of Engineering Mechanics **124**(4), 455–461 (1998)
8. Beck, J.L., Yuen, K.V.: Model selection using response measurements: Bayesian probabilistic approach. Journal of Engineering Mechanics **130**(2), 192–203 (2004)
9. Beer, M., Ferson, S., Kreinovich, V.: Imprecise probabilities in engineering analyses. Mechanical systems and signal processing **37**(1), 4–29 (2013)
10. Beer, M., Ferson, S., Kreinovich, V.: Imprecise probabilities in engineering analyses. Mechanical Systems and Signal Processing **37**(1), 4 – 29 (2013). DOI http://dx.doi.org/10.1016/j.ymssp.2013.01.024
11. Beer, M., Kreinovich, V.: Interval or moments: Which carry more information? Soft Computing **17**(8), 1319–1327 (2013). DOI 10.1007/s00500-013-1002-1
12. Beer, M., Liebscher, M., Möller, B.: Structural design under fuzzy randomness. In: Proceedings of the NSF workshop on Reliable Engineering Computing, pp. 215–234 (2004)
13. de Berg, M., Cheong, O., van Kreveld, M., Overmars, M.: Computational Geometry. Springer, Berlin, Heidelberg (2008). DOI 10.1007/978-3-540-77974-2
14. Betz, W., Papaioannou, I., Straub, D.: Numerical methods for the discretization of random fields by means of the Karhunen-Loeve expansion. Computer Methods in Applied Mechanics and Engineering **271**, 109–129 (2014). DOI 10.1016/j.cma.2013.12.010
15. Biondini, F., Bontempi, F., Malerba, P.G.: Fuzzy reliability analysis of concrete structures. Computers and Structures **82**(13-14), 1033–1052 (2004). DOI 10.1016/j.compstruc.2004.03.011
16. de Boor, C., Ron, A.: On multivariate polynomial interpolation. Constructive Approximation **6**(3), 287–302 (1990). DOI 10.1007/BF01890412
17. Boulkaibet, I., Marwala, T., Friswell, M., Khodaparast, H.H., Adhikari, S.: Fuzzy finite element model updating using metaheuristic optimization algorithms. arXiv preprint arXiv:1701.00833 (2017)
18. Bulgakov, B.V.: Fehleranhäufung bei kreiselapparaten. Ingenieur-Archiv **11**(6), 461–469 (1940). DOI 10.1007/BF02088988
19. Bulgakov, B.V.: On the accumulation of disturbances in linear os- cillatory systems with constant coefficients (in russian). Proceedings of the USSR Academy of Sciences **51**, 343–345 (1946)
20. Butlin, T.: Anti-optimisation for modelling the vibration of locally nonlinear structures: An exploratory study. Journal of Sound and Vibration **332**(26), 7099–7122 (2013). DOI 10.1016/j.jsv.2013.06.028
21. Campi, M.C., Calafiore, G., Garatti, S.: Interval predictor models: Identification and reliability. Automatica **45**(2), 382–392 (2009)

22. Catallo, L.: Genetic anti-optimization for reliability structural assessment of precast concrete structures. Computers and Structures **82**(13-14), 1053–1065 (2004). DOI 10.1016/j.compstruc.2004.03.018
23. Chen, L., Rao, S.: Fuzzy finite-element approach for the vibration analysis of imprecisely-defined systems. Finite Elements in Analysis and Design **27**(1), 69–83 (1997). DOI 10.1016/S0168-874X(97)00005-X
24. Chen, S., Lian, H., Yang, X.: Interval static displacement analysis for structures with interval parameters. International Journal for Numerical Methods in Engineering **53**(2), 393–407 (2002). DOI 10.1002/nme.281
25. Cheung, S.H., Beck, J.L.: Bayesian model updating using hybrid monte carlo simulation with application to structural dynamic models with many uncertain parameters. Journal of engineering mechanics **135**(4), 243–255 (2009)
26. Ching, J., Chen, Y.C.: Transitional markov chain monte carlo method for bayesian model updating, model class selection, and model averaging. Journal of engineering mechanics **133**(7), 816–832 (2007)
27. Choi, C.K., Yoo, H.H.: Stochastic modeling and vibration analysis of rotating beams considering geometric random fields. Journal of Sound and Vibration **388**, 105 – 122 (2017). DOI http://dx.doi.org/10.1016/j.jsv.2016.10.030
28. Chowdhary, K., Najm, H.N.: Bayesian estimation of karhunen–loève expansions; a random subspace approach. Journal of Computational Physics **319**, 280 – 293 (2016). DOI https://doi.org/10.1016/j.jcp.2016.02.056
29. Civanlar, M.R., Trussell, H.J.: Constructing membership functions using statistical data. Fuzzy sets and systems **18**(1), 1–13 (1986)
30. Comba, J.L.D., Stolfi, J.: Affine arithmetic and its applications to computer graphics (1993)
31. Crespo, L.G., Kenny, S.P., Giesy, D.P.: Interval predictor models with a linear parameter dependency. Journal of Verification, Validation and Uncertainty Quantification **1**(2), 021007 (2016)
32. Crombecq, K., Couckuyt, I., Gorissen, D., Dhaene, T.: Space-filling sequential design strategies for adaptive surrogate modelling. In: The first international conference on soft computing technology in civil, structural and environmental engineering (2009)
33. De Munck, M., Moens, D., Desmet, W., Vandepitte, D.: An efficient response surface based optimisation method for non-deterministic harmonic and transient dynamic analysis. CMES - Computer Modeling in Engineering and Sciences **47**(2), 119–166 (2009). DOI 10.3970/cmes.2009.047.119
34. De Oliveira, V., Kedem, B., Short, D.A.: Bayesian prediction of transformed gaussian random fields. Journal of the American Statistical Association **92**(440), 1422–1433 (1997)
35. Degrauwe, D., Lombaert, G., Roeck, G.D.: Improving interval analysis in finite element calculations by means of affine arithmetic. Computers & Structures **88**(3–4), 247 – 254 (2010). DOI http://dx.doi.org/10.1016/j.compstruc.2009.11.003
36. Dempster, A.P.: Upper and lower probabilities induced by a multivalued mapping. The annals of mathematical statistics pp. 325–339 (1967)
37. Deng, Z., Guo, Z., Zhang, X.: Non-probabilistic set-theoretic models for transient heat conduction of thermal protection systems with uncertain parameters. Applied Thermal Engineering **95**, 10–17 (2016)
38. Deng, Z., Guo, Z., Zhang, X.: Interval model updating using perturbation method and radial basis function neural networks. Mechanical Systems and Signal Processing **84**, 699–716 (2017)
39. Di, W., Wei, G.: Uncertain static plane stress analysis with interval fields. International Journal for Numerical Methods in Engineering **110**(13), 1272–1300 (2016). DOI 10.1002/nme.5457. URL https://onlinelibrary.wiley.com/doi/abs/10.1002/nme.5457
40. Do, D.M., Gao, W., Song, C.: Stochastic finite element analysis of structures in the presence of multiple imprecise random field parameters. Computer Methods in Applied Mechanics and Engineering **300**, 657 – 688 (2016). DOI http://dx.doi.org/10.1016/j.cma.2015.11.032
41. Dogan, M., Van Dam, R.L., Liu, G., Meerschaert, M.M., Butler, J.J., Bohling, G.C., Benson, D.A., Hyndman, D.W.: Predicting flow and transport in highly heterogeneous alluvial aquifers. Geophysical Research Letters **41**(21), 7560–7565 (2014)
42. Dolbow, J., Belytschko, T.: A finite element method for crack growth without remeshing. International journal for numerical methods in engineering **46**(1), 131–150 (1999)

43. Donders, S., Vandepitte, D., Van de Peer, J., Desmet, W.: The short transformation method to predict the frf of dynamic structures subject to uncertainty. In: Proc. of ISMA, pp. 3043–3054 (2004)
44. Donders, S., Vandepitte, D., de Peer, J.V., Desmet, W.: Assessment of uncertainty on structural dynamic responses with the short transformation method. Journal of Sound and Vibration **288**(3), 523 – 549 (2005). DOI http://doi.org/10.1016/j.jsv.2005.07.003. Uncertainty in structural dynamicsUncertainty in structural dynamics
45. Dong, W., Shah, H.C.: Vertex Method for Computing of Fuzzy Variables. Fuzzy Sets and Systems **24**, 65–78 (1987). DOI 10.1016/0165-0114(87)90114-X
46. Dorigo, M., Birattari, M., Stutzle, T.: Ant colony optimization. IEEE computational intelligence magazine **1**(4), 28–39 (2006)
47. Dubois, D., Prade, H.: Possibility theory: an approach to computerized processing of uncertainty. Springer Science & Business Media (2012)
48. Elishakoff, I.: An idea of uncertainty triangle. The Shock and Vibration Digest **22**(10), 1 (1990)
49. Elishakoff, I.: Possible Limitations of Probabilistic Methods in Engineering. Applied Mechanics Reviews **53**(2), 19 (2000). DOI 10.1115/1.3097337
50. Elishakoff, I.: Possible limitations of probabilistic methods in engineering. Applied Mechanics Reviews **53**(2), 19–36 (2000)
51. Elishakoff, I., Miglis, Y.: Novel parameterized intervals may lead to sharp bounds. Mechanics Research Communications **44**, 1 – 8 (2012). DOI http://doi.org/10.1016/j.mechrescom.2012.04.004
52. Elishakoff, I., Sarlin, N.: Uncertainty quantification based on pillars of experiment, theory, and computation. Part I: Data analysis. Mechanical Systems and Signal Processing **74**, 54–72 (2016). DOI 10.1016/j.ymssp.2015.04.035
53. Elishakoff, I., Sarlin, N.: Uncertainty quantification based on pillars of experiment, theory, and computation. Part II: Theory and computation. Mechanical Systems and Signal Processing2 **74** (2016)
54. Engl, H.W., Hanke, M., Neubauer, A.: Regularization of inverse problems, vol. 375. Springer Science & Business Media (1996)
55. Faes, M.: Interval methods for the identification and quantification of inhomogeneous uncertainty in finite element models. Ph.D. thesis, KU Leuven, Department of Mechanical Engineering (2017)
56. Faes, M., Broggi, M., Beer, M., Moens, D.: Failure probability under uncertain surrogate model predictions. In: Proceedings of the joint ICVRAM ISUMA UNCERTAINTIES conference (2018)
57. Faes, M., Broggi, M., Patelli, E., Govers, Y., Mottershead, J., Beer, M., Moens, D.: A multivariate interval approach for inverse uncertainty quantification with limited experimental data. Mechanical Systems and Signal Processing **118**, 534–548 (2019). DOI 10.1016/j.ymssp.2018.08.050. URL https://doi.org/10.1016/j.ymssp.2018.08.050 https://www.sciencedirect.com/science/article/pii/S0888327018305946?via%3Dihub
58. Faes, M., Cerneels, J., Vandepitte, D., Moens, D.: Identification of Interval Fields for Spatial Uncertainty Representation in Finite Element Models. In: Proceedings of the VII European Congress on Computational Methods in Applied Sciences and Engineering (ECCOMAS Congress 2016), vol. 3, pp. 6091–6098 (2016). DOI 10.7712/100016.2243.4995. URL http://www.eccomasproceedia.org/conferences/eccomas-congresses/eccomas-congress-2016/2243
59. Faes, M., Cerneels, J., Vandepitte, D., Moens, D.: Identification and quantification of multivariate interval uncertainty in finite element models. Computer Methods in Applied Mechanics and Engineering **315**, 896–920 (2017). DOI 10.1016/j.cma.2016.11.023. URL http://dx.doi.org/10.1016/j.cma.2016.11.023
60. Faes, M., Cerneels, J., Vandepitte, D., Moens, D.: Influence of measurement data metrics on the identification of interval fields for the representation of spatial variability in finite element models. PAMM **16**(1), 27–30 (2017). DOI 10.1002/pamm.201610008. URL https://onlinelibrary.wiley.com/doi/abs/10.1002/pamm.201610008
61. Faes, M., Moens, D.: Identification and quantification of spatial interval uncertainty in numerical models. Computers and Structures **192**, 16–33 (2017). DOI 10.1016/j.compstruc.2017.07.006
62. Faes, M., Moens, D.: Multivariate dependent interval finite element analysis via convex hull pair constructions and the extended transformation method. Computer Methods in Applied Mechanics and Engineering **347**,

85 – 102 (2019). DOI https://doi.org/10.1016/j.cma.2018.12.021. URL http://www.sciencedirect.com/science/article/pii/S0045782518306200
63. Fang, S.E., Zhang, Q.H., Ren, W.X.: An interval model updating strategy using interval response surface models. Mechanical Systems and Signal Processing **60-61**, 909–927 (2015). DOI 10.1016/j.ymssp.2015.01.016
64. Farkas, L., Moens, D., Donders, S., Vandepitte, D.: Optimisation study of a vehicle bumper subsystem with fuzzy parameters. Mechanical Systems and Signal Processing **32**, 59–68 (2012)
65. Farley, B., Clark, W.: Simulation of self-organizing systems by digital computer. Transactions of the IRE Professional Group on Information Theory **4**(4), 76–84 (1954). DOI 10.1109/TIT.1954.1057468
66. Fedele, F., Muhanna, R.L., Xiao, N., Mullen, R.L.: Interval-Based Approach for Uncertainty Propagation in Inverse Problems. Journal of Engineering Mechanics **4**(1), 1–7 (2014). DOI 10.1061/(ASCE)EM.1943-7889.0000815
67. Ferson, S., Ginzburg, L.R.: Different methods are needed to propagate ignorance and variability. Reliability Engineering & System Safety **54**(2), 133 – 144 (1996). DOI http://dx.doi.org/10.1016/S0951-8320(96)00071-3
68. Ferson, S., Kreinovich, V., Ginzburg, L., Myers, D.S., Sentz, K.: Constructing probability boxes and dempster-shafer structures. Tech. rep., Technical report, Sandia National Laboratories (2003)
69. Ferson, S., Moore, D.R., Van Den Brink, P., Estes, T., Gallagher, K., Connor, R., Verdonck, F.: Bounding uncertainty analyses. Application of uncertainty analysis to ecological risks of pesticides (2010)
70. Ferson, S., Siegrist, J.: Verified computation with probabilities. In: Uncertainty Quantification in Scientific Computing, pp. 95–122. Springer (2012)
71. Fisher, R.: Presidential address by professor ra fisher, sc. d., frs. The Indian Journal of Statistics **4**(1), 14–17 (1938)
72. Fleissner, F., Haag, T., Hanss, M., Eberhard, P.: Analysis of granular chute flow based on a particle model including uncertainties. Trends in Computational Contact Mechanics pp. 121–134 (2011)
73. Gabriele, S., Brancaleoni, F., Spina, D.: Model updating of pescara benchmark: interval vs. traditional method. In: Journal of Physics: Conference Series, vol. 305, p. 012083. IOP Publishing (2011)
74. Gabriele, S., Valente, C.: An interval-based technique for fe model updating. International Journal of Reliability and Safety **3**(1-3), 79–103 (2009)
75. Gotz, M., Leichsenring, F., Graf, W., Michael, K.: Four types of dependencies for fuzzy analysis. In: Proceedings of the 6th European Conference on Computational Mechanics (ECCM). ECCOMAS (2018)
76. Govers, Y., Haddad Khodaparast, H., Link, M., Mottershead, J.E.: A comparison of two stochastic model updating methods using the DLR AIRMOD test structure. Mechanical Systems and Signal Processing **52-53**(1), 105–114 (2015)
77. Graf, W., Götz, M., Kaliske, M.: Analysis of dynamical processes under consideration of polymorphic uncertainty. Structural Safety **52**, 194 – 201 (2015). DOI https://doi.org/10.1016/j.strusafe.2014.09.003. URL http://www.sciencedirect.com/science/article/pii/S0167473014000861. Engineering Analyses with Vague and Imprecise Information
78. Gratiet, L.L., Marelli, S., Sudret, B.: Metamodel-based sensitivity analysis: polynomial chaos expansions and gaussian processes. Handbook of Uncertainty Quantification pp. 1–37 (2016)
79. Gull, S.F.: Bayesian inductive inference and maximum entropy, pp. 53–74. Springer (1988)
80. Haag, T., González, S.C., Hanss, M.: Model validation and selection based on inverse fuzzy arithmetic. Mechanical Systems and Signal Processing **32**, 116–134 (2012)
81. Haag, T., Hanss, M.: Model assessment using inverse fuzzy arithmetic. Information Processing and Management of Uncertainty in Knowledge-Based Systems. Applications pp. 461–470 (2010)
82. Haag, T., Hanss (sup.), M., Moens (cosup.), D., Gaul (cosup.), L.: Forward and Inverse Fuzzy Arithmetic for Uncertainty Analysis with Applications to Structural Mechanics. Phd thesis, Universit{ä}t Stuttgart (2012)
83. Haag, T., Herrmann, J., Hanss, M.: Identification procedure for epistemic uncertainties using inverse fuzzy arithmetic. Mechanical Systems and Signal Processing **24**(7), 2021–2034 (2010)

84. Haddad Khodaparast, H., Govers, Y., Adhikari, S., Link, M., Friswell, M.I., Mottershead, J.E., Sienz, J.: Fuzzy model updating and its application to the DLR AIRMOD test structure. In: P. Sas, D. Moens, H. Denayer (eds.) Proceedings of the International Conference on Uncertainty in Structural Dynamics, USD 2014, pp. 4509–4522. {KU} {L}euven, Leuven, Belgium (2014)
85. Hansen, E., Walster, G.W.: Global optimization using interval analysis: revised and expanded, vol. 264. CRC Press (2003)
86. Hansen, P.C.: Rank-deficient and discrete ill-posed problems: numerical aspects of linear inversion. SIAM (1998)
87. Hanss, M.: The transformation method for the simulation and analysis of systems with uncertain parameters. Fuzzy Sets and Systems **130**(3), 277–289 (2002). DOI 10.1016/S0165-0114(02)00045-3
88. Hanss, M.: An approach to inverse fuzzy arithmetic. In: 22nd International Conference of the North American Fuzzy Information Processing Society, NAFIPS 2003, pp. 474–479 (2003). DOI 10.1109/NAFIPS.2003.1226831
89. Hanss, M.: The extended transformation method for the simulation and analysis of fuzzy-parameterized models. International Journal of Uncertainty, Fuzziness and Knowledge-Based Systems **11**(06), 711–727 (2003). DOI 10.1142/S0218488503002491
90. Hanss, M.: Applied Fuzzy Arithmetic: an Introduction with Engineering Applications. Springer, Berlin (2005)
91. Hanss, M., Gauger, U., Turrin, S.: Fuzzy arithmetical robustness analysis of mechanical structures with uncertainties. In: Internat. Conf. on Computational Structures Technology, Gran Canaria, Spain (2006)
92. Hanss, M., Klimke, A.: On the reliability of the influence measure in the transformation method of fuzzy arithmetic. Fuzzy Sets and Systems **143**(3), 371–390 (2004)
93. Hanss, M., Turrin, S.: A fuzzy-based approach to comprehensive modeling and analysis of systems with epistemic uncertainties. Structural Safety **32**(6), 433–441 (2010)
94. Harvey, C.R., Zhou, G.: Bayesian inference in asset pricing tests. Journal of Financial Economics **26**(2), 221–254 (1990)
95. Hoffman, F.O., Hammonds, J.S.: Propagation of uncertainty in risk assessments: The need to distinguish between uncertainty due to lack of knowledge and uncertainty due to variability. Risk Analysis **14**(5), 707–712 (1994). DOI 10.1111/j.1539-6924.1994.tb00281.x
96. Hristopulos, D.T.: Spartan gibbs random field models for geostatistical applications. SIAM Journal on Scientific Computing **24**(6), 2125–2162 (2003)
97. Hsu, C.W., Lin, C.J.: A comparison of methods for multiclass support vector machines. IEEE transactions on Neural Networks **13**(2), 415–425 (2002)
98. Huelsenbeck, J.P., Ronquist, F., Nielsen, R., Bollback, J.P.: Bayesian inference of phylogeny and its impact on evolutionary biology. science **294**(5550), 2310–2314 (2001)
99. Hughes, T.J., Cottrell, J.A., Bazilevs, Y.: Isogeometric analysis: Cad, finite elements, nurbs, exact geometry and mesh refinement. Computer methods in applied mechanics and engineering **194**(39), 4135–4195 (2005)
100. Imholz, M., Vandepitte, D., Moens, D.: Analysis of the effect of uncertain clamping stiffness on the dynamical behaviour of structures using interval field methods. In: Applied Mechanics and Materials, vol. 807, pp. 195–204. Trans Tech Publ (2015)
101. Imholz, M., Vandepitte, D., Moens, D.: Derivation of an Input Interval Field Decomposition Based on Expert Knowledge Using Locally Defined Basis Functions. In: 1st ECCOMAS Thematic Conference on International Conference on Uncertainty Quantification in Computational Sciences and Engineering, pp. 1–19 (2015)
102. Imholz, M., Vandepitte, D., Moens, D.: Application of interval fields to fit experimental data on deepdrawn components. Proceedings of the joint ICVRAM ISUMA UNCERTAINTIES conference (2) (2018)
103. Jaynes, E.T.: Information theory and statistical mechanics. Phys. Rev. **106**, 620–630 (1957). DOI 10.1103/PhysRev.106.620
104. Jaynes, E.T.: Information theory and statistical mechanics. ii. Phys. Rev. **108**, 171–190 (1957). DOI 10.1103/PhysRev.108.171
105. Jinglai, W., Zhen, L., Yunqing, Z., Nong, Z., Liping, C.: Interval uncertain method for multibody mechanical systems using chebyshev inclusion functions. International Journal for Numerical Methods in Engineering **95**(7), 608–630 (2013). DOI 10.1002/nme.4525. URL https://onlinelibrary.wiley.com/doi/abs/10.1002/nme.4525
106. Kandel, S., McCulloch, R., Stambaugh, R.F.: Bayesian inference and portfolio efficiency. Review of Financial Studies **8**(1), 1–53 (1995)

107. Katafygiotis, L.S., Beck, J.L.: Updating models and their uncertainties. ii:model identifiability. Journal of Engineering Mechanics **124**(4), 463–467 (1998)
108. Kennedy, J.: Particle swarm optimization. In: Encyclopedia of machine learning, pp. 760–766. Springer (2011)
109. Kennedy, M.C., O'Hagan, A.: Bayesian calibration of computer models. Journal of the Royal Statistical Society: Series B (Statistical Methodology) **63**(3), 425–464 (2001)
110. Khodaparast, H.H., Mottershead, J.E., Badcock, K.J.: Interval model updating with irreducible uncertainty using the Kriging predictor. Mechanical Systems and Signal Processing **25**(4), 1204–1206 (2011). DOI 10.1016/j.ymssp.2010.10.009
111. der Kiureghian, A., Ditlevsen, O.: Aleatory or epistemic? Does it matter? Structural Safety **31**(2), 105–112 (2009). DOI 10.1016/j.strusafe.2008.06.020
112. Klimke, A., Nunes, R.F., Wohlmuth, B.: Fuzzy Arithmetic Based on Dimension-Adaptive Sparse Grids: a Case Study of a Large-Scale Finite Element Model Under Uncertain Parameters. International Journal of Uncertainty, Fuzziness and Knowledge-Based Systems **14**(05), 561–577 (2006). DOI 10.1142/S0218488506004199
113. Kononenko, I.: Bayesian neural networks. Biological Cybernetics **61**(5), 361–370 (1989)
114. Köylüoglu, H., Elishakoff, I.: A comparison of stochastic and interval finite elements applied to shear frames with uncertain stiffness properties. Computers & Structures **67**(1-3), 91–98 (1998). DOI 10.1016/S0045-7949(97)00160-0
115. Kulpa, Z., Pownuk, A., Skalna, I.: Analysis of linear mechanical structures with uncertainties by means of interval methods. Computer Assisted Mechanics and Engineering Sciences **5**(4), 443–477 (1998)
116. Lava, P., Cooreman, S., Coppieters, S., De Strycker, M., Debruyne, D.: Assessment of measuring errors in DIC using deformation fields generated by plastic FEA. Optics and Lasers in Engineering **47**(7-8), 747–753 (2009). DOI 10.1016/j.optlaseng.2009.03.007
117. Legault, J., Langley, R., Woodhouse, J.: Physical consequences of a nonparametric uncertainty model in structural dynamics. Journal of Sound and Vibration **331**(25), 5469 – 5487 (2012). DOI http://doi.org/10.1016/j.jsv.2012.07.017
118. Manson, G.: Calculating frequency response functions for uncertain systems using complex affine analysis. Journal of Sound and Vibration **288**(3), 487–521 (2005). DOI 10.1016/j.jsv.2005.07.004
119. de Marsily, G., Delay, F., Teles, V., Schafmeister, M.T.: Some current methods to represent the heterogeneity of natural media in hydrogeology. Hydrogeology Journal **6**(1), 115–130 (1998). DOI 10.1007/s100400050138
120. Martin, J.D., Simpson, T.W.: Use of Kriging Models to Approximate Deterministic Computer Models. AIAA Journal **43**(4), 853–863 (2005). DOI 10.2514/1.8650
121. Marwala, T., Mdlazi, L., Sibisi, S.: Finite element model updating using bayesian approach. arXiv preprint arXiv:0705.2515 (2007)
122. Massa, F., Ruffin, K., Tison, T., Lallemand, B.: A complete method for efficient fuzzy modal analysis. Journal of Sound and Vibration **309**(1-2), 63–85 (2008). DOI 10.1016/j.jsv.2007.06.004
123. Massa, F., Tison, T., Lallemand, B.: A fuzzy procedure for the static design of imprecise structures. Computer Methods in Applied Mechanics and Engineering **195**(9-12), 925–941 (2006). DOI 10.1016/j.cma.2005.02.015
124. McCulloch, W.S., Pitts, W.: A logical calculus of the ideas immanent in nervous activity. The bulletin of mathematical biophysics **5**(4), 115–133 (1943). DOI 10.1007/BF02478259
125. McDonald, D.B., Grantham, W.J., Tabor, W.L.: Response surface development for global/local optimization using radial basis functions. In: Aiaa 2000-4776. AIAA, Long Beach, CA, USA (2005)
126. McWilliam, S.: Anti-optimisation of uncertain structures using interval analysis. Computers {&} Structures **79**(4), 421–430 (2001). DOI 10.1016/S0045-7949(00)00143-7
127. Mehrez, L., Doostan, A., Moens, D., Vandepitte, D.: Stochastic identification of composite material properties from limited experimental databases, Part II: Uncertainty modelling. Mechanical Systems and Signal Processing **27**(1), 484–498 (2012). DOI 10.1016/j.ymssp.2011.09.001
128. Missoum, S., Lacaze, S., Amabili, M., Alijani, F.: Identification of material properties of composite sandwich panels under geometric uncertainty. Composite Structures (2017). DOI http://dx.doi.org/10.1016/j.compstruct.2017.07.020
129. Modares, M., Venkitaraman, S.: Reliable condition assessment of structures using hybrid structural measurements and structural uncertainty analyses. Structural Safety **52**, 202–208 (2015)

130. Moens, D., De Munck, M., Desmet, W., Vandepitte, D.: Numerical dynamic analysis of uncertain mechanical structures based on interval fields. In: IUTAM symposium on the vibration analysis of structures with uncertainties, pp. 71–83. Springer (2011)
131. Moens, D., De Munck, M., Vandepitte, D.: Envelope frequency response function analysis of mechanical structures with uncertain modal damping characteristics. Computer Modelling in Engineering & Sciences **22**(2), 129–149 (2007)
132. Moens, D., Hanss, M.: Non-probabilistic finite element analysis for parametric uncertainty treatment in applied mechanics: Recent advances. Finite Elements in Analysis and Design **47**(1), 4–16 (2011). DOI 10.1016/j.finel.2010.07.010
133. Moens, D., Vandepitte, D.: An interval finite element approach for the calculation of envelope frequency respons functions. International journal for numerical methods in engineering **61**(14), 2480–2507 (2004)
134. Moens, D., Vandepitte, D.: Recent advances in non-probabilistic approaches for non-deterministic dynamic finite element analysis. Archives of Computational Methods in Engineering **13**(3), 389–464 (2006). DOI 10.1007/BF02736398
135. Moens, D., Vandepitte, D.: Interval sensitivity theory and its application to frequency response envelope analysis of uncertain structures. Computer Methods in Applied Mechanics and Engineering **196**(21-24), 2486–2496 (2007). DOI 10.1016/j.cma.2007.01.006
136. Möller, B.: Fuzzy randomness–a contribution to imprecise probability. ZAMM-Journal of Applied Mathematics and Mechanics/Zeitschrift für Angewandte Mathematik und Mechanik **84**(10-11), 754–764 (2004)
137. Möller, B., Beer, M.: Fuzzy randomness: uncertainty in civil engineering and computational mechanics. Springer Science & Business Media (2013)
138. Möller, B., Beer, M., Graf, W., Sickert, J.U.: Time-dependent reliability of textile-strengthened rc structures under consideration of fuzzy randomness. Computers & Structures **84**(8), 585–603 (2006)
139. Möller, B., Beer, M., Reuter, U.: Theoretical basics of fuzzy randomness-application to time series with fuzzy data. In: CD Proc. of 9th Int. Conf. On Structural Safety and Reliability ICOSSAR, vol. 5 (2005)
140. Möller, B., Graf, W., Beer, M.: Fuzzy structural analysis using alpha-level optimization. Computational Mechanics **26**(6), 547–565 (2000). DOI 10.1007/s004660000204
141. Möller, B., Graf, W., Beer, M.: Fuzzy structural analysis using α-level optimization. Computational Mechanics **26**(6), 547–565 (2000)
142. Möller, B., Graf, W., Beer, M.: Safety assessment of structures in view of fuzzy randomness. Computers & Structures **81**(15), 1567–1582 (2003)
143. Monelli, D., Mai, P.: Bayesian inference of kinematic earthquake rupture parameters through fitting of strong motion data. Geophysical Journal International **173**(1), 220–232 (2008)
144. Moore, R.E.: Interval arithmetic and automatic error analysis in digital computing. Ph.D. thesis, Stanford University, Department of Mathematics (1962)
145. Moore, R.E.: Methods and applications of interval analysis. SIAM (1979)
146. Moore, R.T.: Interval Analysis, vol. 4. Prentice Hall, Englewood Cliffs (1966). DOI 10.1016/0016-0032(67)90590-X
147. Mottershead, J., Friswell, M.: Model updating in structural dynamics: a survey. Journal of sound and vibration **167**(2), 347–375 (1993)
148. Muhanna, R.L., Mullen, R.L.: Uncertanty in mechanics problems- interval based approach. Journal of engineering mechanics **127**(6), 557–566 (2001)
149. Muhanna, R.L., Mullen, R.L., Zhang, H.: Penalty-Based Solution for the Interval Finite-Element Methods. Journal of Engineering Mechanics **131**(October), 1102–1112 (2005). DOI 10.1061/(ASCE)0733-9399(2005)131:10(1102)
150. Mullen, R.L.M.H.Z.R.L.: Combined axial and bending stiffness in interval finite-element methods. Journal of Structural Engineering **133**(12), 1700–1709 (2007). DOI 10.1061/(ASCE)0733-9445(2007)133:12(1700)
151. Muscolino, G., Santoro, R., Sofi, A.: Explicit sensitivities of the response of discretized structures under stationary random processes. Probabilistic Engineering Mechanics **35**, 82–95 (2014)
152. Muscolino, G., Santoro, R., Sofi, A.: Explicit reliability sensitivities of linear structures with interval uncertainties under stationary stochastic excitation. Structural Safety **52**, 219–232 (2015)
153. Muscolino, G., Sofi, A.: Stochastic analysis of structures with uncertain-but-bounded parameters via improved interval analysis. Probabilistic Engineering Mechanics **28**, 152–163 (2012). DOI 10.1016/j.probengmech.2011.08.011

154. Muscolino, G., Sofi, A.: Bounds for the stationary stochastic response of truss structures with uncertain-but-bounded parameters. Mechanical Systems and Signal Processing **37**(1), 163–181 (2013)
155. Nicolaï, B.M., Egea, J.A., Scheerlinck, N., Banga, J.R., Datta, A.K.: Fuzzy finite element analysis of heat conduction problems with uncertain parameters. Journal of Food Engineering **103**(1), 38–46 (2011). DOI 10.1016/j.jfoodeng.2010.09.017
156. Nocedal, J., Wright, S.J.: Numerical Optimization. Springer (1999). DOI 10.1007/b98874
157. Oberkampf, W., DeLand, S., Rutherford, B., Diegert, K., Alvin, K.: A new methodology for the estimation of total uncertainty in computational simulation. In: A new methodology for the estimation of total uncertainty in computational simulation, pp. 3061–3083 (1999)
158. Oberkampf, W.L., Trucano, T.G., Hirsch, C.: Verification, validation, and predictive capability in computational engineering and physics. Applied Mechanics Reviews **57**(5), 345–384 (2004)
159. Otto, K., Antonsson, E.: Imprecision in engineering design. ASME J. Mech. Des **117**, 25–32 (1995)
160. Patelli, E., Govers, Y., Broggi, M., Gomes, H.M., Link, M., Mottershead, J.E.: Sensitivity or bayesian model updating: a comparison of techniques using the dlr airmod test data. Archive of Applied Mechanics pp. 1–21 (2017). DOI 10.1007/s00419-017-1233-1
161. Pota, M., Esposito, M., Pietro, G.D.: Transforming probability distributions into membership functions of fuzzy classes: A hypothesis test approach. Fuzzy Sets and Systems **233**, 52 – 73 (2013). DOI http://dx.doi.org/10.1016/j.fss.2013.03.013
162. Qiu, Z., Elishakoff, I.: Antioptimization of structures with large uncertain-but-non- random parameters via interval analysis. Computer methods in applied mechanics engineering **7825**(96), 361–372 (1998)
163. Qiu, Z., Wang, X.: Vertex solution theorem for the upper and lower bounds on the dynamic response of structures with uncertain-but-bounded parameters. Acta Mechanica Sinica/Lixue Xuebao **25**(3), 367–379 (2009). DOI 10.1007/s10409-008-0223-5
164. Rao, M.R., Mullen, R.L., Muhanna, R.L.: A new interval finite element formulation with the same accuracy in primary and derived variables. International Journal of Reliability and Safety **5**(3/4), 336 (2011). DOI 10.1504/IJRS.2011.041184
165. Rao, S., Berke, L.: Analysis of uncertain structural systems using interval analysis. AIAA Journal **35**(4), 727–735 (1997). DOI 10.2514/3.13572
166. Rao, S.S., Chen, L.I.: Numerical Solution of Fuzzy Linear Equations in Engineering Analysis. International Journal for Numerical Methods in Engineering **846**(March 1997), 829–846 (1998)
167. Rao, S.S., Sawyer, J.P.: Fuzzy finite element approach for the analysis of imprecisely defined systems. AIAA Journal **33**(12), 2364–2370 (1995)
168. Rossi, P.E., Allenby, G.M.: Bayesian statistics and marketing. Marketing Science **22**(3), 304–328 (2003)
169. Rupert, C., Miller, C.: An analysis of polynomial chaos approximations for modeling single-fluid-phase flow in porous medium systems. Journal of Computational Physics **226**(2), 2175 – 2205 (2007). DOI http://dx.doi.org/10.1016/j.jcp.2007.07.001
170. Sadeghi, J., De Angelis, M., Patelli, E.: Frequentist history matching with interval predictor models. Applied Mathematical Modelling (2018)
171. Scionti, A., Lardeur, P.: Experimental and numerical study of the intra/inter variability of an acoustic windscreen. In: Proceedings of the International Conference on Noise and Vibration Engineering ISMA 2006, pp. 1999–2003. Leuven, Belgium (2006)
172. Sentz, K., Ferson, S.: Combination of evidence in Dempster-Shafer theory, vol. 4015. Citeseer (2002)
173. Serhat Erdogan, Y., Gundes Bakir, P.: Inverse propagation of uncertainties in finite element model updating through use of fuzzy arithmetic. Engineering Applications of Artificial Intelligence **26**(1), 357–367 (2013). DOI 10.1016/j.engappai.2012.10.003
174. Shafer, G., et al.: A mathematical theory of evidence, vol. 1. Princeton university press Princeton (1976)
175. Sim, J., Qiu, Z., Wang, X.: Modal analysis of structures with uncertain-but-bounded parameters via interval analysis. Journal of Sound and Vibration **303**, 29–45 (2007). DOI 10.1016/j.jsv.2006.11.038
176. Simoen, E., Roeck, G.D., Lombaert, G.: Dealing with uncertainty in model updating for damage assessment: A review. Mechanical Systems and Signal Processing **56–57**, 123 – 149 (2015). DOI https://doi.org/10.1016/j.ymssp.2014.11.001

177. Singh, P., Deschrijver, D., Dhaene, T.: A balanced sequential design strategy for global surrogate modeling. In: Simulation Conference (WSC), 2013 Winter, pp. 2172–2179. IEEE (2013)
178. Sofi, A.: Structural response variability under spatially dependent uncertainty: Stochastic versus interval model. Probabilistic Engineering Mechanics **42**, 78–86 (2015). DOI 10.1016/j.probengmech.2015.09.001
179. Sofi, A., Muscolino, G.: Static analysis of Euler-Bernoulli beams with interval Young's modulus. Computers and Structures **156**, 72–82 (2015). DOI 10.1016/j.compstruc.2015.04.002
180. Sofi, A., Muscolino, G., Elishakoff, I.: Natural frequencies of structures with interval parameters. Journal of Sound and Vibration **347**, 79–95 (2015). DOI 10.1016/j.jsv.2015.02.037
181. Sofi, A., Muscolino, G., Elishakoff, I.: Static response bounds of Timoshenko beams with spatially varying interval uncertainties. Acta Mechanica **226**(11), 3737–3748 (2015). DOI 10.1007/s00707-015-1400-9
182. Sofi, A., Romeo, E.: A novel interval finite element method based on the improved interval analysis. Computer Methods in Applied Mechanics and Engineering **311**, 671 – 697 (2016). DOI http://dx.doi.org/10.1016/j.cma.2016.09.009
183. Soize, C.: Construction of probability distributions in high dimension using the maximum entropy principle:Applications to stochastic processes, random fields and random matrices. International Journal For Numerical Methods In Engineering **76**, 1583–1611 (2008). DOI 10.1002/nme
184. Soize, C.: Generalized probabilistic approach of uncertainties in computational dynamics using random matrices and polynomial chaos decompositions. International Journal for Numerical Methods in Engineering **81**(8), 939–970 (2010). DOI 10.1002/nme.2712
185. Soize, C.: A computational inverse method for identification of non-gaussian random fields using the bayesian approach in very high dimension. Computer Methods in Applied Mechanics and Engineering **200**(45), 3083–3099 (2011)
186. Spanos, P., Ghanem, R.: Stochastic finite element expansion for random media. Journal of engineering mechanics **115**(5), 1035–1053 (1989)
187. Sraj, I., Maître, O.P.L., Knio, O.M., Hoteit, I.: Coordinate transformation and polynomial chaos for the bayesian inference of a gaussian process with parametrized prior covariance function. Computer Methods in Applied Mechanics and Engineering **298**, 205 – 228 (2016). DOI https://doi.org/10.1016/j.cma.2015.10.002
188. Stefanou, G.: The stochastic finite element method: Past, present and future. Computer Methods in Applied Mechanics and Engineering **198**(9-12), 1031–1051 (2009). DOI 10.1016/j.cma.2008.11.007
189. Stein, M., Beer, M., Kreinovich, V.: Bayesian approach for inconsistent information. Information sciences **245**, 96–111 (2013)
190. Sudret, B.: Meta-models for structural reliability and uncertainty quantification. arXiv preprint arXiv:1203.2062 (2012)
191. Sunaga, T.: Theory of an interval algebra and its application to numerical analysis. Japan Journal of Industrial and Applied Mathematics **26**(2), 125–143 (1958)
192. Taylor, B.N., Kuyatt, C.E.: Guidelines for evaluating and expressing the uncertainty of NIST measurement results. US Department of Commerce, Technology Administration, National Institute of Standards and Technology Gaithersburg, MD (1994)
193. Teichert, W.H.: Reasons for Uncertainty and their Consequence. In: Proceedings of the 23rd International Conference on Noise and Vibration Engineering, ISMA, pp. 961–966. Leuven (1998)
194. Thacker, B.H., Doebling, S.W., Hemez, F.M., Anderson, M.C., Pepin, J.E., Rodriguez, E.A.: Concepts of model verification and validation. Tech. rep., Los Alamos National Lab., Los Alamos, NM (US) (2004)
195. Titurus, B., Friswell, M.: Regularization in model updating. International Journal for numerical methods in engineering **75**(4), 440–478 (2008)
196. Tonon, F., Bernardini, A.: A random set approach to the optimization of uncertain structures. Computers & structures **68**(6), 583–600 (1998)
197. Troffaes, M., Destercke, S.: Probability boxes on totally preordered spaces for multivariate modelling. International Journal of Approximate Reasoning **52**(6), 767–791 (2011). DOI 10.1016/j.ijar.2011.02.001
198. Turrin, S., Hanss, M., Selvadurai, A.: An approach to uncertainty analysis of rockfall simulation. CMES: Computer Modeling in Engineering & Sciences **52**(3), 237–258 (2009)

199. Van Der Herten, J., Deschrijver, D., Dhaene, T.: Fuzzy local linear approximation-based sequential design. In: Computational Intelligence for Engineering Solutions (CIES), 2014 IEEE Symposium on, pp. 17–21. IEEE (2014)
200. Vandepitte, D., Moens, D.: Quantification of uncertain and variable model parameters in non-deterministic analysis. In: IUTAM Symposium on the Vibration Analysis of Structures with Uncertainties, vol. 27, pp. 15–28. Saint Petersburg (2011). DOI 10.1007/978-94-007-0289-9
201. Vanmarcke, E.H., Grigoriu, M.: Stochastic Finite Element Analysis of Simple Beams. Journal of Engineering Mechanics **109**(5), 1203–1214 (1983). DOI 10.1061/(ASCE)0733-9399(1983)109:5(1203)
202. Verhaeghe, W., Desmet, W., Vandepitte, D., Joris, I., Seuntjens, P., Moens, D.: Application of interval fields for uncertainty modeling in a geohydrological case. In: ECCOMAS Thematic Conference - COMPDYN 2011: 3rd International Conference on Computational Methods in Structural Dynamics and Earthquake Engineering: An IACM Special Interest Conference, Programme. Corfu, Greece (2011)
203. Verhaeghe, W., Desmet, W., Vandepitte, D., Joris, I., Seuntjens, P., Moens, D.: Application of interval fields for uncertainty modeling in a geohydrological case. In: Computational Methods in Stochastic Dynamics, pp. 131–147. Springer (2013)
204. Verhaeghe, W., Desmet, W., Vandepitte, D., Moens, D.: Uncertainty assessment in random field representations: An interval approach. In: Annual Conference of the North American Fuzzy Information Processing Society - NAFIPS, pp. 1–6. El Paso, TX (2011). DOI 10.1109/NAFIPS.2011.5752048
205. Versteeg, H.K., Malalasekera, W.: An introduction to computational fluid dynamics: the finite volume method. Pearson Education (2007)
206. Walker, W.E., Harremoës, P., Rotmans, J., van der Sluijs, J.P., van Asselt, M.B., Janssen, P., Krayer von Krauss, M.P.: Defining uncertainty: a conceptual basis for uncertainty management in model-based decision support. Integrated assessment **4**(1), 5–17 (2003)
207. Wang, C., Qiu, Z., Wang, X., Wu, D.: Interval finite element analysis and reliability-based optimization of coupled structural-acoustic system with uncertain parameters. Finite Elements in Analysis and Design **91**, 108–114 (2014)
208. Wang, C., Qiu, Z., Wang, X., Wu, D.: Interval finite element analysis and reliability-based optimization of coupled structural-acoustic system with uncertain parameters. Finite Elements in Analysis and Design **91**, 108 – 114 (2014). DOI https://doi.org/10.1016/j.finel.2014.07.014. URL http://www.sciencedirect.com/science/article/pii/S0168874X14001553
209. Wang, M., Huang, Q.: A new hybrid uncertain analysis method for structural-acoustic systems with random and interval parameters. Computers & Structures **175**, 15 – 28 (2016). DOI https://doi.org/10.1016/j.compstruc.2016.07.001. URL http://www.sciencedirect.com/science/article/pii/S0045794916305466
210. Warmus, M.: Calculus of approximations. Bulletin de l'Academie Polonaise de Sciences **4**(5), 253–257 (1956)
211. Wasfy, T.M., Noor, A.K.: Multibody dynamic simulation of the next generation space telescope using finite elements and fuzzy sets. Computer Methods in Applied Mechanics and Engineering **190**(5-7), 803–824 (2000). DOI 10.1016/S0045-7825(99)00445-4
212. Weyl, H.: Elementare Theorie der konvexen Polyeder. Comentarii Mathematici Helvetici **7**(1), 290 – 306 (1934)
213. Witteveen, J.A., Bijl, H.: Effect of randomness on multi-frequency aeroelastic responses resolved by unsteady adaptive stochastic finite elements. Journal of Computational Physics **228**(18), 7025 – 7045 (2009). DOI http://dx.doi.org/10.1016/j.jcp.2009.06.013
214. Wu, B., Gao, W., Wu, D., Song, C.: Probabilistic interval geometrically nonlinear analysis for structures. Structural Safety **65**, 100 – 112 (2017). DOI http://dx.doi.org/10.1016/j.strusafe.2017.01.002
215. Wu, D., Gao, W.: Hybrid uncertain static analysis with random and interval fields. Computer Methods in Applied Mechanics and Engineering **315**, 222–246 (2017). DOI 10.1016/j.cma.2016.10.047
216. Xia, B., Yu, D.: Optimization based on reliability and confidence interval design for the structural-acoustic system with interval probabilistic variables. Journal of Sound and Vibration **336**, 1–15 (2015). DOI 10.1016/j.jsv.2014.10.012
217. Xiao, N., Fedele, F., Muhanna, R.: Interval-based parameter identification for structural static problems. arXiv preprint arXiv:1408.3430 (2014)

218. Xiaojun, W., Zhiping, Q.: Interval finite element analysis of wing flutter. Chinese Journal of Aeronautics **21**(2), 134–140 (2008)
219. Xu, M., Du, J., Wang, C., Li, Y.: Hybrid uncertainty propagation in structural-acoustic systems based on the polynomial chaos expansion and dimension-wise analysis. Computer Methods in Applied Mechanics and Engineering **320**, 198 – 217 (2017). DOI https://doi.org/10.1016/j.cma.2017.03.026. URL http://www.sciencedirect.com/science/article/pii/S004578251631461X
220. Xu, M., Qiu, Z.: A dimension-wise method for the static analysis of structures with interval parameters. Science China: Physics, Mechanics and Astronomy **57**(10), 1934–1945 (2014). DOI 10.1007/s11433-014-5445-x
221. Yan, W.J., Katafygiotis, L.S.: A novel bayesian approach for structural model updating utilizing statistical modal information from multiple setups. Structural Safety **52, Part B**, 260 – 271 (2015). DOI https://doi.org/10.1016/j.strusafe.2014.06.004. Engineering Analyses with Vague and Imprecise Information
222. Yin, H., Yu, D., Lü, H., Yin, S., Xia, B.: Hybrid finite element/statistical energy method for mid-frequency analysis of structure- acoustic systems with interval parameters. Journal of Sound and Vibration **353**, 181–204 (2015)
223. Yu, M., Bao, H., Ye, J., Chi, Y.: The effect of random porosity field on supercritical carbonation of cement-based materials. Construction and Building Materials **146**, 144 – 155 (2017). DOI http://dx.doi.org/10.1016/j.conbuildmat.2017.04.060
224. Zadeh, L.: Fuzzy sets. Information and Control **8**(3), 338–353 (1965). DOI 10.1016/S0019-9958(65)90241-X
225. Zadeh, L.A.: The concept of a linguistic variable and its application to approximate reasoning-iii. Information sciences **9**(1), 43–80 (1975)
226. Zadeh, L.A.: The concept of a linguistic variable and its application to approximate reasoning—i. Information sciences **8**(3), 199–249 (1975)
227. Zadeh, L.A.: The concept of a linguistic variable and its application to approximate reasoning—ii. Information sciences **8**(4), 301–357 (1975)
228. Zadeh, L.A., et al.: Calculus of fuzzy restrictions. Electronics Research Laboratory, University of California (1975)
229. Zhu, H., Zhang, L., Xiao, T., Li, X.: Generation of multivariate cross-correlated geotechnical random fields. Computers and Geotechnics **86**, 95 – 107 (2017). DOI http://dx.doi.org/10.1016/j.compgeo.2017.01.006
230. Zhu, Y., Zhang, L.: Finite element model updating based on least squares support vector machines. Advances in Neural Networks–ISNN 2009 pp. 296–303 (2009)
231. Zienkiewicz, O.C., Taylor, R.L., Taylor, R.L.: The finite element method, vol. 3. McGraw-hill London (1977)